"DENOISING ECG SIGNALS BASED ON WAVELET TRANSFORM HYBRID WITH MACHINE LEARNING ALGORITHMS"

A THESIS

Submitted by

Submitted for the Partial Fulfillment of the
Degree of Doctor of Philosophy
By

S. Balasubramanian

Enrollment No: MUIT0118038095

Under the Supervision
of
Dr. Mahaveer Singh Naruka

Professor, MUIT, Lucknow

Maharishi School of Engineering & Technology

Session 2018-19

Maharishi University of Information Technology

Sitapur Road, P.O. Maharishi Vidya Mandir
Lucknow, 226013

ABSTRACT

The biggest cause of mortality worldwide is cardiovascular disorder, therefore cardiovascular fitness of the human heart has been a fascinating topic for decades. The electrocardiogram (ECG) signal is a comprehensive non-invasive method for determining cardiac health. Various health practitioners use the ECG signal to ascertain critical information about the human heart. A non-stationary biological signal electrocardiogram (ECG) helps us to diagnose heart problems. Because the artefacts that contaminate the data have similar frequency characteristics to the signal itself, reducing noise in electrocardiography signals is a critical and significant challenge. Filtering approaches, for example, were shown to be ineffective in removing these interferences. As a result, in order to achieve adequate noise-removal performance, electrocardiography signals require a novel and efficient denoising approach.

For denoising ECG signals, wavelet techniques including DWT and EWT are hybridized together via machine learning methods. The suggested technique is assessed on ECG data gathered from MIT-

BIH Database, which included artefacts including baseline wander and muscle contraction noise. The algorithm's efficacy on a range of signal kinds is determined by calculating parameters. The findings suggest the recommended denoising method is simple for designing and are used in electrocardiography data.

The noisy ECG signal is denoised in this study using the suggested adaptive switching mean filter (ASMF) and discrete wavelet transform (DWT) optimized with the Enhanced African Vulture Optimization (AVO) method. Prior to adding white Gaussian noise, the input ECG signals are first extracted from the MIT-BIH ARR dataset. Then the corrupted ECG signals are denoised by DWT from which the threshold is optimized by an Enhanced African Vulture Optimization (AVO) algorithm to obtain the optimum threshold. The AVO algorithm is enhanced by Whale Optimization Algorithm (WOA). Additionally, ASMF is tuned by the Enhanced AVO algorithm. The tests are done in the MIT-BIH dataset and the proposed filter built using the EAVO algorithm, attains a significant enhancement in reliable parameters, according to the testing results in terms of SNR, mean difference (MD),

peak reconstruction error (PRE), mean square error (MSE), normalized root mean squared error (NRMSE), maximum error (ME), and normalized root mean error (NRME) with existing algorithms namely, PSO, AOA, MVO, etc.

Keywords: ECG signal denoising, discrete wavelet transform, African Vulture optimization, whale optimization, adaptive switching mean filter, and MIT-BIH dataset.

TABLE OF CONTENTS

LIST OF TABLES

LIST OF FIGURES

ABBREVATIONS

ECG	Electrocardiogram
EMR	Electronic Medical Recordings
PSD	Power Spectral Density
EMF	Electromagnetic Field
ARV	Averaged Rectified Value
MIT	Massachusetts Institute of Technology
HPF	High Pass Filter
LPF	Low Pass Filter
LMS	Least Mean Square
RLS	Recursive Least Squares
ANC	Adaptive Noise Cancellers
WT	Wavelet Transform
STFT	Short-Time Fourier Transform
ANFIS	Adaptive Neuro-Fuzzy Inference System
ICA	independent component analysis
ANN	Artificial Neural Network
LLMS	Leaky LMS Algorithm
PCA	Principal Component Analysis
MGGD	Multivariate Generalised Gaussian Distribution
IVUS	Intravascular Ultrasonography
MAP	Most Extreme a Posteriori
WHO	World Health Organization
DWT	Discrete Wavelet Transform
EWT	Empirical Wavelet Transform
HBO	Honey Badger Optimization
NRMSE	Normalized Root-Mean-Square Error
ME	Maximum Error
PRE	Peak Reconstruction Error
MD	Mean Difference
SNR	Signal-to-Noise Ratio
NRME	Normalized Root Maximum Error
CC	Correlation Coefficient
MSE	Mean Square Error
AVO	African Vulture Optimization

CHAPTER 1

INTRODUCTION

1.1 Electrocardiograms

Electrocardiograms (ECGs) have been widely utilized to store the electrical impulses of the heart from 1901, thanks to William Einthoven's invention [1]. The medical community has been able to detect and diagnose heart abnormalities like cardiac arrhythmias, myocardial infarction, and heart failure with greater accuracy. Biomedical signals are produced by physiological processes within the organism. Signals may be produced by every living thing, from gene and protein sequences to brain and cardiac rhythms. These signals might be studied or tracked in order to understand certain elements of a physiologic system. The cardiac signal, or ECG, is the most frequent signal utilised by clinicians to evaluate heart irregularities in medical care. The ECG is a time-based image of cardiac electrical activity that is often used to diagnose heart problems. Based on the most current statistics of World Health Organization's, in all parts of the world, cardiovascular diseases remain the major cause of mortality [2].

The heart activity is represented by electrocardiography (ECG), which is primarily an electrical signal. It's presented as a graph. Electrodes (3 or 12 leads) are linked externally to the surface of the

thorax, legs, and hands to record the data. The potentials generated by cardiovascular muscle action are plotted on the ECG. Physicians utilize it widely to anticipate and treat a variety of cardiovascular disorders. The QRS complex, along with P, T, and U waves, each of which is associated with a particular occurrence that takes place within a single cardiac cycle, are just a few of the unique entities that may be seen on an ECG. The combination of these entities and knowledge of the ECG scale allows for the calculation of heart rate and the detection of rhythm disorders such as atrial fibrillation, atrial flutter, cardiac arrhythmia, sinus tachycardia, and sinus bradycardia, among other things. The axis deviation of the QRS complex, for example, is a symptom of ventricular hypertrophy, anterior and posterior fascicular block, and other disorders that can be detected by shape analysis.

ECG equipment may now generate time series ECG data (amplitude and time) as well as the paper ECG record, which is frequently scanned and saved in digital format. Given that a significant proportion of paper ECG records have yet to be digitised, a variety of techniques have been proposed to efficiently convert paper ECG records into digitally recorded ECG signals. Electronic Medical Recordings (EMR) are increasingly being utilised to maintain patient information and digitally preserve ECG records [3]. Integrating EMR with digitised ECG signals might possibly aid in the collection of data needed for prediction algorithms.

The signal produced by the ECG is low amplitude voltage, and because of the numerous artefacts sources that might degrade it, the ECG signal recording should account for this. The most prevalent causes of ECG noise include equipment, power line interference, and biological systems surrounding the heart. Organic systems such as the heart are complex, and they are constantly influenced by other organic systems or subsystems in the environment. As a result, heart signals frequently include signals from other regions of the body, such as electromyography (EMG) signals. Removing unnecessary signal components from an ECG signal can lead to better signal interpretation. As a result, signal processing is employed to minimise noise in a wide range of ECG systems.

1.2 ECG and Noise

The ECG (electrocardiogram) displays the heart’s electrical movements as a series of electrical waves for each pulse as illustrated in Figure 1.1. The signals in the ECG is made up of five valleys and peaks denoted as T, R,Q, S, and P, that represent cardiac actions. Atrial depolarization represents the frequency P, the frequencies T are the three electrical entities that make up an ECG trace (ventricular repolarization) and ventricular depolarization represents the QRS complex. An ECG signal's normal frequency range is 0.05–50 Hz, with the wave P is situated among 0.67 and 5 Hz, the QRS complex is situated between 10 and 50 Hz, and the wave T falling between 1 and 7 Hz.

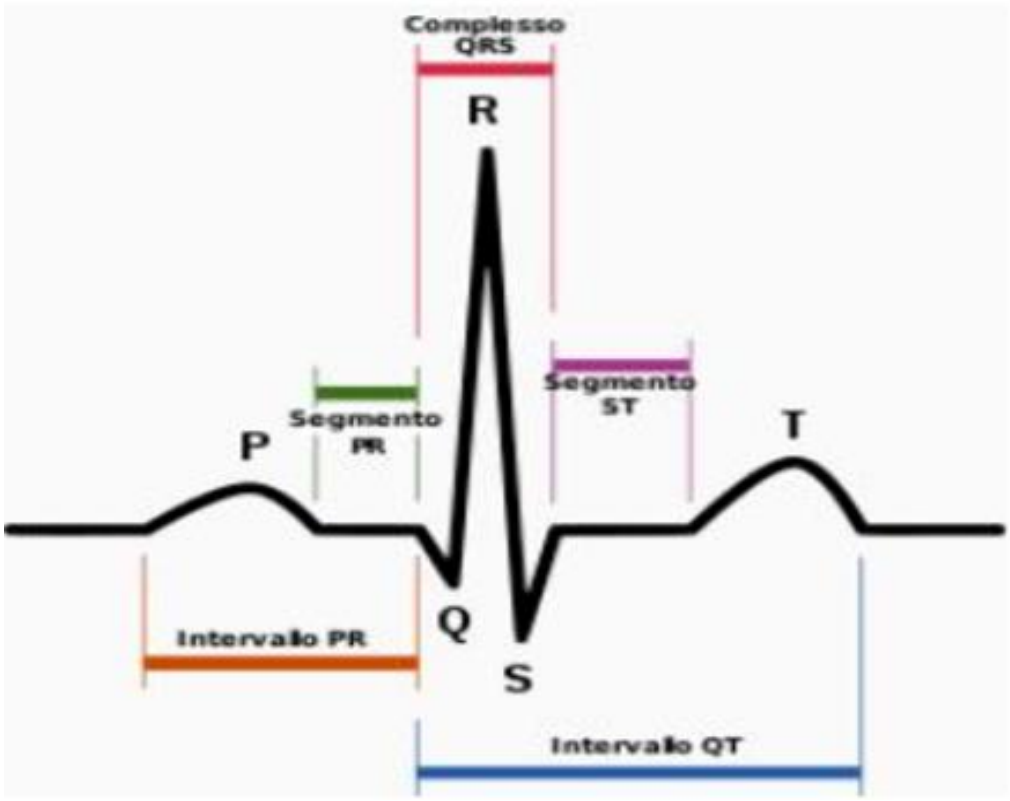

Figure 1.1: Representation of a Pulse in ECG

Various artefacts impact the ECG signal during capture and transmission. A multitude of noise sources can distort the ECG signal, which can be categorised based on their power spectral density (PSD). Electromyogram (EMG) artefacts, power line interference, and additive white Gaussian artefacts are samples of high-frequency artefacts with their major power spectral density located in larger frequencies according to the frequency spectrum of ECG. The low-frequency artefacts are baseline wandering which affects the signals of ECG in the lower frequency band. Furthermore, a variety of artefacts can contaminate ECG, including electrodes, motion artefacts, and muscle artefacts, the

most of which PSD overlap ECG signal spectrum and are thus the most difficult to eliminate.

1.3 Artefacts in the ECG

Unfortunately, the recorded ECG contains not just components created by the heart's electrical activity, but it is also contaminated with artefacts that can interfere with or interrupt the signal, resulting in data loss. The shape of these artefacts can be similar to that of an ECG [4]. The most common ECG artefacts are as follows:

- Power line artefacts have a 50 / 60 Hz frequency, based on the country.

- The lack of contact between the electrodes and the saturating skin causes steep voltage fluctuations. Furthermore, variations in the impedance between the skin and the electrode caused by the electrode's movement as a result of the patient's movement create some fast baseline jumps that may saturate.

- Muscle contractions produce electrical activity that ranges from dc to 10kHz.

- The most common source of baseline drift is respiration at extremely low frequencies, about 0.1-0.3 Hz [7].

The presence of artefacts in the ECG signal makes it difficult to analyse. This happens because the artefacts and the signal have a significant spectral frequency overlap. Because there hasn't been much research done on artefact identification and removal, the literature available on the issue is restricted. Bala Gopakumaran et al. [24] investigated ECG artefacts recorded by four most important patient observer was created by (Phillip Medical Systems, Andover, MA; Ivy Biomedical Systems, Bradford,; Datex Ohmeda, Helsinki, Finland; and CT GE Medical Systems, Milwaukee, WI). They recommend the measures that reduce the surgical artefacts. Although those procedures can reduce the appearance of artefacts in general, they are ineffective at removing or eliminating them.

1.4 Analysing the Artefacts in the ECG

1.4.1 Baseline Drift

Baseline wander/baseline drift indicates the effect of a signal's base axis (x-axis) 'wandering' or shifting up and down instead of being straight. The signal deviates from its usual baseline, which is a zero-mean signal. Patient movement, breathing, and improper electrodes (electrode-skin impedance) cause baseline drift (respiration). Baseline wander has a frequency content of 0.5 Hz. On the other hand, increased physical activity while exercising or a stress test increases frequency content. Figure 1.2 shows a visual representation of baseline drift.

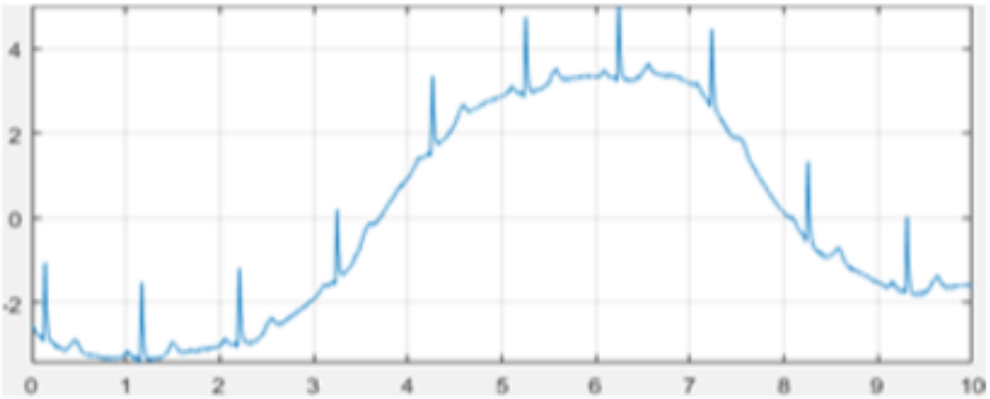

Figure 1.2: Representation of Baseline Drift

1.4.2 Power line interference

An artefact in the ECG and any other bioelectrical signal recorded from the human skin is frequently caused by the electromagnetic fields produced by power lines. This sort of noise is characterised by sinusoidal interference at 50 (or 60) Hz with several harmonics. Narrowband noise makes ECG analysis and interpretation more difficult due to inaccurate demarcation of low-amplitude waveforms and the possibility of false waveforms being formed. Electromagnetic field (EMF) interference induced by alternating current fields in power lines or adjacent machinery is the major source of interference. The pictorial representation of power line is shown in Figure 1.3.

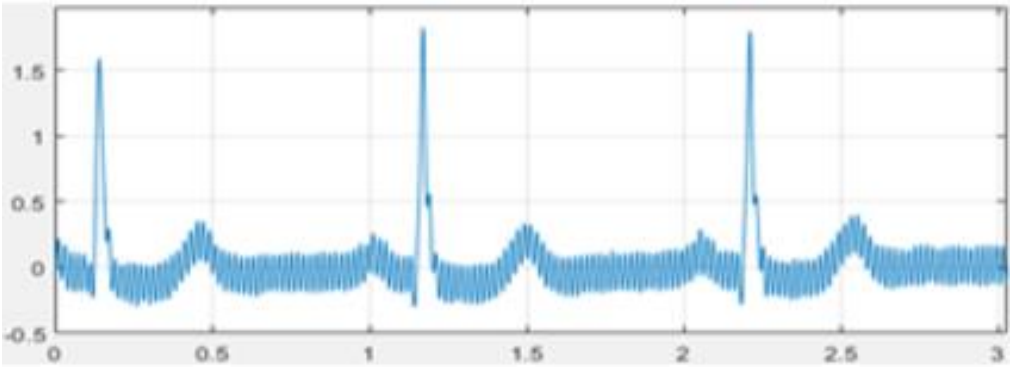

Figure 1.3: Representation of Power Line Interference

1.4.3 Electromyogram (EMG) Noise

Muscle noise is a significant issue occurs in various ECG methodologies, particularly in recordings made while exercising, because ECG waves with lesser amplitudes can completely covered. Narrowband filtering does not diminish muscle noise, but it does provide a lot more difficult filtering problem since muscle activity's spectral content overlaps the PQRST complexes significantly. Figure 1.4 depicts a visual depiction of EMG noise.

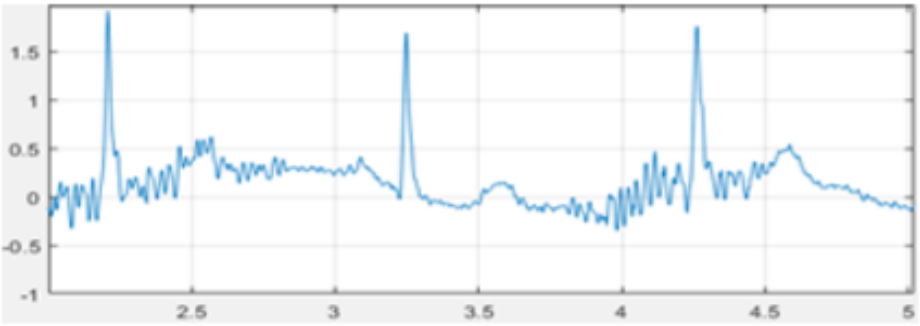

Figure 1.4: Representation of EMG Noise

1.4.4 Electrode Motion Artefacts

Skin stretching alters the impedance of the skin around the electrode, which results in abnormal electrode motion. While motion artefacts have signal characteristics similar to baseline wander, their spectral content significantly overlaps the PQRST complex, making them more challenging to avoid. Between 1 and 10 Hz, they are most prevalent. Large-amplitude waveforms that resemble QRS complexes can be seen as a result of these abnormalities on the ECG. In ambulatory ECG monitoring, where they are the most common cause of inaccurately reported heartbeats, electrode motion artefacts are especially problematic. The pictorial representation of electrode motion artefacts is shown in Figure 1.5.

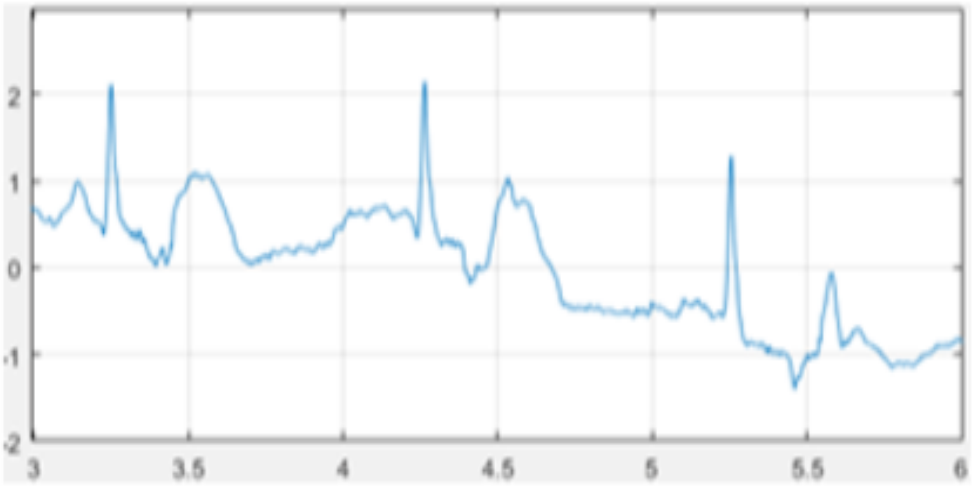

Figure 1.5: Representation of Electrode Motion Artefacts

1.5 Signal Recording

EMG data recorded near the heart typically contain ECG interferences, however in places where electrocardiogram contamination is limited, a clean EMG signal can be acquired. Figure 1.6 shows five sets of two-channel clean EMG data from the right biceps and deltoid muscles collected over five minutes. Applications for hand prosthesis control and hand motion prediction are the main reasons to use these muscles. Figure 1.6 shows five pairs of left pectoral is major muscle-related two-channel ECG abnormalities. To taint the EMG signal, this signal is necessary. The polluted EMG signal generated by merging the clean EMG signal with the ECG artefact is shown in Figure 1.6. On the wrist, the reference electrodes were placed.

For example, ANC, ANN, and ANFIS all need the recording of the ECG artefact as well as the associated ECG signal. As a result, the ECG signal in Figure 1.6 was recorded at V5. The patients' EMG signals were captured as they sat in a chair and exercised their biceps and deltoid muscles twice. Between each activity, a rest period was considered. The subjects were told to lie absolutely comfortably while the ECG and ECG artefacts were recorded.

On the biceps muscles, deltoid, and pectoralis major, the SENIAM standard was utilised to determine electrode placement. At the Biological Systems Control Lab, ECG and EMG data were gathered using the Power Lab/16SP equipment (ML795 from AD Instrument).

Five 21.4+/-1.94 year old guys (tallness= 177+/-3.67 cm, weight= 72.6+/-13.37 kg) were selected from the population subsequently receiving informed permission.

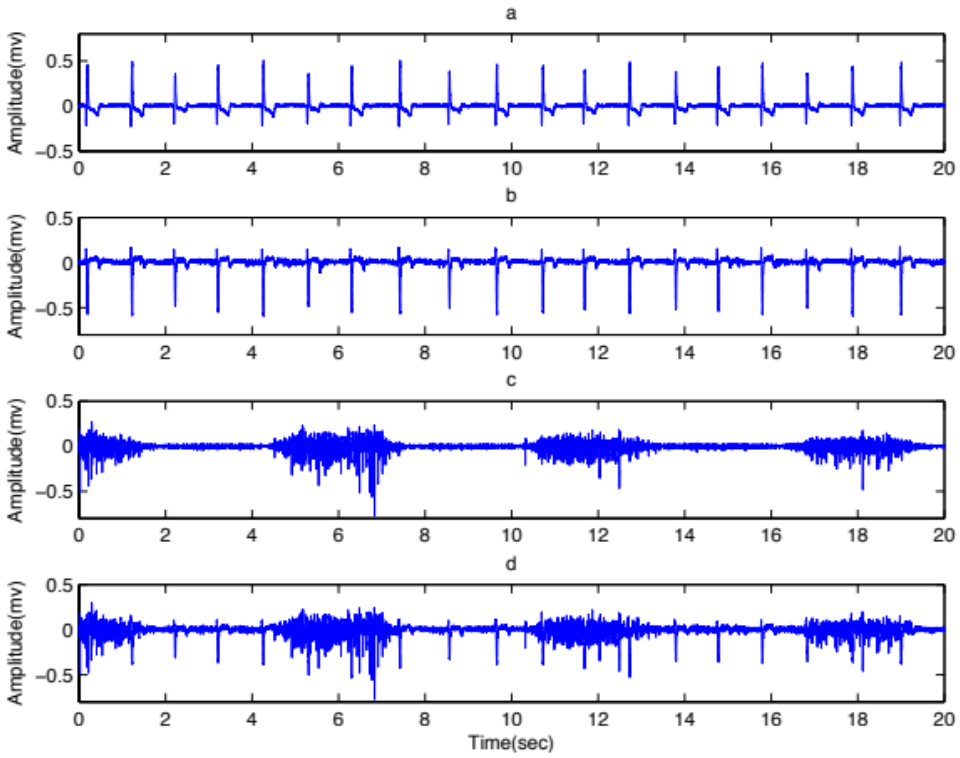

Figure 1.6: (a) Clean ECG (b) Artefacts ECG (c) Clean EMG (d) Corrupted EMG

SKINTAC FRG1, 32 x 41 mm, pre- clotted Ag-AgCl bipolar electrodes were implanted on the skin's surface to record the signals. The electrodes were spaced apart by 30 mm [37]. In order to prepare the skin, it was shaved, lightly abraded, and cleaned with alcohol. Below 10,000 ohms of impedance were maintained. These electrodes' EMG signals

were examined using a biological amplifier. To reduce the influence of high frequency noise and avoid aliasing, the raw EMG signals were band-pass filtered with an analogue filter from 0.3 to 500 Hz before pre-amplification and sampling.

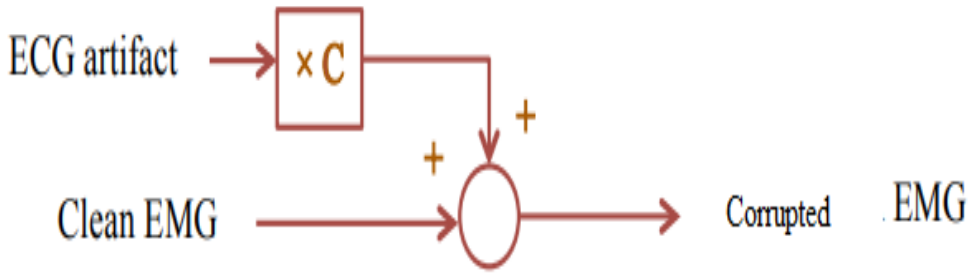

Figure 1.7: Corrupted EMG Signal Framework

EMG frequencies were isolated from power line interference using a notch filter (centred at 50 Hz). 2000 Hz sample frequency was used to record the signals. The comparable artefacts free EMG signal must be given alongside, the polluted EMG signal in order to enable a quantitative comparison of the techniques. As a result, the polluted EMG signal was produced as precisely as feasible for this investigation. The contaminated EMG signal was created, as seen in Figure 1.7, by multiplying the artefact free EMG frequencies from the right side's biceps and deltoid muscles by a factor (C=0.65) and merging them with the ECG artefacts from the left side's pectoral is major muscle. The polluted EMG signals had their SNR value adjusted to zero (dB). This study looks at how various techniques impact the target signal while accounting for the starting SNR. Ten channels of polluted EMG signals

were produced after using this approach to analyse a 60-second slice of data from each channel collected from five healthy people.

1.6 Artefact Removal Approaches

Hybrid approach, gating method, ANC, spike clipping, HPF, ICA, wavelet-ICA, ANN, template subtraction, wavelet transform, and ANFIS were utilized to explore the effectiveness of ECG artefact removal methods.

1.6.1 High Pass Filter

ECG distortions were removed from EMG data using a FIR high pass filter with a Hamming window (length=100) and cutoff frequencies of 10, 20, 30, and 60 Hz. The 30 Hz cutoff frequency outperforms all others. When cutoff frequencies of 10 and 20 Hz are used, a substantial amount of noise is still present in the cleaned signal; however, when cutoff frequencies of 50 Hz are used, a large quantity of useable signal is lost.

1.6.2 Spike Clipping

Spike clipping is evaluated by Eqn. (1.1), which depends on a threshold level ($Thres$). If the recorded signal's amplitude ($r_i(n)$) reaches this amount, the signal's amplitude is restricted at this level. The denoised signal is $\widehat{sp}(n)$.

$$\widehat{sp}(n) = \begin{cases} r_i(n) & |r_i(n)| < Thres \\ Thres & |r_i(n)| > Thres \end{cases} \quad (1.1)$$

1.6.3 Gating Approach

The gating approach is similar to the clipping technique in that it needs the determination of a threshold. If the recorded signal's amplitude ($r_i(n)$) reaches this amount, the signal is clamped to zero (Eqn. (1.2)) . The thresholding procedure determines the method's performance.

$$\widehat{sp}(n) = \begin{cases} r_i(n) & |r_i(n)| < Thres \\ 0 & |r_i(n)| > Thres \end{cases} \quad (1.2)$$

1.6.4 Hybrid Approach

ECG artefacts were removed from EMG data using a hybrid method [18]. It combines a spike clipping method with an HPF, as seen in Figure 1.3. Adaptive thresholding is used to implement the spike-clipping mechanism in this approach. The amplitude of previous samples, as well as a gain chosen by the user, defines the threshold. The averaged rectified value (ARV) for polluted signal is computed in each iteration of the spike-clipping method across a window of N times. The ARV's gain is then set to a certain value. A spike that appears above the cutoff level is trimmed and put below it. One of the method's drawbacks is that

evaluating the spike-clipping procedure in each cycle takes a lengthy time.

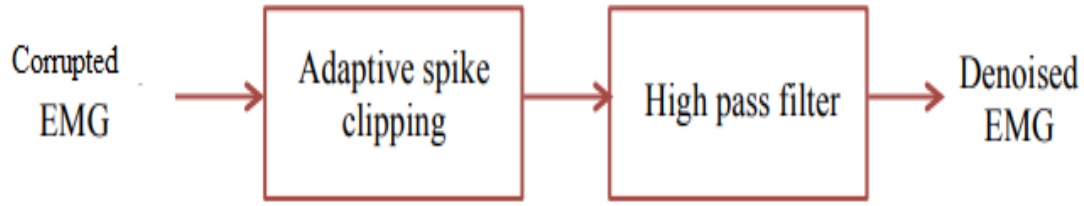

Figure 1.7: Hybrid Approach Framework

1.7 Types of Denoising Techniques

There are two strategies for denoising are,

- Spatial domain filtering methodologies
- Transform domain filtering methodologies

1.7.1 Spatial domain filtering Techniques

The filters spatial are a common technique for removing visual noise. There are two types of spatial filters: linear and nonlinear.

1.7.1.1 Linear Filtering Technique

In the realm of remote sensing, spatial domain filtering is done in the pixel grey geometric space, which allows a quick filtering

procedure if the contract is linear, and the filter is called a linear filter.In terms of MSE, an optimal linear filter is a mean or average filter for noise reduction. In the presence of noise that depends on the signal, it may also blur clear edges, erase lines, and obscure other crucial visual characteristics.

1.7.1.2 Nonlinear Filtering Technique

These filters are frequently helps to diminish the interference and identify the edges. A frequent sort of filter is the median filter. The spatial filters also use low-pass filtration in pixel groups, based on the assumption that noise dominates a larger regional frequency spectrum. Typically, spatial filters eliminate picture noises; nevertheless, blurring the image obscures the image's edges. To tackle these drawbacks, most upgraded median filters, including Rank Conditioned Rank Selection, Weighted Median Adaptive Filter, and Multilevel Hybrid Median Filter, are now offered.

1.7.2 Transform domain filtering Techniques

The analysis function or the choice of bases is used to classify transform domain filter approaches. Wavelet domain and spatial frequency filtering are two types of analytic functions.

1.7.2.1 Spatial Frequency Filtering Technique

This filter is known as a low-pass filter since it uses FFT (frequency domain based filter). The frequency domain based filter smoothes down the frequency domain effective signal and changes the cutoff frequency to separate noise parts. Cut-off frequency and filter working behaviour impact the time consumption of these techniques.

1.8 ECG Database

Since 1975, the Massachusetts Institute of Technology (MIT) has collaborated with Boston's Beth Israel Hospital (now the Beth Israel Deaconess Medical Centre) to create a database to aid studies in arrhythmia analysis and related topics. The database of the Massachusetts Institute of Technology Beth Israel Hospital (MIT-BIH) was one of their first important accomplishments. In 1980, the database was completed and distributed. In addition to being used for basic research on cardiac dynamics at more than 500 locations across the world, the database was the first freely accessible set of standard test material for assessing arrhythmia detectors [34].

The MIT-BIH Arrhythmia Database contains 48 half-hour samples of two-channel ambulatory ECG recordings. These findings are from a group of 47 participants who were part of a mixed sample of inpatients (60%) and outpatients (40%) who were examined by the BIH Arrhythmia Laboratory. There contains 25 males and 22 women in the

study, with ages ranging from 32 to 89. Since its debut in September 1999, around half of PhysioNet's database (25 of 48 full records and reference annotation files for all 48 records) has been made publicly accessible [35]. The extra 23 signal files, which were previously exclusively accessible via the MIT-BIH Arrhythmia Database CD-ROM, were made available to the public in February 2005 [36]. The recordings were digitalized across a 10 mV range at 360 samples per second, each channel.

1.9 ECG Denoising Techniques

The denoising techniques used to eradicate the artefacts in the ECG are,

- FIR filter
- Adaptive filter
- Wavelet filter

1.9.1 FIR Filter

Based on how the system's unit pulse responds, the digital filters are categorised as IIR or FIR filters. The FIR system's impulse response is time-constrained, but the IIR system's impulse response is unbounded. Since IIR filters are typically built with feedback mechanisms, the current response of an IIR filter is a function of the

present, past, and prior values of the excitation as well as the prior value of the response. However, the FIR filter's response is frequently implemented using structures that do not provide feedback, therefore the response is totally dependent on the current and previous input values [37]. FIR filters are popular because of the merits described as follows:

- Exact linear phase
- Filter start-up transients have finite length
- Always stable
- Linear design approaches
- Hardware implementation

1.9.2 Adaptive Filter

The filter coefficients (parameters) are modified over time in adaptive filtering. In order to minimise error, it responds to variations in signal quality. Channel equalisation, Adaptive noise cancellation, frequency tracking, and system identification are just a few of the applications available [38]. Figure 1.6 depicts the overall framework of an adaptive filter.

The signal input is denoted as a0(n) in Figure 1.8. Eqn. (1.3) gives the vector form of a0(n). There are artefacts in this input signal. In

other terms, as described in Eqn. (1.4), d0(n) represents the intended signal sum and the artefacts as v0(n).

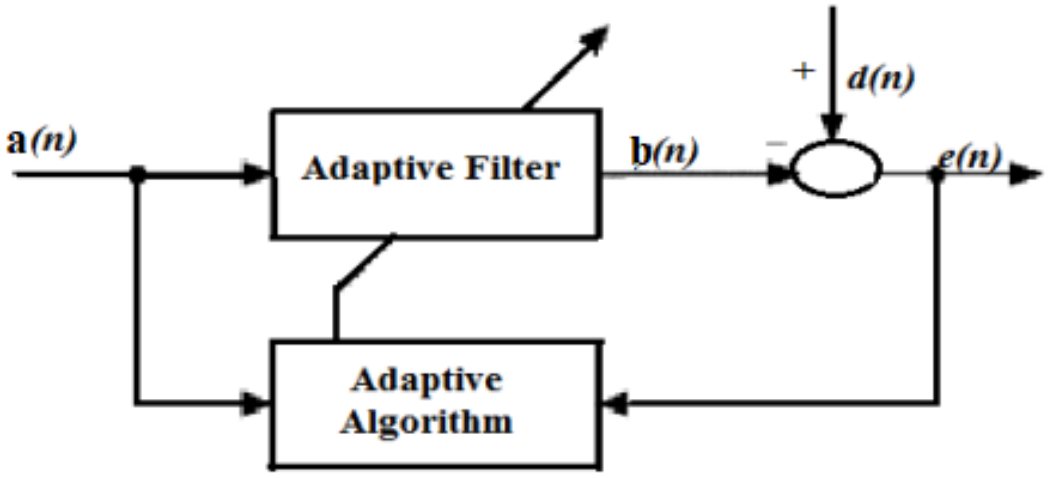

Figure 1.8: Adaptive Filter Outline

$$a0(n) = [a0(n), a0(n-1), \ldots, a0(n-N-1)]^T \tag{1.3}$$

$$a0(n) = d0(n) + v0(n) \tag{1.4}$$

The outline of the adaptive filters is the Finite Impulse Response. Such systems' impulse responsiveness is equivalent to the filter coefficients. The N filter order coefficients are denoted as,

$$Co(n) = [co_n(0), co_n(1), \ldots, co_n(N-1)]^T \tag{1.5}$$

The outcomefor an adaptive filter is b0(n) which is written as,

$$b(n) = C(n)^T a(n) \tag{1.6}$$

The difference between the intended and estimated signals is the error signal or cost function.

$$e(n) = d(n) - b(n) \tag{1.7}$$

Furthermore, the variable filter constantly changes the filter coefficients.

$$W0(n+1) = W0(n) - \Delta W0(n) \tag{1.8}$$

Here, $\Delta W0(n)$isthe filter coefficients' adjustment factor.

1.9.2.1 Handling of Adaptive Filter

Filters lessen the effect of artefacts in a signal to enhance the SNR at the filter's output. Various filter categories are available depending on the application. This thesis employs adaptive linear filters,

with the filtered output changing over time. A filter can be made one of two ways.

- Frequency selective filters including Filter with Low Pass (LPF), Filter with High Pass (HPF), and Notch Filter use the Classical method. The spectral components of the message signal and the artefact are monitored to reduce SNR. The most crucial thing to keep in mind is that these filters can only be applied if the frequency ranges of the input signal and the artefact are different.

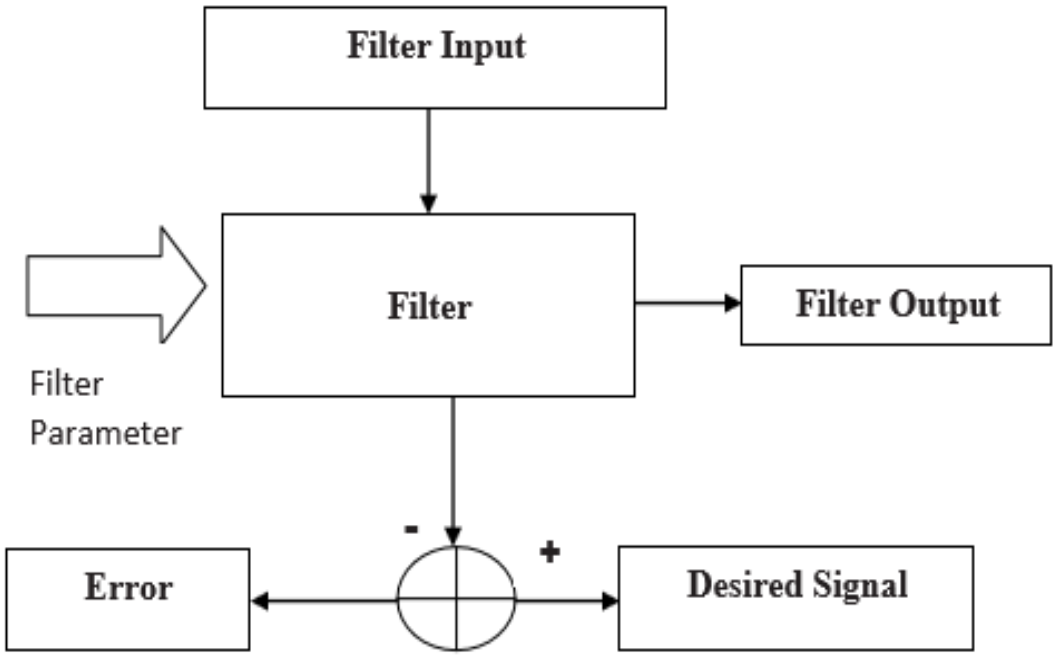

Figure 1.9: Wiener Filter

- Another option is to apply optimization theory to develop better filters using optimal filter design. The optimum filter design is the best for reducing artefacts if the statistical character of the stochastic process is understood in advance. As shown in Figure 1.9, the primary purpose is to reduce the MSE, or the dissimilarity among the filter outcome and the desired signal.

Non-stationary noise signals are those whose statistical features shift over time. The wiener filtration method is theoretically acceptable in these scenarios but difficult to execute in practise.

The adaptive filter is superior for this since it is self-designing. The adaptive filter structure is comprised of an adaptation algorithm. It keeps track of the input samples and changes the filter tap weights as needed. The adaptive algorithm begins the learning phase under specified conditions with an unknown input vector. As a consequence, depending on the received signals, attempts are made to develop the best filter design possible.

1.9.2.2 Features of Adaptive Approaches

The primary function of an adaptive filter is to minimise an objective function. It is possible to condition this objective function to have a continuous form by properly selecting it. The following elements contribute to the preferences of one algorithm over another.

- Convergence Rate
- Misadjustment
- Tracking
- Computational Requirement

1.9.3 Linear Adaptive Filter

The adaptation algorithm for the application of linear filters can be obtained in several different ways. Two techniques are that develops linear filters are,

- Stochastic Gradient Approach
- Least Squares Estimation

1.9.3.1 Stochastic Gradient Approach

The linear adaptive filter is implemented using a transversal filter structure in this manner. The MSE stands for the cost function, which is also known as index performance. The MSE is the variation among the outcome of the transversal filter with the desired signal. The MSE, which is a second order function, is the cost function of the transversal filter's tap weights. The error performance surface is a multidimensional paraboloid structure that comes from MSE's reliance

on unknown filter coefficients. The filter coefficients corresponding to the least feasible location on the gradient are determined by the wiener solution.

The transversal filter structures' adaptive algorithm may be changed at two separate levels. To find the best wiener solution, an adaption algorithm is first chosen. To optimise the adaptation process, the steepest descent approach is applied. The gradient vector, which is based on two key factors, determines the steepest descent technique. The first vector is the vector of adjustment among the desired signal and the input vector. The gradient vector estimate is then calculated using the correlation matrix's instantaneous values. As a result, the method developed is named as Least Mean Square (LMS) method.

In every case, the LMS approach, which is straightforward and reliable, has the potential to deliver good outcomes. The LMS algorithm's principal drawbacks are its sluggish convergence rate and susceptibility to variations in the hermitian matrix-based input data vector. The LMS is a basic and dependable algorithm that may produce excellent results in any situation. In non-stationary signals, the adaptation of MSE behaviour changes over time. The LMS algorithm is also responsible for continuously tracking the error performance surface, which is linked to the volatility of the input data vector.

1.9.3.2 Least Squares Estimation

The least squares strategy is used in another notion for developing the linear adaptive filter. The cost function, which is equal to the total of the weighted error squares, is reduced using least squares. The error, also known as the residue, is the discrepancy among the intended frequency and the filtered outcome. The filter coefficients are determined block by block using the least squares approach. A stream of input data is organised sequentially into a block of data with equal lengths. The filtering procedure in block estimation is accomplished block by block. The adaptive filter coefficients are organised on a sample basis in order to accommodate recursive adaptation.

Recursive least squares (RLS) adaptations include the Kalman filter. The Kalman filtering technique is distinct in that it calculates the average value of the input samples applied to the linear adaptive filter at a certain time.

1.9.4 Adaptive Noise Cancellation's Importance in Biotelemetry

A filter must eliminate various distortions from the ECG signal before monitoring to present an accurate signal. FIR and IIR filters, which give exact frequency characteristics, are commonly used to change the signal frequency content. By obtaining the real frequency characteristics, Fourier Transform analysis is utilised to evaluate design methods. However, these design methods do not make it clear to users

which frequency characteristic is the best, i.e. which filter type successfully separates signals from noise. This decision is based on the source qualities or the user's signal understanding. The use of optimal filter theory to identify the structure's most acceptable frequency characteristics is offered. The divergence of the actual and desired filter responses prefers the wiener filter theory to MMSE for analysis. The error surface parameter simply represents the representation of the MSE for the linear filter's variable parameter.

When non-stationary signals are met with time-varying forms of optimal filter, the wiener filter is not used. Only if the information fits the features of the input data is prior statistical data of the information necessary to process the Wiener filter and the optimal solution offered. Without this, data is impossible to understand entirely, and weiner filter improvement is no longer possible. As a result, the recursively based adaptive filter, which is a self-designed filter that produces approximated results even when all of the relevant signal's data is unavailable, is favoured. This method begins with a pre-determined set of beginning values that are relevant to the present situation. In a statistical sense, the algorithm's Optimum Weiner solution is found after a certain number of rounds.

Adaptive filtering has been a prominent method for processing biological data such as ECG analysis in recent years. Adaptive filters allow for the identification of time-varying potentials as well as the monitoring of dynamic signal fluctuations. They also vary their nature in

relation to the quantity of incoming data samples, allowing for the evaluation of signal pattern changes. One of the best approaches to get rid of artefacts in biotelemetry applications is to use LMS-based adaptive noise cancellers (ANC's).

1.9.5 Wavelet Filter

The WT is quite similar as Fourier transform. The FFT's core functions are sines and cosines. Wavelets, mother wavelets, or studying wavelets, as well as scaling functions, are more complicated wavelet transform basis functions. Wavelet analysis divides the original (or mother) wavelet into shifted and scaled variations. The wavelet transform is excellent for non-stationary signals like the ECG since it is a multi-resolution analysis [39].

1.9.5.1 Wavelet Transform

The signal frequency modules are analysed by using the tool Fourier transform. However, when Fourier transform is applied to the full time axis, it is unable to determine when a given frequency increases. A sliding window is used in the short-time Fourier transform (STFT) to find a spectrogram that incorporates both time and frequency information. However, there is another problem: the window's length limits frequency resolution. The wavelet transforms looks to be a viable solution to the problem. Small wavelets with low duration are used in wavelet

transformations (WT). The time and frequency resolutions in the time-frequency plane in WT change when doing a multi-resolution analysis.

A signal a0(t) belonging to the integrable square subspace $L^2(R)$ describes the terms of scaling operation $\varphi_{j,k}(t)$ and mother wavelet operation $\omega_{j,k}(t)$ in the wavelet transform (t). j is the dilation or frequency visibility parameter, while k is the location parameter.

$$a0(t) = \sum_{k} x_{j0,k}\, \varphi_{j0,k}(t) + \sum_{j=j0}^{\infty} \sum_{k} y_{j,k}\, \omega_{j,k}(t) \tag{1.9}$$

Here, x and y are the coefficients for $\varphi_{j,k}(t)$ and $\omega_{j,k}(t)$.

1.10 Role of Bio-inspired Algorithms for Denoising

The desired coefficients in the filters are selected and optimised using bio-inspired computation-based methodologies. It is feasible to adapt the filter weights to fit varying picture and noise characteristics using population-based alternative hybrid algorithms. With the ultimate goal of decreasing noise in multidimensional siganls, a bio-inspired metaheuristic optimization strategy was used. The evolutionary algorithms are built on the soft computing notion, which includes concepts like fitness functions, cycles, and probabilistic conditions. Finding the right bio-inspired algorithm for picture denoising,

on the other hand, is a difficult challenge. Machine learning principles are integrated with a bio-inspired algorithm to increase the performance of denoising approaches.

1.11 Motivation

Signal processing is a discipline that is always evolving and improving. Every day, new and novel procedures and processes are produced. Signal processing engineers and scientists may use these approaches to extract useful information from a range of signals. There is no one approach that can help with the analysis of all forms of data in the field of signal denoising. Given the significance of ECG analysis in medical science, there are hundreds of methods for analysing the information and sending signals in numerous ways. However, no single strategy is totally reliable or durable.

1.12 Background and Problem Description

ECG artefacts in surface EMG data have drawn a lot of attention in recent years. ECG artefacts in EMG data must be removed when signal quality is crucial. Since their frequency spectra overlap so significantly, it is extremely challenging to remove ECG artefacts from EMG data. Depending on the kind of muscle and the quantity of fatty tissue, the frequency range of surface EMG impulses is 0 to 400 Hz. ECG impulses have a frequency range of 0 to 200 Hz, with frequencies under 45 Hz providing the most strength [5].

To remove ECG artefacts, researchers used a a hybrid technique, template subtraction, a gating method, spike clipping, artificial neural network (ANN), high-pass filter (HPF), wavelet transform, adaptive neuro-fuzzy inference system (ANFIS), adaptive noise canceller (ANC), wavelet-ICA, and independent component analysis (ICA). Traditional high-pass filters are an easy and quick fix, but they are inefficient for a few software's, including hand motion regulator, since they lose a lot of important information from EMG signals. The QRS complex identification must be exact, and the ECG signals must be stationary for the subtraction technique to work.

Additionally, the use of pre-defined QRS templates is required [6]. The gating approach is arguably the most used way for eliminating ECG signals, however it misses parts of the EMG signal that cover the QRS complexes. Additionally, ANC has recently been employed to eliminate ECG artefacts; but, due to its high computational expense, it is not suited for usage in real-world applications. The wavelet transform is a low-cost online method that does not need a large number of inputs. However, certain artefacts remain in the original signal, thus this method only removes portion of the desired signal. The ICA technique is an online method for processing multi-channel signals that increases hardware complexity. ANN and ANFIS approaches offer the best performance of all of these methods, but their results might be enhanced when combined with other techniques for specific applications [7].

1.13 Scope and Proposes

The goal of this study is to see how adaptive signal processing can help with ECG denoising. The major goal is to learn how adaptive filters function and to investigate how well they perform in biological signal denoising. The following are the major activities to complete this task:

- In this study, the ECG signals from different sources will be used to determine the efficiency of the denoising procedure for high and poor quality ECG data. The ECG signal is taken from a high-resolution record in the Beth Israel Hospital database at the Massachusetts Institute of Technology (MIT-BIH).

- White Gaussian noise will be the noise under study. In ECG recordings, these are the most prevalent sounds. In the case of the ECG signal, simulated and actual noise signals will be investigated, and the denoising performance for simulated and real sounds will be compared.

- The adaptive methods employed in the denoising process should take minimal computing resources and high efficiency into account. For this situation, the Honey Badger Optimization algorithm and African Vulture Optimization algorithm, an adaptive filter with weight technique, will be investigated.

- This method has a cheap computing cost and a high efficiency. It is sometimes referred to as FIR filtering for the same signal and noises, with the goal of recognising the differences between the two approaches.

1.14 Thesis Organization

The proposed thesis can be systematized as follows:

Chapter 1describes the basic introduction of the suggested thesis which describes the importance of ECG signals, retrieving the ECG signals, denoising approaches, wavelet transforms and the role of optimization algorithms in denoising.

Chapter 2 presents the review of literatures, review findings, research gaps and problem formulation of the research work.

Chapter 3 presents an improved Empirical Wavelet Transform with Honey Badger Optimization for ECG signal denoising.

Chapter 4 presents the design of ECG signal denoising utilized discrete wavelet transform with African Vulture Optimization algorithm.

Chapter 6 concludes the thesis by highlighting the research contributions and the future direction for denoising ECG signals.

CHAPTER 2

LITERATURE SURVEY

2.1 Introduction

Despite the fact that digital formats became widespread in the late 1990s, many healthcare organisations still print ECG signals on paper. Digital storage options for ECG signals are becoming more popular as healthcare data become more digitised. This is because of benefits such as increased storage capacity, mobility, and accessibility. The lack of a common digital format is due to the considerable variation in ECG equipment types and the private interests of ECG manufacturers. The American Heart Association and the Common Standards for Quantitative Electrocardiography have made several attempts to standardise ECG forms. To minimise noise in ECG readings, signal processing methods are necessary. This stage is crucial for correctly detecting the waves in the ECG signal, which is crucial for monitoring and diagnosing.

2.2 Adaptive Filtering

Given that all ECG signals are nonlinear, adaptive filtering is the method most frequently employed to reduce signal noise. The author [8] examined the performance of RLS and LMS adaptive techniques and found that RLS-based adaptive filters outperform LMS-based adaptive

filters. To reduce artefacts in ECG, the author [9] devised a set of simple and fast sign-based normalised adaptive filters that outperform multiplier-free update loops in terms of computing efficiency. When comparing the performance of adaptive filters with and without reference noise, the authors [10] found that adaptive filters without reference noise perform better since noise in the primary signal may or may not correlate with the adaptive filter's reference input.

The author [11] developed a framework for a resilient VSSNLMS method based on cost function optimization in the filter update norm with a time-variant constraint. The experts put this to the test in terms of detecting and eliminating echo applications. Another VSSNLMS method for the reduction of echo was proposed by the author [12]. Previously established techniques, according to the authors, dealt with accurate modelling simulations in which the adaptive filter's length equalled the length of the simulated system. In actuality, acoustic echo pathways are quite lengthy; therefore having a filter that is shorter than the path would be advantageous. They used that method in their solution after that. The article [13], provide the mean square performance for a partial update filter. A Normalized Subband Adaptive Filter can enhance the NLMS convergence rate (NSAF).

The authors proposed a block-based multichannel LMS method in [14] if any prior knowledge about the input signal existed. To account for the incomplete acquisition problem where the needed data is non-stationary, a new equation based on block based cross-relation has been

devised. A performance review is part of this contribution. A fractional normalised filtered-error based LMS approach is proposed in [15] for secondary route modelling. A fractional update is combined with the standard LMS integral operator, which is derived from the Riemann-Liouville differ integral operator. By employing zero-mean binary inputs, this method is utilised to reduce noise from the principal path. An anti-noise signal is developed using improved secondary route modelling to reduce noise influence and filter inaccuracy. It is tested using the specified approach for various techniques by altering the step size and fractional orders.

The authors offer a wavelet-based sub-band adaptation filter approach in their study [16] for isolating a scant ECG signal in a busy environment. This fusion methodology keeps a high degree of consistency while sharpening the extraction accuracy.

Widrow and Hoff [17] introduce LMS adaptive approach that is now broadly utilised in a variety of applications, including adaptive noise cancellation, channel equalisation [18], and system identification [19]. The resilience, low computational cost, and ease of hardware implementation of the LMS methodology are the key reasons for its popularity [20]. The following are some of the key features of the LMS algorithm:

- Without performing matrix inversion, the optimum filter solution may be effectively calculated. The autocorrelation and cross correlation matrices are also unnecessary.

- A step-size, is easily chosen to modify the algorithm's convergence speed and stability.

- In tackling several practical adaptive signal processing issues, the approach is resilient and reliable.

The leaky LMS algorithm (LLMS) was created to solve the numerical instability of the filter in the digital version of the LMS algorithm. A leakage prevents overflow in finite-precision by permitting a trade-off between lowering the MSE and minimising the energy in the filter coefficients. This is achieved by incorporating a regularisation term in the cost operation of the LMS algorithm.

When compared to the LMS method with a fixed step-size, the variable step size LMS (VSSLMS) technique was created to achieve the balance necessary for faster convergence time and lower MSE. By choosing a large step size at the start and giving each filter coefficient an independent time-varying step-size, the adaptation process can improve convergence speed. As the VSSLMS algorithm approaches the steady-state solution, the step size decreases, lowering MSE.

Traditional adaptive algorithms, such as LMS and its variations, Kalman filters [21], and RLS are susceptible to strongly correlated inputs, have limited convergence, and consume a lot of power. Furthermore, the adaptive methods outlined above are unable to use a priori knowledge of the system structure, such as sparsity. For the adaptive filtering approach to work well, it may be necessary to use such a priori information.

A parallel lookup table (LUT) updates concurrent filtering, and weight-update functions-based pipelined adaptive filter architecture is suggested by the author [22], which greatly improves performance. Instead of the usual adder-based shift accumulation, conditional signed bring accumulation is utilised for DA-based inner-product calculations to reduce sampling time and area complexity. By using a fast bit clock for carry-save accumulation and a considerably slower bit clock for all other operations, the recommended device uses less energy.

2.3 Wavelet Transform

Mashud Khan et al. [21] suggest a wavelet-based SNR technique in their work. Artefacts evolve in lockstep with the main ECG signal, according to this technique. For multi-scale signal decomposition, the symmlet mother wavelet was utilised, which allows for precise noise estimates and removal with little processing. Bingo W. et al. [6] proposed a few fuzzy criteria for selecting the best post filters, pre and multi

wavelets at different noise levels. Despite better denoising speed, selecting a membership function has remained tricky.

In [24] the author suggested a wavelet-based denoising approach. This method is beneficial in that, unlike adaptive filtering techniques, it does not require an a priori reference. As a wavelet basis function, the discrete Meyer wavelet was used. A novel thresholding function that joins the properties of thresholding soft and hard is also suggested.

In D. Zhang [23] presents a DWT-based technique for removing baseline wander. To minimise high-frequency noise, the shrinkage approach employs E-Bayes posterior median. For decomposition levels up to 6, a Symlet wavelet of order 8 is employed.

The building of statistically matched wavelet filter banks has been thoroughly researched by R. Crandall [26], and has been presented as a constrained optimization issue. To examine the coding gain performance of matched filter banks built using the KLT's Vis-&-Vis approach, the parametric study must be broadened. Let h stand for the filter coefficients in a 2M-dimensional vector and Rxx stand for the covariance matrix of a process. The matching wavelet that maximises energy compaction may be formulated using the goal function.

According to Major Joseph O. Chapa [27], the bulk of orthonormal multi-resolution analyses (OMRA) applications utilise

Daubechies, Meyer, or Lemarie's wavelets. The wavelet matching the target signal, though, would be amazing. This paper first presents a way for generating the scaling function from the wavelet, and then it gives the wavelet the specifications that assure an OMRA, in order to generate an OMRA using a wavelet that has been least squares matched to a signal of interest.

A wavelet-based method for removing structured noise from data, such as impulsive spikes or unwanted harmonic components, was introduced by Phillip L. Ainsleigh [28]. Wavelets' time- and frequency-localization skills allow for better noise identification and signal distortion than direct data filtering for this type of noise. This method is used to analyse data from multipath interference transfer functions and impulsive noise time series.

Morlet introduced the Wavelet transform in early 1980 to assess seismic data, according to E. Farahabadi et al. [29]. The test signal or signal to be studied is divided into multiple sub-bands with different scales, and we simply compare or correlate the signal with shifted and scale wavelet. Since it is compatible with multi-resolution investigations and localization in time and frequency domain.

2.4 Meliorating ECG Image

The primary work of this research is to enhance the quality of ECG signals and reduce artefacts. A thorough review of the literature

was carried out to discover the many approaches to improving the ECG signal using adaptive linear filters and other traditional techniques [30]. To discover the variances in the input data samples, Thakor et al., 1991, created an ANC structure that functions as an LMS adaption method.

Because of its capacity to capture pulse fluctuations quickly, this design is appropriate for ambulatory ECGs [31].The LMS's reference signal is an important requirement for improving the ECG signal. The reference signal is a deterministic orthonormal features-based function. The LMS algorithm's core function is based on estimating the tap weights for each iteration when a new sample comes. However, according to a research, the LMS algorithm's convergence characteristics limit the tap weight estimate to achieve the wiener solution converge [32].

As a result, Block LMS (BLMS), an adaptation algorithm [33], was devised to solve the constraint. On the occurrence of the block gradient, the adaptive filter coefficients are calculated. BLMS is commonly used for stochastic systems with stationary signals. With the help of ANCs, this work may be completed.

The author of [34] created a strategy for eliminating the Motion Artifact [MA] which hybridizes the LMS and the Normalized LMS (NLMS) methodologies. The suggested approach eliminates the artefacts while maintaining the ECG signal. In [35], the author developed a VLMS technique for real-time remote healthcare applications. In the

literature, several strategies for enhancing the efficiency of the LMS algorithm have been offered.

To negate the Baseline Wander (BW), Sayadi et al., introduced a bionic wavelet transform [36]. Montazeri et al. suggested a novel approach for obtaining the foetal ECG from the mother's ECG [37]. Using Principal Component Analysis (PCA), Langley et al., presented a technique to improve the ECG signal [38]. When compared to traditional filters, the adaptive filter is the most effective in cancelling the maternal ECG. They also confirmed that the recommended method yields superior outcomes. This approach has a significant computational complexity problem, which is a critical characteristic in biological signal processing applications. The number of LMS algorithms reported in the literature is significant, but there is little emphasis on reducing computing complexity, which is an important parameter in healthcare applications. To overcome the computational complexity difficulties, sign algorithms are integrated with the LMS method in this thesis. Adaptive algorithms in real-time applications such as continuous ECG monitoring must have a fast convergence speed while being computationally simple.

Rahman et al. developed an efficient ANC to lower the adaptive filter's computing cost [39]. The sign method has the benefit of requiring fewer computations, which is enabled via the signum function. Three types of sign algorithms have been documented in the literature: the Sign Sign Approach (SSA), the Sign Approach(SA), and the Sign

Regressor (SR) approach. In comparison to the previous LMS algorithm, all of the sign methods need half multiplications.

2.5 Different types of Noises in denoising

Noise estimation is the most important method in image processing approaches. This suggests that noise level estimation has an impact on the picture denoising approach's output. Asem Khmag et al [40] suggested an automated noise computation approach for AWGN (additive white Gaussian noise) based on local statistics. Even if the original image noise level is known, current denoising algorithms cannot provide outstanding results for photos with intricate details. The noise level is calculated using a blind picture denoising technique using a patch-based estimate approach. This approach chooses an image with a low rank and eliminates high frequency sections from the damaged image. The noise levels of the chosen sections are also calculated by Principal Component Analysis (PCA). This denoising approach is used with undecimated wavelet-based denoising methods and PCA in the case of blind denoising to obtain the picture's features. The findings demonstrate that this technique performs well even in circumstances with additive noise. When paired with other noise estimating techniques, this method produces better performance, higher-quality images, and saves time.

Cho, D& Bui [13] proposed a universal estimate technique in the wavelet domain based on multivariate statistical theory to produce

denoised coefficients from a noisy image. Photographic effects such as Poisson, speckle, salt & pepper, and Gaussian noise are all frequent. Random variations in the picture pixels occurred in images of various circumstances and quality. The primary goal of the researchers was to erase these blemishes from the digital image. A parametric multivariate generalised Gaussian distribution (MGGD) model was used to precisely mimic the sample distribution. In addition, research was undertaken among Daubechies wavelets employing wavelets image denoising techniques and satellite images in order to obtain adequate findings. The PSNR measure was utilised to estimate the image denoising procedure's implementation.

After several years of research, the discipline of picture denoising was well-established. Many practical problems in disciplines like geometric modelling, computer vision, medical imaging, and computer graphics still use pictures in irregular domain collections like graphs. Poisson–Gaussian mixed and Poisson noise reduction of pictures on graphs was studied by Wang and Yang [12]. Based on the observed characteristics of noisy images, a wavelet frame-based variation model for picture restoration was developed. Consider a -regularized term and a weighted fidelity term for the corresponding model, which allows for the usage of tight wavelet frame conversion on maps to safeguard essential characteristics like image edges and textures.

The images were damaged due to impulse and Gaussian disturbances, thus a cascade step technique was used to denoise them. Ali

Awad [10] developed an approach based on the early elimination of aberrant values, which would aid in the later removal of noisy tiny components. The first phase used the intensity difference approach, whereas the succeeding phases used principal component analysis. In the following step, the smallest noisy components were deleted, followed by the smallest ones that represented the remaining noise in succeeding stages. Finally, the restored picture acquired by that approach performs better in PSNR and has high visual quality.

Ashek Ahmmed [14] proposed the additive noise corrupted digital picture denoising technique. The filter bank of dyadic Gabor, which decomposes the noisy picture into distinct scales Gabor coefficients, provided the information of localised frequency. Denoising was done in the transform domain using Gabor coefficient thresholding using phase preserve and non-phase preserve thresholds. The Bayes Shrink thresholding was used in the non-phase preserve technique. Finally, every channel Gabor coefficient threshold had generated a denoised picture. For smoothly moving pictures, it was discovered that the modified Bayes Shrink approach outperforms both Bayes Shrink and phase preserve methods and works best for high-contrast images.

2.6 Noise Detection Methodologies

Mitra et al. [9] presented a narrative approach to reduce intravascular ultrasonography (IVUS) in speckle noise. Because of the known impedances of the reflected ultrasound from dissipates, IVUS,

which is a conventional coronary course that analyses the imaging convention, is degraded by speckle noise. The presence of such noise has an impact on the categorization and division of these images. The non-neighborhood channel has been proposed and implemented in wavelet space to trim noise obstacles and improve visual IVUS comprehension features. Finally, a correlation study was carried out using various channels, including anisotropic dispersion, nonlinear middle channel, and mathematical nonlinear dissemination channel.

A de-dotting strategy based on wavelet change and rapid two-sided channel is offered for enhancing ultrasound clinical imaging. Based on the real characteristics of the ultrasonic clinical picture in the wavelet area, Ju Zhang et al. [8] produced an improved edge work wavelet based on the general edge work wavelet. The sum of Gaussian conveyance and Laplace dispersion, respectively, is used to describe the coefficients of the wavelet without the sign of the noise and the speckle noise. To derive another shrinkage computation for the wavelet, the bayesian greatest posteriori evaluation is modified.

In the wavelet field, Jing Tian et al [17] investigate the topic of image despeckling. By combining a non-parametric measurable model into a Bayesian derivation system, a most extreme a posteriori (MAP) evaluation based picture despeckling technique is provided. The suggested non-parametric model describes the wavelet coefficients' insignificant circulation.

Sameera V Mohd Sagheer et al [28] suggested a method in which the image's recurrence sections are obtained using wavelet decay, and then the bayesian structure is integrated to assess the noise in the high recurrence segments. By going via a dedicated guided channel, low-recurrence noise portions are de-speckled. The suggested scheme was compared to several recent research, such as Bayesian non-nearby techniques channel (OBNLM), wavelet evaluation based on rapid reciprocal filtering, and non-parametric model.

Yongjian Yu et al [29] discuss the induction of speckle lessening anisotropic dispersion (SRAD), a dissemination strategy optimised to radar imaging and ultrasonic applications. The edge-sensitive dispersion in images with additional material noise is known as regular anisotropic dissemination, whereas the edge-sensitive dispersion in images with speckles is known as SRAD. At first, the Frost and Lee channels may serve as halfway differential conditions, and then we deduce SRAD by permitting edge-touchy anisotropic propagation inside this uncommon circumstance.

Sara Parrilli et al. [30] projected a fresh approach to despeckling manufactured opening radar (SAR) images based on wavelet-area shrinkage and nonlocal separation concepts. It appears to be the design of square coordinating three-dimensional computation, which was recently presented for additional substance white Gaussian noise denoising, but it changes its major handling stages to account for the peculiarities of images in the SAR. When the wavelet shrinkage is made

utilising the additional substance signal-subordinate noise technique and finding the ideal nearby direct least mean-square-blunder assessor in the wavelet space, a measure for probabilistic similarity is used for coordinating the square.

Jong-Sen Lee [31] uses neighbourhood mean and difference to construct computational methods such as contrast improvement and noise filtering on two-dimensional photo clusters. These computations are nonrecursive and do not need the use of any changes. They have comparable characteristics in that each pixel is treated independently. As a result, when used in continuous sophisticated picture handling applications and when an equivalent processor may be used, this technology has a noticeable amount of leeway. Every pixel's previous mean and fluctuation are derived from its surrounding mean and difference in both the added substance and multiplicative situations. The noise sifting computations are then obtained using the basic mean-square mistake assessor in its simplest configuration.

Victor S. Ice and colleagues [32] in this study, a model for the radar imaging measure is developed, as well as a strategy for smoothing noisy radar images. The radar image is polluted by multiplicative noise, according to the imaging model. For smoothing radar images, the model suggests the utilitarian kind of an ideal (least MSE) channel. The channel is made flexible by using privately evaluated border esteems to provide the lowest MSE gauges inside homogenous zones of an image while maintaining the edge structure.

2.7 Wavelet Based Denoising

For image segmentation, K.P. Baby et al [33] suggested a multi-level thresholding approach based on the Krill Herd Optimization (KHO) algorithm. To find the best threshold value, the Krill Herd Optimization primary function of Kapur'sor Otsu's was maximised. The development of an ideal threshold for multi-level thresholding lowered the computational time of the suggested technique. Different benchmark pictures were used to illustrate the computing competency of the KHO-based multi-level thresholding. Bacterial Foraging (BF) , Moth-Flame Optimization (MFO), Particle Swarm Optimization (PSO), and Genetic Algorithm (GA) were used to compare the suggested method to current multi-level thresholding strategies, and the outcomes illustrates that the recommended strategy performed better.

The wavelet approach is a useful technique for recovering infinite-dimensional objects such as images, densities, and curves. Wavelet techniques were utilised to effectively reduce noise because they have a high capacity to achieve signal energy at certain energy transformation values. It was also dependent on the wavelet coefficients are being shrunk in wavelet area. Mitiche et al [34] introduced a denoising approach based on shrinkage and DT-CWT. DTCWT was used to denoise the medical pictures utilising soft and hard thresholding approaches. The denoised picture findings demonstrated superior accuracy and smoothness stability than the SWT and DWT. SSIM

(Structural Similarity Index Measure) and PSNR were used as comparative measurements.

The Poisson process was used to produce photon shot noise, which is the most prevalent cause of noise in optical microscope images. The DWT, on the other hand, has several flaws, such as aliasing, lack of directional selectivity, and shift variance. Ufuk Bala [35] used the DT-CWT in denoising method to overcome these issues. The denoising strategy was founded on the notion that, in the presence of Poisson noise, approximation coefficients may be used to forecast threshold values for wavelet coefficients. Other denoising algorithms were compared to the proposed method. As a result, in image quality measures, the recommended strategy produced improved results. The effects of the suggested technique's contrast enhancement on collagen fiber images were also investigated. This technique also allows for the rapid and effective development of images captured in low-light situations.

A unique adaptive singular value decomposition (ASVD) and dual-tree complex wavelet transform-based Partial Discharge (PD) signal denoising approach was suggested by Mohsen et al (DTCWT). ADTCWT was used to denoise from PD signals in accordance with PD signal and noise on the basis of choosing the best singular values on DTCWT-level decomposition. The major processes in denoising in power transformers were PD signal examination and diagnosis. Experimental sets and simulations were used to estimate the new adaptive DTCWT (ADTCWT) method. Different criteria were used to

compare the ADTCWT algorithm against the DT-CWT and ASVD approaches for noise reduction.

Daubechies wavelet is the most frequent and widely utilised ortho-normal wavelet. The mother wavelet was selected to be the Daubechies wavelet. These wavelets are compactly supported and orthogonal, therefore there will be no overlaps during signal restoration. Daubechies was chosen because of its precise answer and low error rate. To improve picture seeing, C Vimala and P Aruna Priya [37] researched the Double Density DTDWT in image denoising. The photos were used in the study, and the results were compared to the Double Density DWT and the discrete wavelet transform. For denoised pictures, the Root Mean Square Error and PSNR values were calculated using all three wavelet approaches. It achieved superior results when compared to previous wavelet approaches.

C. Vimala and P. ArunaPriya [38] presented DT-DWT based intelligent approaches for picture denoising. The existence of noise in an image causes misinformation, hence picture quality augmentation was an essential problem for proper image diagnostics. To simulate true artefacts deterioration, these photos were distorted by various noise levels. As a consequence, the recommended system has a high PSNR when compared to the effective strategies.

2.8 Various Filer Methodologies

2.8.1 Bilateral Filer

Image denoising has gained prominence in the realm of medical imaging (MI). Maintaining data-bearing structures like edges and surfaces while increasing PSNR to improve visual quality is the major challenge in image denoising. A technique to bilateral filtering based on optimization was created by Elhoseny and Shankar [39] for MI denoising. Swarm-based optimization of the Dragonfly (DF) and Modified Firefly (MFF) algorithms is utilised to pick these parameters. The settings were chosen using PSNR and vector root mean square error, two multi-objective fitness functions (VRMSE). The CNN classifier is also used to categorise denoised images as abnormal or normal.

Yang et al. [40] demonstrated edge-preserving denoising utilizing twin support vector machines on non-sub sampled shearlet transform (NSST). It is a spatially adaptive non sub sampled transform based on the Bayesian approach for the application of natural picture denoising. Optimal approximation, directional selectivity, and approximate shift variance are among the functions included. It breaks down the noisy picture into sub-bands. Geometric regularity is used to create the feature vector for each pixel in the noisy picture. To train Twin Support Vector Machines, the detailed coefficients of NSST are separated into information relevant coefficients (TSVM). Finally, the

adaptive threshold is used to get the denoised image. The results are compared using distinct strategies on various images.

Speckle noise degrades the low-resolution pictures produced by ultrasonic imaging. For medical applications, picture quality enhancing techniques are therefore required. Rodrigues et al. [21] introduced a quick bilateral filter based on S-median thresholding for speckle noise reduction and picture quality enhancement. S-median thresholding results are compared to those of other thresholding approaches. PSNR has improved by 14.13 percent, structural characteristics have improved by 4.96 percent, and contour preservation has improved by 0.70 percent, respectively. This method reduces speckle noise while preserving contour information and spatial domain properties.

For prioritising infrared images, reducing image noise, and preserving image features related to a shelter room, Zhang [22] proposed combining bilateral denoising with 2D-DWT. The wavelet transform is applied to decompose the image without affecting the low frequency components. With the use of a bilateral filter, the image is rebuilt, keeping three high frequency components. The combination of wavelet transforms and bilateral filters produced improved denoising results with acceptable visual quality, making it appropriate for use in coal mine emergency shelters. However, as compared to edge-preserving smoothing, the fundamental drawback of bilateral filtering is its high computational cost.

Because speckle noise is multiplicative, SAR picture analysis is difficult. As a consequence, Choi and Jeong [13] developed the Speckle Reducing Anisotropic Diffusion technique for removing speckle noise (SRAD). It uses a guided filter for to decrease speckle noise and preserve edge information. To remove the multiplicative noise, the image is filtered. A logarithmic transformation is used to convert the multiplication noise into additive noise. DWT is then used to split the picture into several resolution images. To demonstrate the superior outcomes, the subjective and objective performances are compared to current algorithms.

2.8.2 Weiner Filer

Tayade and Bhosale [4] offer a DT-CWT and Wiener filter-based denoising technique. In medical image denoising, the Wavelet Transform is a mathematical operation framework. Wavelet algorithms are ideal for removing noise because they can collect signal energy at low energy transformation values. On further examination, the image enhancement technique performed by DTCWT is used to produce multiple frequency bands. In this procedure, the attributes of precision and smoothness are balanced. The following performance, as assessed by PSNR and SSIM, regulates the quality of the denoised image.

For noisy image suppression, Long kumer and Gupta [5] introduced the DWT approach. It takes advantage of both the Weiner filter's approximation coefficient and soft thresholding approaches. The

noisy pictures are created by feeding the Weiner filter salt and pepper noise as well as Gaussian noise. Finally, the noisy images are denoised using a thresholding-based coefficient model. The method's performance is measured using metrics such as MSE and PSNR.

Wavelet coefficient reduction techniques will remove noise from distorted images in the wavelet area. Mitiche et al [6] introduce one of the wiener filter-based DTCWT techniques. To denoise medical pictures, it uses either a hard or a soft thresholding approach. In comparison to DWT and SWT, the Wiener filter-based techniques seamlessly balance the accuracy. PSNR and SSIM are used to assess the quality of denoised images.

2.8.3 Median Filer

For the purpose of eliminating salt and pepper artefacts, Erkan et al. [7] suggested employing an Iterative Mean Filter (IMF). The surrounding pixel values are taken into account in IMF to identify noise and remove high density noise. However, a broad window affects the precision of noise reduction. As a result, while picture filtering, new grey values are applied to the core pixels. Finally, image enhancement is performed to provide a better denoising picture. In comparison to other filter approaches, the testing findings suggest that it produces high-quality reformed pictures. The effect of a median filter, on the other hand, is harder to analyse.

Chen et al. [8] designed a novel approach for avoiding blur and edge loss in medical applications by integrating both DWT and median filters. Image capture, storage, processing, and reconstruction are the four elements of this denoising operation. The captured pictures are made up of impulse and Gaussian noise, with the original images being saved for parameter and data preservation. Wavelet decomposition is used in the image processing module to divide the medical picture into four sub bands. Improved wavelet thresholds handle the high frequency coefficient. After wavelet threshold processing, median filtering is applied to three high frequency sub bands. The final image is rebuilt, with the benefits of this method including the use of multiple median filters. Medical images with excellent accuracy were generated using changed filter coefficients. The results are compared to those of the contourlet, wavelet, and DTCWT schemas.

2.8.4 Fuzzy Filer

In fuzzy modelling methodologies, the disadvantages of the pixel domain are taken into account. By using a fuzzy smoothing process, the zero-order Takagi–Sugeno fuzzy model was able to reduce additive noise. Zhang et al. [19] suggested an adaptive fuzzy filtering approach for determining fuzzy model parameters for noisy picture data. Both stochastic and deterministic mathematical analyses are available. The filtering model's robustness is assessed in order to calculate upper bound magnitude estimate errors. The fuzzy-filtering algorithm does not need the inference of Gaussian noise.

2.8.5 Whitening Filer

In underwater applications, image denoising is an important and improving method. Underwater exploration is being researched for territorial defence and marine scientific purposes. In underwater acquired mages, the noise energy spectrum density does not fit inside a specific range. Abdul wahed and Kamil [10] investigated many basic functionalities of a DWT-based image denoising approach. For denoising images with a whitening filter, the properties of coloured noise are converted to white noise. Erkan et al. [7] suggested using an Iterative Mean Filter to remove salt and pepper artefacts (IMF). The symlet, bi-orthogonal, and Debauchiese wavelet bases recommended the denoising method to use the pre-whitening filter for creating conspicuous images.

2.9 Thresholding techniques

Erkan et al. [7] suggested using an Iterative Mean Filter to remove salt and pepper artefacts (IMF).However, the SURE-LET method uses point wise thresholding, which ignores the wavelet transform's intrascale information. As a result, the local wiener filter, as described in Zhang, is designed to combine the point-wise thresholding function with the SURE-LET approach. Wavelet transformations are compared subjectively and objectively to the performance of a hybridised thresholding-based denoising technique.

Bhandari et al. used evolutionary algorithms to compare the increasing sub-band adaptive thresholding function for various wavelet filters to denoise satellite pictures. Adaptive thresholding parameters are obtained using the Cuckoo Search (CS) method, PSO, and ABC. The quantitative and visual findings based on Meyer wavelet filter demonstrated the greater flexibility and efficiency of the CS method. For satellite pictures, the Meyer wavelet-based CS algorithm's denoising method provided the best results in terms of PSNR, SNR, and MSE.

Based on linear Bayesian maximum a posteriori (MAP) estimation, Sun et al. [28] suggested a sparse representation model for image denoising. A linear Bayesian MAP evaluator is built to obtain the most probable one behind the annotations after producing a pre-probability distribution in the demonstration vector. This is excellent for resolving typical image inversion issues. Furthermore, to address the picture denoising issue, a closed form solution with a few feasible approximations is constructed. All feasible patches are extracted and sorted into several sub groups using structural patterns in this novel technique. To estimate the MAP parameters, the K-SVD technique is used to train several dictionaries.

The current media communication field's evolution, as well as the demand for high-quality visual information, has prompted the creation of several picture denoising algorithms based on DWT. Gaussian noise clearly distorts visual information communicated in image form. This is a common problem in image processing. Translation

invariant and wavelet thresholding together can reduce random noise using wavelet denoising technique due to their capacity to acquire signal energy at particular energy transformation levels. For image denoising, Hassan and Saparon proposed a wavelet threshold and image denoising translation invariant technique. The outcomes revealed improved visual performance and PSNR.

Adaptive thresholding and k-means clustering-based picture denoising methods were reported by Yahya et al.. It's a hybrid of block-matching hard-thresholding and 3D filtering (BM3D). In the heavy and mild noise areas, gentle and strong thresholding are used, respectively. Adaptive thresholding is used to achieve optimum noise reduction and high spatial frequency detail. Because of the capacity of k-means clustering to locate meaningful candidate-blocks, this clustering is acceptable in the final evaluation. It separates the denoised image into many sections and locates the boundaries between them. By using k-means clustering, the reference blocks help to decrease bad matching. PSNR and SSIM's performance is compared to that of reference methods.

2.10 Wavelet Coefficient based Denoising Methodologies

In DWT, the multi-resolution topology may be used to investigate multiple frequencies at different resolutions. Yan et al. used non-local dictionary learning decomposition levels to apply wavelet sparsity and multi-resolution structure to noisy images. Additionally, hard and universal thresholds are used to determine the best threshold

value. The proposed strategy produced higher compression ratio, lower MSE, and improved PSNR.

The shearlet transform is used for pre-processing, and the kernel smoother is used with variable texture and feature attributes. The image filtering with shearlet transform is the first stage in this two-step technique. The filter weight coefficients of Yaroslavsky are estimated in the second stage. Simulations on 2D pictures distorted by additive white Gaussian noise are used to verify the theoretical conclusions. The pseudo-Gibbs and shearlet-like artefacts were effectively suppressed using this strategy.

Speckle noise is a typical occurrence in ultrasound pictures used in clinical diagnosis in the medical field. This makes it challenging to automatically diagnose ailments from ultrasound images. A speckle noise reduction strategy based on wavelet coefficients was proposed by Sahu et al. To create noise-free coefficients, the Bayesian technique is utilised. The wavelet and noisy coefficients are defined, respectively, by the Gaussian Probability Density Function (PDF) and the Cauchy prior. The Maximum A Priori estimator is then used to produce the noise-free wavelet coefficients (MAP). The appropriate variance of the impacted wavelet coefficients is evaluated using the Median Absolute Deviation (MAD) evaluator. PSNR (21.48 percent), SSIM (1.82 percent), Edge Preserving Index (EPI) (7.68 percent), and Correlation coefficient (ρ) (1 percent) had better experimental outcomes than the other approaches.

With the aid of a multi-scale product rule, wavelet thresholding and adaptive wavelet thresholding are used to maintain edge features and decrease blur. Vijay et al. created an improved wavelet threshold function. This function denoizes the wavelet coefficients for dissecting detail in a picture with Gaussian noise. The wavelet distortion is calculated using the reconstructed image's approximation coefficients. The results show that the advanced threshold function has a higher influence on denoising than hard and soft thresholds. The threshold for different layers of wavelet will be changed when denoising. The approach that is advised combines the wavelet enhanced threshold with the benefits of the median filter.

2.11 Machine Learning Denoising Methodologies

Sensor noise in aircraft images degrades image quality, which has ramifications in satellite photography applications. As a result, deep learning techniques are used to eliminate noise from satellite data. The supervised learning is the deep learning technique that denoises data the most. It needs tough-to-obtain noisy and artefacts free picture pairings, which are challenging to get in real time. For satellite imaging, Song et al. developed a wavelet sub band cycle consistent adversarial network (WavCycleGAN) based denoising approach. To compensate for the lack of balancing data, the proposed unsupervised learning strategy employs cycle consistency loss and adversarial effect loss. In order to properly show high-frequency components as margins and comprehensive information, the wavelet-subband domain learning programme is also

offered. The efficiency of the noise reduction approach is demonstrated by the vertical stripe removal and wave noises of satellite sensor image findings.

Stripe noise degrades the quality of infrared imaging systems. As a result, noise reduction is carried out via destroying algorithms, which struggle to maintain balance. To address this problem, a wavelet-deep neural network with a transform domain was suggested by Guan et al. [12]. To correctly estimate the noise with the lowest predicted load, it completely considers the inherent qualities of complementary information among the stripe noise and the coefficients of different frequency sub bands. In addition, directional regularisation is employed to extract scene features of stripe noise and to retrieve many other details properly. In terms of quantity and quality estimations, extensive testing of simulated and real-world data indicated that the suggested technique surpasses various established de-striping methods.

Su et al. [15] suggested a deep learning and mapping (DLM) system for detecting changes in ternary tasks in imbalanced pictures. It is based on a deep learning method that uses feature extraction from two pictures and two networks. On both photos, the auto-encoder is employed as a feature extractor for stacked denoising at first. The mapping functions are derived from the utilised stack mapping network after sample selection to build links between each class and the features. Finally, a comparison is done between the features and the clustered final trinity map.

Deep learning and model-based optimization algorithms are used to handle picture noise concerns. However, model-based optimization takes longer, and while deep learning is quicker, Convolution Neural Network (CNN) performance is subpar. Liu et al. [18] suggested a deep residual learning model that incorporates both multi-scale and dilated residual convolution groups to avoid the discussed effects. The use of a multi-scale convolution group reveals the patterns and field receptive expansion. To keep the denoising performance and enhance the training process, batch normalisation and residual connection are also used. After that, the hybrid dilated convolution is used to reduce gridding artefacts. Finally, the denoising performance produces enhanced outcomes.

Ding et al. [20] suggested a convolution nerve-based image mixing noise reduction technique. The traditional filter desiccation algorithm can only remove one noise and is hence ineffective. As a result, this method achieves picture super-resolution in order to create a de-convolution layer that expands the image. Magnification factor is one of the de-convolution processes that eliminate image interference and noise. The de-convolution layer's magnifying impact is terrible. The algorithm showed good noise reduction results in the experiments, making it ideal for various noisy images. It can also help with image indexing and visual effects.

Blind and Universal Image denoising is a unique model that can denoise images with any amount of noise. For additive Gaussian

noise reduction, El Helou and Süsstrunk [17] suggested using a deep learning image denoiser. It is based on a blind and universal picture that is logically founded. The network under consideration is based on fusion denoising, an optimum denoising method. It is theoretically derived from a Gaussian image assumption. Synthetic trials revealed an additive noise level that obscured the networks' generalisation power. The genuine images are denoised using the fusion denoising network. This strategy increased the PSNR results, which in turn improved the colour image performance.

2.12 Bio-inspired Algorithms for Denoising

Threshold optimum for wavelet image denoising was given by Zhao et al. [23] Wavelet conversion to a unique signal and wavelet selection were completed first. The GA technique was used to find the best threshold after wavelet decomposition of each level. To get final signals, the coefficients were quantized in high level at each level and the end inverse transition was applied to the coefficients. In order to utilise the best image threshold, a genetic algorithm was devised. The suggested strategy quickly obtained the appropriate threshold and shown good competence in a comparison of threshold techniques.

For satellite image denoising in the wavelet transform, Noorbakhsh Amiri et al proposed a population-based Harris Hawks Optimization Technique (CMDHHO). Noise suppression techniques based on CMDHHO and TNN were compared to the de-noising

outcomes. This technology is computationally efficient and improves processing quality and quantity while speeding up the process. Optimized noise suppression outperforms TNN-based picture de-noising in the lab. Finally, the PSNR and SSIM data were compared using several de - noising techniques.

Jonatas et al [34] suggested a hybrid genetic method for picture denoising (HGA). The sounds deformed the digital photos, which were then repaired without losing the texture, corners, or edges. HGA stands for a denoising approach combined with a genetic algorithm. As local search and mutation operators, this strategy employs various complex denoising algorithms and filtration strategies during evolution. Gaussian noise of various level combinations corrupted a collection of digital communities often the scientific community utilized it as a standard. During the studies, a fresh set of Satellite Aperture Radar (SAR) pictures warped by increased speckle noise were employed. The suggested method was then compared to many other approaches, and the findings were presented.

Jeevitha and Amutha [33] use discrete wavelet transforms to build a block-based scrambling technique (DWT). The corners of the original image are extracted using this procedure. This approach comprises three phases: decomposing the DWT-plane, generating edge map sequences, and scrambling the DWT-level. The first phase is decomposing the images into various DWT-planes. The deriche edge detector technique was used in the second step to examine the corner

maps. To divide neighbouring pixels into various rows and columns, DWT-level scrambling was utilised. The tight association between neighbouring pixels deteriorates in this way. This strategy reduces time while also improving pixel correlation.

To eliminate noise from satellite images, Asokan and Anitha offer a mix of bilateral filter and nature-inspired optimization techniques. The Gaussian noise in the satellite picture is removed using an Adaptive Cuckoo Search (ACS) technique with a bilateral filter to denoise the image. Other typical ways blur the edges of satellite photos, but our method does not. By removing Gaussian noise from the picture, it protects the corners and other crucial information connected to satellite images. It was quicker and less complicated than previous ways. The algorithm's limitation was that it couldn't completely eliminate the noise, so it suppressed it inside the image.

Pan et al. [37] developed a unique pre-trained convolutional neural network for image denoising. This suggested article divides the synthetic aperture radar (SAR) pictures into LF bands and HF bands. In addition to additive white Gaussian noise, the Multi-channel Logarithm with Gaussian Denoising (MuLoG) structure featured a pre-trained fast and scalable denoising convolutional neural network (FFDNet) (AWGN). This approach removes unnecessary noise from both single channel and multiple channel SAR videos.

The stationary bionic wavelet transforms (SBWT) and the 1-D double-density complex DWT algorithms are suggested by Talbi [40] as a denoising technique for the EKG (ECG). SBWT, which provides the coefficients ce1 and ce2, initially reduced the artefacts in the ECG data. The coefficient ce1 stands for stationary Bionic, whereas ce2 stands for approximation one. The coefficients ce1 can remove white artefacts from the ECG data using the soft thresholding procedure. The ce2 coefficients can be denoised using the 1-D double-density complex DWT denoising approach. The ECG signals were taken from the MIT-BIT dataset, which includes ECG signals with additive Gaussian white noise and various SNR values.

Bhargava and Sivakumar [39] suggest a non-local approach of packing multi patches based on directionality and multi-scale decomposition for eliminating noise from non-subsampled contourlet images. The Guided filter with picture statistics is also used in the local framework to decrease noise, such as edges, texturing, and other artefacts. A non-local strategy of packing multi patches filters is used to address low frequency sounds in the base subband and edges with moderate textural components in the detail scale. Image statistics are also employed in a guided filter to improve the visual impression of a denoised image.

For robust denoising, Papageorgiou et al. used a greedy technique. For the estimate and modelling of outliers, the authors devised sparse modelling. The bulk of the outliers were successfully discovered

using this greedy strategy. For recovering denoised images from noisy photographs, including anonymous noise patterns, Zhu et al.[23] developed a novel blind image denoising technique. It's a learning-based method for recovering a clean image from a noisy image containing different types of noise. Jia et al. suggested a novel TV-Stokes model with a beautiful geometrical structure for picture deblurring. It kept an image's textures, edges, and other information. Even in very blurred and highly noised images, it produced better results.

By incorporating super pixel segmentation into low rank representation, Fan et al. presented a unique denoising approach. It eliminates outliers and different sorts of noise from hyper-spectral images' spatial information in order to generate homogenous zones. Shahdoosti et al. [32] proposed using a hidden Markov tree to denoise noisy pictures using a combination of one-sided exponential densities. To avoid pseudo-Gibbs occurrences, this approach employs a dual contourlet transform. To minimise picture noise, it consisted of one Gaussian distribution and two one-sided exponential distributions.

Chandra et al. [30] conceived and implemented an enhanced high-speed adaptive filter-based denoising architecture on the Xilinx FPGA tool. It outperforms the existing wavelet based technique and adaptive filter architectures. It is required to decrease the distortions generated by multiple sources of noise in the case of an ECG. Vargas and Veiga (2020) [27] presented a denoising approach by genetic algorithm minimization of a new noise dissimilarity estimate as a new ECG

denoising approach (GAMNVE). In the noisy ECG signal, the GAMNVE approach uses the DWT and processes the wavelet coefficients by reducing a new noise variance estimate. The genetic algorithm was used to achieve this reduction. On the other hand, individual variances make ECG denoising problematic, mainly for DCG.

As a result, Hao et al., [35] developed a multi-lead model-based denoising scheme in which an inherently tailored guided filter is used for denoising. A patient-specific statistical prototype is made for each individual using a sparse auto-encoder (SAE), which can efficiently maintain complete signal properties. As a result, the statistical model's directed signal can operate well in the guided filter. The suggested technique can handle ECG readings with irregular heartbeats and hence increase disease identification accuracy.

WT-based filter bank design for ECG denoising was implemented by Kumar et al., [24]. In comparison to earlier built architectures, the introduced strategy only has three low-pass filters and one high-pass filter. A multi-lead model has been suggested by Hao et al., [33], in which to denoise ECG data a guided filter is essentially fitted. A sparse auto-encoder (SAE), which can effectively maintain particular signal attributes, will be used. As a result, the statistical model's directed signal can accomplish well in the guided filter.

Georgieva-Tsaneva [27] reviews the WT-based denoising method and provides an effectual algorithm for denoising in non-

stationary signals that uses an adaptive threshold scheme, detailed and approximate coefficients processing, and the level of decomposition. The denoising procedures allow specifying the decomposition level, wavelet basis, and testing signal size, as well as calculating the denoising process assessment features.

The Adaptive Dual Threshold Filter (ADTF) was suggested by Jenkal et al. [38] for the denoising of ECG data. The suggested design is not excessively complex and just utilises a small amount of resources. Wavelet denoising is one of the most used denoising methods for ECG data. The feeble a characteristic of ECG signals may, however, are diminished during the noise filtering process because of the frequency overlap between the EMG and the ECG.

A modified wavelet design approach is presented by Wang et al. [19] and used for ECG signal denoising. The wavelet is constructed using the optimal filter coefficients, which are derived by predicting the amplitude-frequency response of the ideal filter.

The Kalman filter-based novel Bayesian structure presented by Hesar and Mohebbi [8] may be used to different ECG morphologies without requiring the use of an existing scheme. For denoising the QRS complex as well as the P and T waves, it uses a filter bank with two adaptive Kalman filters. These filters' parameters are continually estimated and updated using the expectation-maximization (EM) technique. And also Manju and Sneha proposed two filters to remove the

noises by Wiener filter and the Kalman filter. The simulation results suggest that the Wiener filter is an excellent filter for denoising the ECG data. However, ECG analysis is a time-consuming operation that necessitates a significant amount of computational power due to the vast amount of data that is essentially evaluated in parallel at high frequencies.

Mejhoudi et al. [15] evaluate the Adaptive Dual Threshold Filter (ADTF) approach for ECG signal denoising as a result using a number of embedded architectures. This technique was used to the MIT-BIH Arrhythmia dataset with a 360 Hz sampling rate in order to validate the assessment.

Swarm intelligence approaches are used in the biomedical signal processing sector by Yadav et al., [12] in the optimization of adaptive noise cancellers. The PSO, SOS, and harmony search (HS) optimization was used to evaluate and update the adaptive filter parameters.

Heart rate signals obtained utilizing non-contact radar systems for use in assisted living situations are focused on by Pravin and Ojha, such signals contain more noise than those measured under clinical settings, necessitating the development of a new signal noise removal approach capable of determining adaptive filters. The wavelet and elliptical filtering methods are investigated in this study for the objective of decreasing noise in ECG readings recorded utilizing assistive

technology. Currently, the most frequent approach to reducing noise from such a waveform is to utilize filters, with the wavelet filter being the most prominent among them. However, in some cases, applying a different filtering approach can result in a waveform with a greater SNR.

2.13 Summary

The noise reduction strategies, filtering-based denoising approaches, transform-based denoising methods and machine learning techniques have all been thoroughly researched. The PSNR, MSE, and SSIM, as well as other metrics like SDME, PC, and SMAPE, are enhanced to be characterised as a better denoising approach, according to the literature review. It contributes significantly to the current research effort in expanding and increasing the performance of image denoising algorithms since an in-depth review of the existing approaches was conducted in a methodical manner.

The focus of this study is on image denoising optimization methods based on WT. Machine learning-based neural network concepts are being investigated for this purpose. In addition, hybrid optimization methods are used to increase efficiency and improve PSNR. These are the most successful noise reduction approaches that have been presented in the field of ECG denoising so far. Though these methods are effective, the performance can be improvised by hybridizing with some other algorithms or filters thereby harvesting the best part of both the techniques.

CHAPTER 3

ECG SIGNAL DENOISING USING OPTIMIZED ADAPTIVE HYBRID FILTER WITH EMPIRICAL WAVELET TRANSFORM

3.1 Introduction

The majority of modern therapeutic gadgets that capture bodily signals have grown smaller and more efficient in recent years. The ECG signal is the signals that are most frequently recorded. Due to the way it shows the monitoring of a patient's heart throughout medical treatment, it may be used to diagnose a variety of cardiac conditions. Muscle artefact (MA), baseline wander (BW), and electrode motion (EM), among other noises (coined artefacts), always degrade recorded ECG data. These sounds have a considerable influence on the ECG waveform, obscuring the ECG signal's weak qualities, making it harder to identify cardiovascular disorders. As a result, signal denoising for ECGs is becoming more significant. As a result, signal denoising for ECGs is becoming more significant. EMG interference, Power line noise, baseline drift, and electrode contact noise all distort the ECG signal, which is a weak non-stationary signal.

Signals from electrocardiography (ECG) are essential for making a variety of heart problems diagnoses. The World Health

Organization (WHO) reports that CVDs kill more people globally than any other cause does each year. The ECG is done with accurate electronic equipment because cardiac pulses may fluctuate significantly and noise can impact decision accuracy. When collecting data to detect ECG signal features and make choices about various cardiac disorders using advanced algorithms, precision measurements are essential. Aberrations and noise, however, can skew even the most exact results. Both internal and external factors, such as the evaporating electrode gel in Parkinson's disease, can result in artefacts.

During the process of collecting and transmitting the ECG signal, high frequency artefacts may pollute it (baseline wandering). Since noise in ECG data might result in incorrect interpretation, it must be eliminated. As a result, much work has gone into establishing mathematical approaches and computing algorithms for accurately extracting ECG patterns from normal (noisy) data for medical reasons during the last few decades. A Fourier transform-based method for extracting frequency domain ECG signal characteristics. However, this technique ignores time resolution, which has an impact on estimating accuracy. Other researches have overcome this issue by analysing time-frequency data without affecting resolution. The wavelet transform-based algorithms were developed with the purpose of discovering medicinal applications. A balance between frequency and temporal resolutions is easier to accomplish in the wavelet domain, and a suitable wavelet may be chosen to provide enough precision.

The ECG readings can quickly reveal cardiac abnormalities. However, the data are still degraded as a result of artefacts introduced into the ECG signals during acquisition. These aberrations degrade the performance of the acquired ECG signals, resulting in incorrect cardiac disease prediction. The White Gaussian artefacts in the ECG data must be removed before the problem can be identified. To eliminate artefacts from ECG data, several denoising techniques can be applied. ECG signal filtering is all about finding a balance between de-noising performance and processing complexity. This research proposes a hybrid methodology that receives the ECG signals and provides a high denoised ECG signal which helps to predict the disease accurately.

ECG signal denoising is a method for separating the real signal from unwanted signals to produce a denoised ECG that enables quick and accurate diagnosis. In order to prevent unforeseen artefacts from influencing the findings, a denoising algorithm should be able to recognise and filter distinct types of noise in the data. The ECG signal can get contaminated during acquisition and transmission by both low-frequency noises like power-line interference and electromyogram noise, as well as high-frequency disturbances such additive white Gaussian noise, power-line interference, and electromyogram noise (baseline wandering). Denoising the ECG signal is necessary because noise might cause inaccurate interpretation. As a result, much work has gone into creating mathematical techniques and computational algorithms that can

properly extract ECG features from normal (noisy) data during the previous few decades.

The contribution of the work is as follows,

- The input of the design is thought to be the ECG signals from the MIT-BIH dataset. A clean signal is combined with white Gaussian noise to produce a noisy signal.

- The denoised ECG signal is decayed by the EWT and the window function is optimized by the proposed Honey Badger Optimization algorithm.

- After the decomposition, the noisy signal is transferred into the Adaptive hybrid filter and its weight parameters are adjusted by the HBO technique. Finally, the denoised ECG signals are obtained from the suggested strategy.

- The success of the proposed approach is verified in terms of NRMSE, SNR, MD, NRME, PRE, ME, and CC with various existing approaches.

3.2 Background

3.2.1 Wavelet Transform

In the mathematician's writings from a long time ago, the wavelet theory is obfuscated. Karl Weirstrass mathematically stated how to build the functions of a family by superimposing the measured forms of a given basis operation in 1873. The term wavelet refers to a tiny wave, and compactness denotes that the window function requirement is supported compactly to a limited length. A wave function is a temporal function that oscillates from time to time. Localized waves, on the other hand, are wavelets. They build up energy over time and are good for analysing transitory signals. Figure 1.3 illustrates the dissimilarity among a wave and a wavelet.

The WT is among the most important signal processing techniques because of its multi-resolution capabilities. In contrast to Fourier transformation, WT is appropriate for non-stationary signals with varying frequency responses. The degree of frequency content similarity between a signal and the chosen wavelet is measured by frequency coefficients. Due to its band-pass like spectrum, these coefficients are estimated as the conversion of the signal and the observed wavelet function. It is also derived as an extended band pass filter. The radian frequency is inversely proportional to the magnitude in this case. Lower frequencies resemble greater scales and lengthier wavelet operations as a result.

Approximations are based on wavelet analysis, which is used to extract information from one of the signals using a high-scale technique. Details of a signal are exploited at lower levels to obtain greater information. Signals are often band-limited, and using finite energy is equivalent, therefore confined scale intervals are employed. Continuous Wavelet Transform, on the other hand, provides much redundant information. Because wavelet families are bi-orthogonal or orthogonal, using a space-saving Discrete Wavelet Transform (DWT) algorithm saves space and avoids superfluous analysis. The DWT is comparable to the subsequent version, which is generally a dyed stage model. The signal to be investigated is amplified using a wavelet function, and its transformation is calculated for each segment formed in wavelet analysis. At low frequencies, the wavelet transform enhances frequency and temporal resolution.

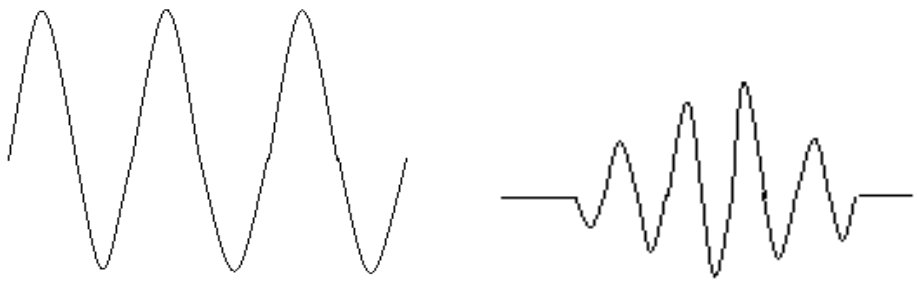

(a) (b)

Figure 3.1: Dissimilarity among Wave and Wavelet (a) wave (b) wavelet

Any signal may be analysed by scaling and translating a single mother wavelet function (Basis function). Because their energy is concentrated throughout time and has wave-like (duration) properties, wavelets allow simultaneous time and frequency analysis of signals. As a result, the wavelet provides a flexible mathematical tool for evaluating statistically unexpected and time-varying (non-stationary) signals, particularly in the region of discontinuities, which is a prevalent property of images with edges that are discontinuous.

3.2.2 Adaptive Filter

An approach containing an adaptive filter includes a linear filter with a transfer function that may be optimised and is controlled by moveable parameters. The majority of adaptive filters were designed in a digital manner owning to the complexity for optimization methods. Adaptive filters are necessary in some situations because certain elements of the intended processing operation are not known or unpredictable. T By receiving feedback in the form of an error signal, the closed loop adaptive filter improves its transfer function. In order to lower the cost, which is essential for the optimum filter performance, the closed loop adaptive method often entails feeding a cost function to an algorithm that determines how to adjust the filter transfer function on the subsequent iteration. The mean square of the error signal is the most typical cost function.

The recording of a heartbeat may be hampered by noise from the AC mains (an ECG). The harmonics and frequency of a power source may change over time. The heartbeat almost probably contains frequency components in the rejected zone, therefore one way to decrease noise is to filter the signal using a notch filter at the mains frequency and its environs. However, this might considerably impair the quality of the ECG.

An adaptive filter could be utilized to reduce the chance of data loss. The adaptive filter would receive data from the patient as well as the mains, enabling it to follow the noise's varying true frequency and exclude it from the recording. In these situations, an adaptive approach often permits a filter with a reduced rejection range, indicating that the output signal quality is better for medical purposes.

3.2.3 LMS Technique

When a tapped delay line in FIR framework is included in the variable filter, the least mean square updating mechanism is simple to implement. The FIR filter's coefficients are typically modified as follows after each sample:

$$C_{l,k+1} = C_{lk} + 2\mu\epsilon_k X_{k-1} \tag{3.1}$$

Here, μ is known as the convergence factor.

Because the LMS approach requires no precise relationship between the X values, it may be used to change both a linear combiner and a FIR filter. The following is the update formula:

$$C_{l,k+1} = C_{lk} + 2\mu\epsilon_k X_{lk} \quad (3.1)$$

The LMS algorithm modifies each weight by a little amount at each time k. If the modification had been made at time k, the error would have been reduced. The accompanying value X and the fault at time k determine the magnitude of each weight shift. The weights that have the most influence on the production have been adjusted the most. The weights should remain the same if the mistake is zero. If the value matching of X is 0, altering the weight has no impact, thus it is left alone.

3.3 Proposed Approach

In this proposed approach, a novel strategy for denoising ECG signal based on Empirical Wavelet Transform (EWT) with honey badger optimization algorithm and weighted adaptive filter is proposed. Initially, the White Gaussian artefacts are included in the ECG signal images obtained from three datasets namely MIT-BIH ARR, BIDMC-CHF and MIT-BIH NSR. Then the acquired ECG signals are denoised using Empirical Wavelet Transform (EWT) in which the window size is optimized with a Honey Badger Optimization (HBO) algorithm to obtain

the optimum value. Finally, the denoised image is again processed with a weighted adaptive filter for enhancing the edge information and improving the denoising performance. Furthermore, the suggested method is compared against current denoising methods. The suggested approach's framework is defined in Figure 3.2.

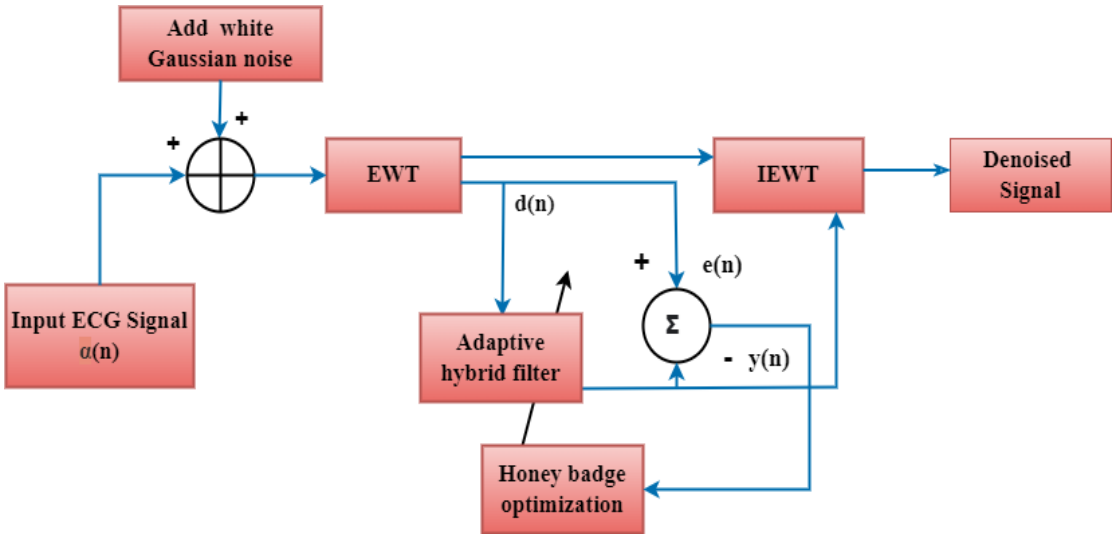

Figure 3.2: Proposed Approach Flow diagram

3.3.1 Empirical Wavelet Transform (EWT)

The EWT was founded by Jerome Gilles in the year 2013 which uses the adaptive wavelet filter bank for decomposing. In the proposed approach the EWT uses weighted adaptive filter for denoising the ECG signals. The EWT works based on segmenting the Fourier afterwards it constructs a group of wavelet filters that helps to retrieve the various modes of the ECG.

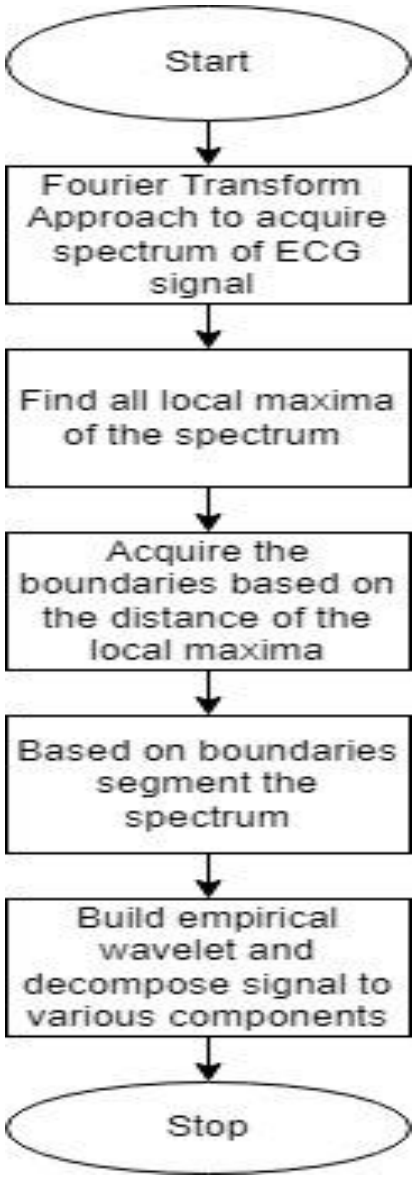

Figure 3.3: Flow Diagram of EWT

If the sections of Fourier are automatically then EWT adapts to adaptive for handling this weighted adaptive filter is designed. The operation of EWT is it locates all of the spectrum's local maxima and then uses the centres of the two neighbouring local maxima as the

Fourier segment borders. Figure 3.3 demonstrates the operation of the EWT.

In the process of denoising, at first white Gaussian noise is introduced to the input ECG signals in various amplitude scales to create synthetic bio-signals contaminated by WGN over a wide range of SNR. Because substantial noise levels deform ECG to such an extent that small magnitude complexes are not discernible, only SNRs greater than 0 dB are evaluated.

EWT is a wavelet that is tailored to the signal being processed. This wavelet is analogous to that of band-pass filters. Empirical wavelets allow signal flexibility. It divides the certain signal into a variety of modes called AM-FM components using this wavelet. The Fourier spectrum of these AM-FM components is compactly supported. Different mode segmentation is equal to Fourier spectrum segmentation in this case. Assume that there are N segments in the Fourier spectrum. Between each segment, there is a limit ω_n. The task of segmenting the spectrum is critical since segmentation allows for adaptation. Our goal is to distinguish the various regions of the spectrum that correspond to various modes. We need a total of $N+1$ borders to divide into N segments by spectrum, but the Fourier spectrum limit is among 0 and π, hence need$n-1$ additional limits. To establish such confines, initially locate the spectrum's local maxima and arrange them in decreasing order. If the algorithm finds M maxima, two scenarios can emerge.

$M \geq N$: Maintain the first $N-1$ maxima once the algorithm discovered sufficient maximum to determine the necessary segments.

$M < N$: Maintain all of the observed maxima because the signal contains fewer modes than expected and set N to the proper value.

The empirical wavelet transform is defined similarly to the classical wavelet transform. The inner product of the Empirical wavelets yields the detail coefficients [17].

$$W_f'(n,t) = (f, \Psi_n) = \int f(\tau)\overline{\Psi_n(\tau - t)}d\tau = (\hat{f}(\omega)\overline{\Psi_n(\omega)})^v \quad (3.1)$$

And the inner product of the scaling function with the approximation coefficients,

$$W_f'(0,t) = (f, \varphi_1) = \int f(\tau)\overline{\varphi_1(\tau - t)}d\tau = (\hat{f}(\omega)\overline{\varphi_1(\omega)})^v \quad (3.2)$$

Where $\overline{\Psi_n(\omega)}$ and $\overline{\varphi_1(\omega)}$ are well-defined by

$$\overline{\Psi_n(\omega)} = \begin{cases} 1 & if|\omega| \leq (1-\gamma)\omega_n \\ cos\left[\frac{\pi}{2}\beta\frac{1}{2\gamma}(|\omega| - (1-\gamma))\right] & if(1-\gamma)\omega_n \leq |\omega| \leq (1+\gamma)\omega_n \\ 0 & otherwise \end{cases} \quad (3.3)$$

The reconstruction is obtained by,

$$f(t) = W_f'(0,t) * \varphi_1(t) + \sum_{n=1}^{N} W_f'(n,t) * \Psi_n(t)$$

$$= \left(\widehat{W}_f(0,\omega)\hat{\varphi}_1 + \sum_{n=1}^{N} W_f'(n,\omega) * \widehat{\Psi}_n(t)\right)^v \quad (3.4)$$

The mid points among the adjacent local maxima are obtained. After, the rectangular window function is applied which is utilized to multiply the midpoints with this window function. Then the inverse Fourier transform is taken.

3.3.2 Rectangular window function

Equations (3.5) and (3.6) gives the weighting function and spectrum of the l-point Rectangular window function. In time domain,

$$\omega_{Rec}(n) = \begin{cases} 1; for \frac{-(l-1)}{2} \leq |n| \leq \frac{l-1}{2} \\ 0; \quad otherwise \end{cases} \quad (3.5)$$

In frequency domain,

$$\omega_{Rec}\left(e^{j\omega}\right) = \frac{sin\left(\frac{\omega l}{2}\right)}{sin\frac{\omega}{2}} \quad (3.6)$$

The window design function outperforms filter design strategies in terms of performance, easiness, and robustness. The performance of a window function with a progressive deterioration to zero has been enhanced. Therefore, to optimize the window function, the

HBO algorithm is introduced. The HBO algorithm is utilized to MSE parameter which is represented in Equation,

$$obj = \min\{MSE\} = \frac{1}{N}\sum_{m=1}^{N}(y(m) - x(m))^2 \quad (3.7)$$

Where, (m) is the pure signal, (m) is output of the filter output and number of sample is signified into ^{N}, that is each MIT-BIH signal.

3.3.3 Adaptive Hybrid Filter

Adaptive filtering is a mechanism for iteratively determining the relationship between two signals. Figure 3.4 demonstrates the flow diagram of an adaptive filter. Where $^{d(n)}$ represent desired signal, $^{x0(n)}$ is the adaptive filter's input signal, $^{y0(n)}$ is the adaptive filter's output signal, and $^{e(n)}$ is the error signal. The difference among signals $^{d0(n)}$ and $^{y0(n)}$ is $^{e0(n)}$ which are mathematically stated as (3.8)-(3.10). The signals in this case are a pair of reference signals and information and the configuration is used to implement a digital filter as a FIR.

$$d0(n) = s0(n) + x0(n) \quad (3.8)$$

$$y0(n) = w0(n) \times x0(n) \quad (3.9)$$

$$e0(n) = d0(n) - y0(n) \quad (3.10)$$

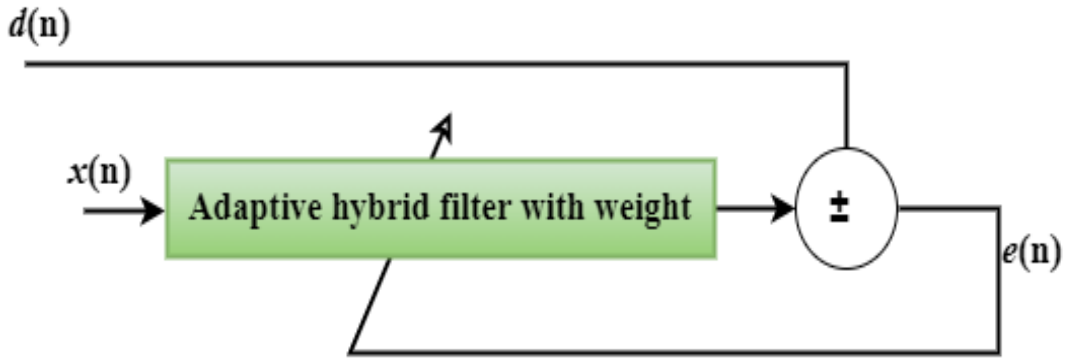

Figure 3.4: Adaptive hybrid filter

In an ECG signal, $q0(n)$ is made up of additive low-frequency and high-frequency components that are unrelated to $s0(n)$. The signal $d0(n)$ is used in this paper comes from the MIT-BIH dataset. The high and low-frequency noise components are $q_1(n)$ and $q_2(n)$, respectively. The adaptive hybrid filter receives the reference noise $q_1(n)$ and $q_2(n)$ to creates the outputs $y_1(n)$ and$y_2(n)$, respectively. The difference between $d(n)$ and $y_1(n)$ is computed as the error signal $e_1(n)$ that fed back to the adaptive hybrid filter in each iteration to alter its weight vector $w_1(n)$. The iteration process will continue until the suggested HBO method minimizes the error $e_1(n)$. The low-frequency noise output signal,$s0(n) + q0'(n)$, is sent to the adaptive hybrid filter's second stage, wherever $e_2(n)$ is figured as the difference between $s0(n) + q0'(n)$ and $y_2(n)$. The adaptive hybrid filter receives $e_2(n)$ and updates its weight vector $w_2(n)$ in each iteration until $e_2(n)$ is minimized. $s0(n)$ is roughly

equal to $s0'(n)$ as the final output signal. The output of the first stage of adaptive hybrid filter, $y_1(n)$ and the output of the second stage $y_2(n)$.

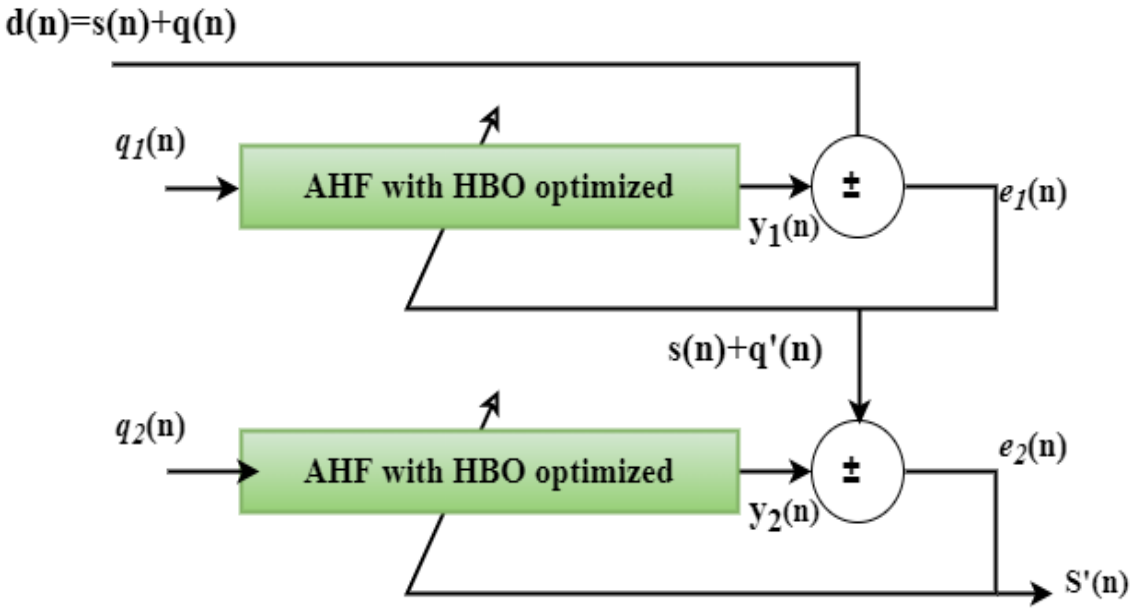

Figure 3.5: Proposed Adaptive Hybrid Filter (AHF)

3.3.4 Honey Badger Optimization - Empirical Wavelet Transform (HBO-EWT)

For diminishing the artefacts interference or frequency dispersion in the acquired ECG signals the Honey Badger Optimization (HBO) algorithm is hybrid with the EWT. The proposed approach finds all the local maxima found in the spectrum of Fourier in a specified window and afterwards the boundaries are segmented. The specified window value is optimized by the HBO algorithm. The foraging features of honey badger are emulated in the HBO approach. It contains two

stages one is digging and the other is honey. The following are the steps followed by the HBO algorithm.

- **Initialization:** The Eqn. (3.11) initializes the total honey badgers and its locations.

$$h_i = min_i + a_1 * (max_i - min_i) \tag{3.11}$$

Here, $h_i$indicates the total number of honey badgers, *i* is the location of the honey badger, a is an arbitrary number varies from 0 to 1 and max_i, min_i are the maximum, minimum bounds.

- **Defining Intensity:** It defines thevictims power and the distance which is computed as follows,

$$I_i = a_2 * \frac{P}{4\pi d_i^2} \tag{3.12}$$

$$P = (h_i - h_{i+1})^2 \tag{3.13}$$

$$d_i = h_{victim} - h_i \tag{3.14}$$

Here, P is the power of the victim and d is the distance of the victim.

- **Modify Density Factor:** Altering the density factor helps to reduce the number of iterations and is computed as follows.

$$\propto = Ct * \exp(\frac{-t}{t_{max}}) \tag{3.15}$$

Here, $\propto$ denotes the density factor, t is the changing time and Ct is the constant value ≥1 by default it is set to 2.

- **Evading local optima:** This contains two stages digging and honey which helps to evade from the local optima.

- **Digging stage:** The digging stage is computed as in Eqn. (3.16).

$$h_{new} = h_{victim} + F * \beta * I * h_{victim} + F * a_3 * \propto * d_i * |\cos(2\pi a_4) * [1 - \cos(2\pi a_5)]| \tag{3.16}$$

Here, the search position is modified based on the flag F.

- Honey stage: The honey stage is computed as in Eqn. (3.17).

$$h_{new} = h_{victim} + F * a_6 * \propto * d_i * a_6 \tag{3.17}$$

The flag F is computed based on the Eqn. (3.18)

$$F = \begin{cases} 1 & if\ a_8 \leq 0.5 \\ -1 & else \end{cases} \tag{3.18}$$

Thus the HBO algorithm integrated with EWT denoise the ECG signal in a better way than other existing approaches and provide better accuracy in diagnosing the disease.

3.4 Results and Discussions

MATLAB2018a software running on a Windows 8.1 operating system is used to simulate the suggested denoising method. White Gaussian noise with 10dB variations is incorporated in the ECG signals. For experimental purposes, the proposed technique is tested on the MIT-BIH ARR, MIT-BIH NSR, and BIDMC-CHF datasets. One of the most well-known ECG databases, the MIT-BIH dataset consists of 48 half-hour snippets from 2-channel ambulatory ECG recordings made at the BIH Arrhythmia Laboratory between 1975 and 1979. The kind of congestive heart failure was determined using data from the BIDMC CHF dataset, which contains 150 signals for testing (CHF). Sinus rhythm signals from the MIT-BIH normal sinus rhythm dataset were utilized for

testing. It comprises 18 ECG recordings from patients who were sent to the same institution's Arrhythmia Laboratory. There were no noticeable arrhythmias in the signals in this database, which included five males between the ages of 26 and 45 and thirteen females between the ages of 20 and 50. There were 142 10-second signals (type NSR) used in total. Figure 3.6 illustrates the datasets, clean ECG signal, artefacts ECG signal and denoised ECG signals.

Dataset	Clean ECG	Artefacts ECG	Denoised ECG
MIT-BIH ARR	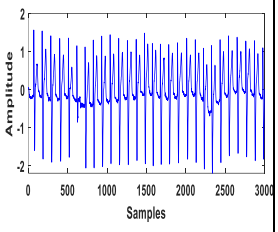	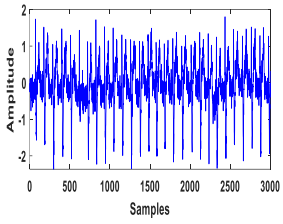	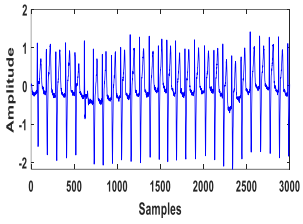
MIT-BIH NSR	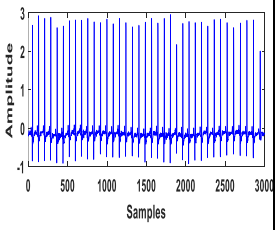	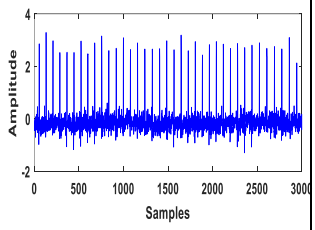	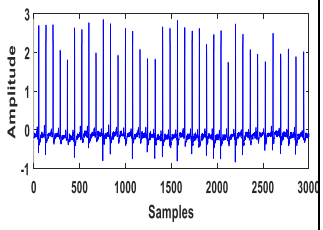

BIDM C-CHF	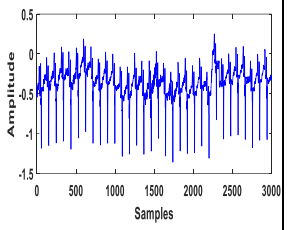	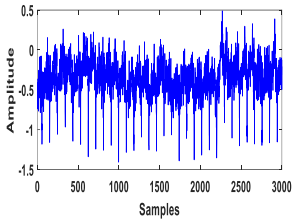	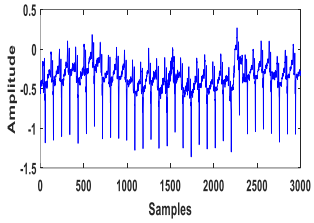

Figure 3.6: Artefacts free ECG Signal, Artefacts ECG Signal and Denoised ECG Signal

Table 3.1 describes the performance of the suggested approach like normalized root-mean-square error (NRMSE), maximum error (ME), peak reconstruction error (PRE), mean difference (MD), mean square error (MSE), correlation coefficient (CC), signal-to-noise ratio (SNR), and normalized root maximum error (NRME) is computed and are compared with other existing approaches such as RLS-based adaptive filter, Multichannel LMS and DWT-based baseline wander. From the readings it is evident that the suggested approach produces superiordenoised signals than the other traditional approaches.

Table 3.1: Performance of the Suggested Methodology compared with other Approaches

Datasets	RLS-based adaptive	Multichannel LMS	DWT- based baseline	Proposed

	filter		wander	
SNR				
MIT-BIH ARR	73.624	75.258	80.158	83.65
MIT-BIH NSR	70.265	73.189	78.529	80.12
BIDMC-CHF	72.221	76.741	84.621	86.21
MSE				
MIT-BIH ARR	2.621e-10	1.984e-10	1.854e-10	2.369e-11
MIT-BIH NSR	3.149e-10	2.956e-10	2.369e-10	1.95e-10

BIDMC-CHF	3.901e-10	3.652e-10	2.689e-10	1.632e-10
ME				
MIT-BIH ARR	8.308e-4	6.325e-4	4.102e-4	6.954e-5
MIT-BIH NSR	1.589e-3	1.360e-3	9.547e-4	7.158e-4
BIDMC-CHF	9.659e-4	7.172e-4	6.984e-4	6.341e-4
MD				
MIT-BIH ARR	-7.052e-7	-4.150e-7	-3.049e-7	-1.10e-7
MIT-BIH	-7.454e-7	-6.894e-7	-5.154e-7	-3.15e-7

NSR				
BIDMC-CHF	-1.025e-6	-6.250e-7	-5.965e-7	-3.87e-7
PRE				
MIT-BIH ARR	4.897e-7	3.564e-7	1.065e-7	5.624e-8
MIT-BIH NSR	9.741e-8	9.654e-8	8.264e-8	6.254e-8
BIDMC-CHF	1.055e-7	9.056e-8	8.364e-8	7.056e-8
NRME				
MIT-BIH ARR	2.904e-1	2.365e-1	2.105e-1	1.250e-1

MIT-BIH NSR	2.981e-1	2.450e-1	2.119e-1	1.354e-1
BIDMC-CHF	3.204e-1	2.415e-1	2.35e-1	1.405e-1
NRMSE				
MIT-BIH ARR	3.647e-5	2.5691e-5	1.9521e-5	1.508e-5
MIT-BIH NSR	3.054e-5	2.641e-5	1.9974e-5	1.689e-5
BIDMC-CHF	3.954e-5	3.564e-5	2.94e-5	1.984e-5
CC				
MIT-BIH	0.9698	0.9788	0.9998	1

ARR				
MIT-BIH NSR	0.9788	0.9788	0.9888	0.9998
BIDMC-CHF	0.9708	0.9715	0.9899	0.9999

Figures 3.7 to 3.13 displays the SNR, NRMSE, MSE, ME, PRE, MD, CC and NRME of proposed and existing RLS-based adaptive filter, Multichannel LMS and DWT-based baseline wander denoising methods. The experimental process is conducted on three MIT-BIH database ECG signals. As can be shown, the suggested method achieves superior SNR values for nearly all signals when compared to the denoising techniques currently in use. Thus, the proposed algorithm is powerful to deal with noises compared to existing denoising methods. Moreover, the MSE and NRMSE values should be least as possible for denoised signals. The proposed approach has reportedly obtained the least amount of ME and NRMSE. In contrast, DWT-based baseline wander, Multichannel LMS, and RLS-based adaptive filter acquired the highest ME and NRMSE when compared to current denoising techniques. These outcomes show that the suggested approach is suited for an efficient denoising procedure. Each coefficient in the wavelet

domains is distributed with noise energy. Among the denoising algorithms other than proposed algorithm DWT-based baseline wander has gained relatively improved denoising performance than existing denoising algorithms.

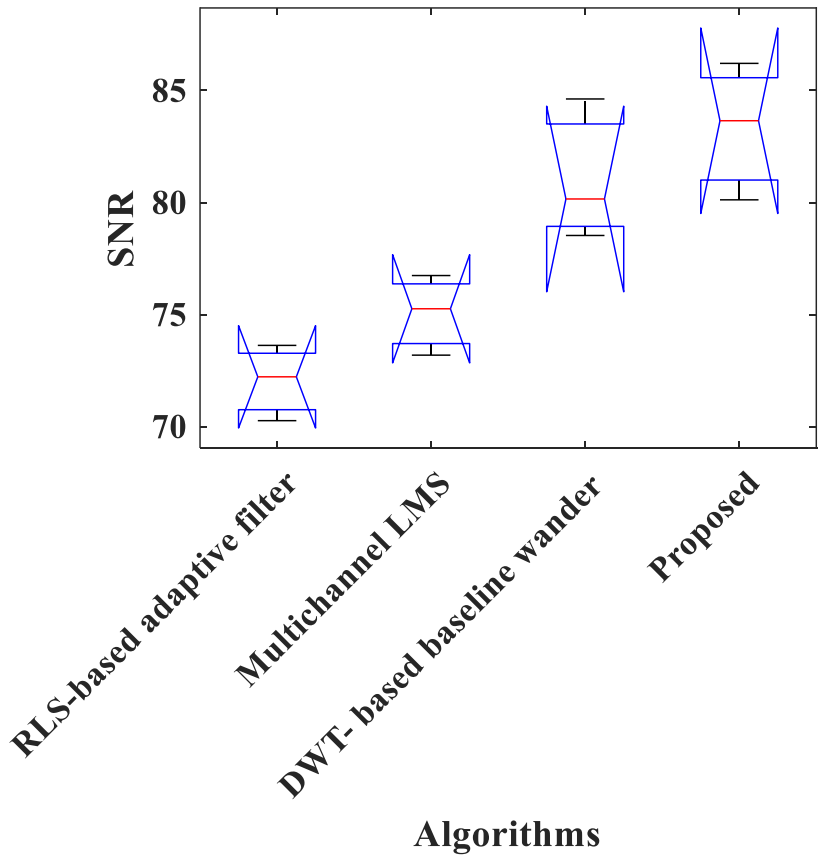

Figure 3.7: Various denoising schemes compared with Suggested scheme in terms of SNR

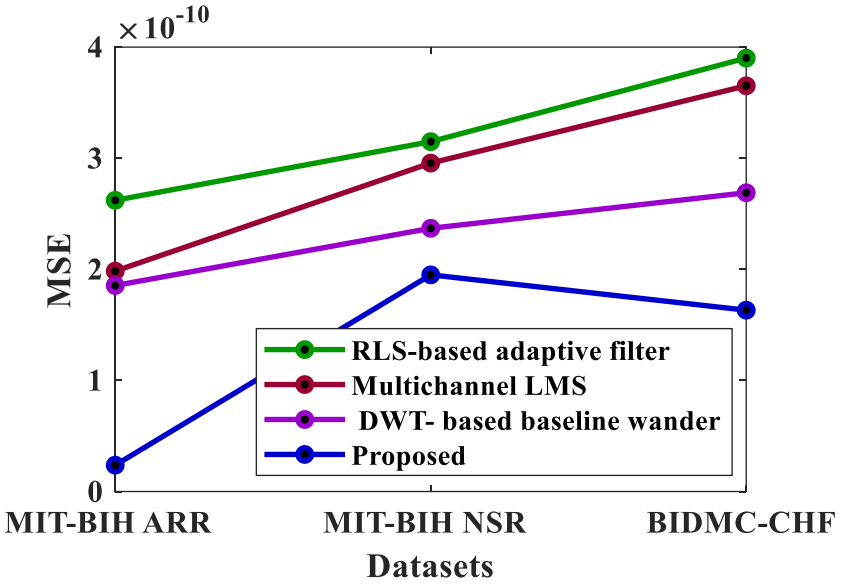

Figure 3.8: Various denoising schemes compared with Suggested scheme in terms of MSE

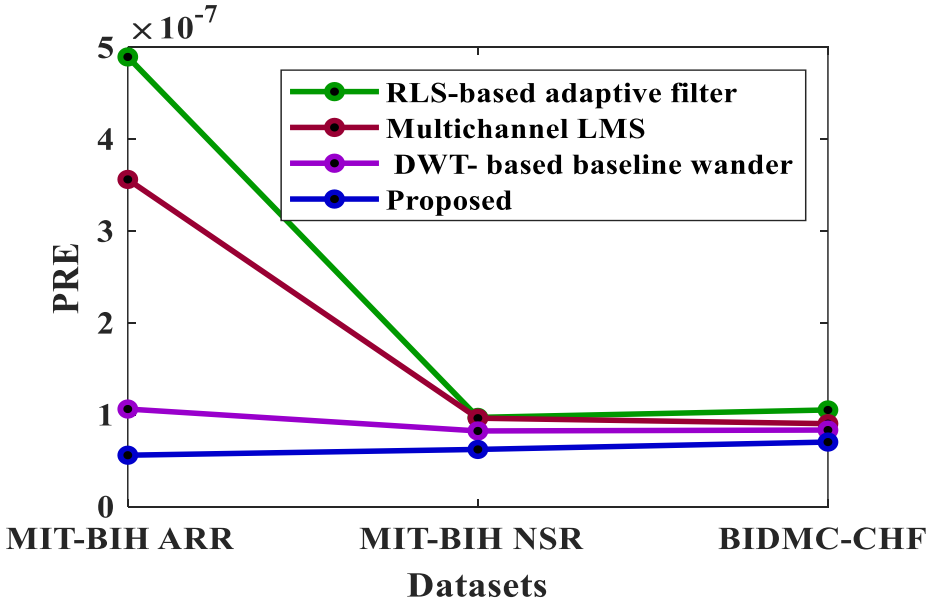

Figure 3.9: Various denoising schemes compared with Suggested scheme in terms of PRE

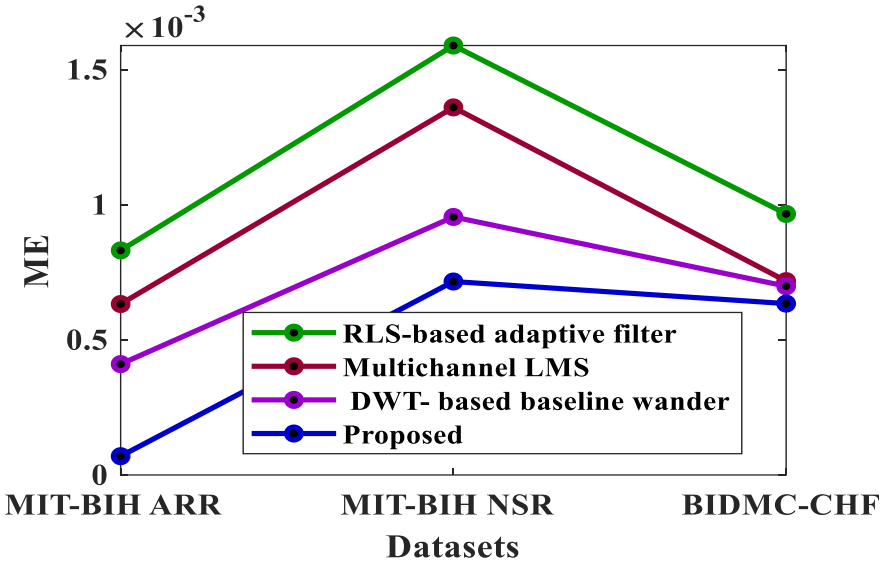

Figure 3.10: Various denoising schemes compared with Suggested scheme in terms of ME

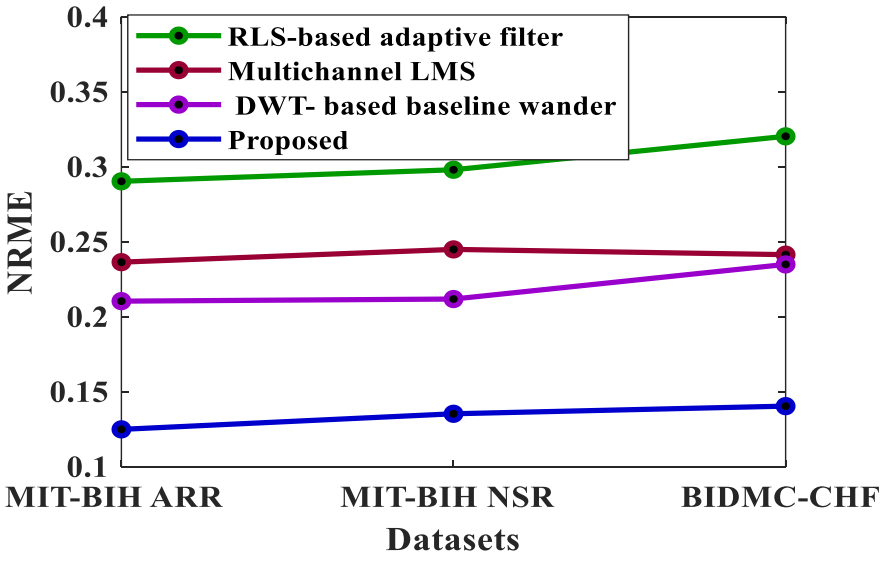

Figure 3.11: Various denoising schemes compared with Suggested scheme in terms of NRME

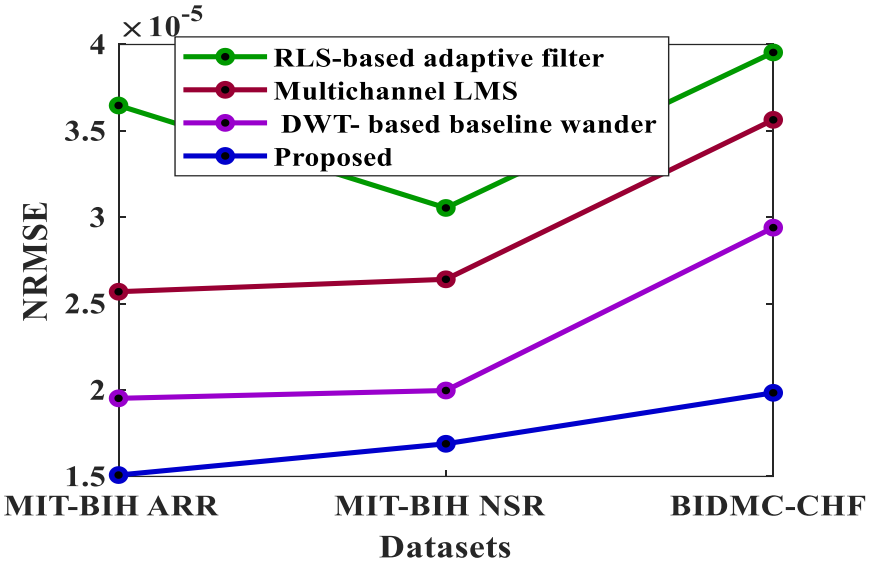

Figure 3.12: Various denoising schemes compared with Suggested scheme in terms of NRMSE

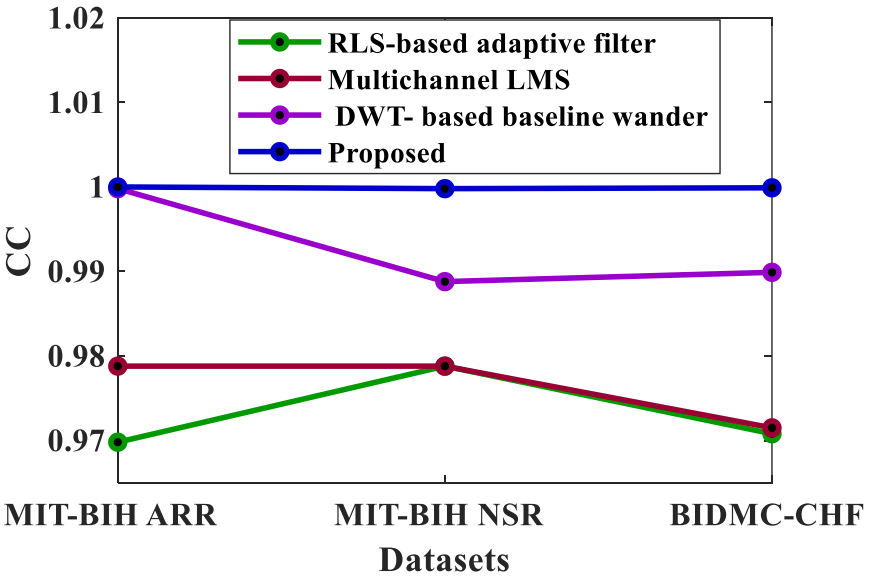

Figure 3.13: Various denoising schemes compared with Suggested scheme in terms of CC

Signal-to-noise ratio (SNR), maximum error (ME), peak reconstruction error (PRE), normalised root mean square error (NRMSE), mean square error (MSE), mean difference (MD), correlation coefficient (CC), and normalised root maximum error (NRME) are computed and are compared with other existing machine learning approaches like PSO, AOA, and MVO. The performance of the proposed approach is described in Table 3.2. The findings demonstrate that suggested HBO with EWT strategy outperforms the other current machine learning approaches in terms of performance.

Table 3.2: Performance of the Suggested Approach compared with other Machine Learning Methodologies

Datasets	PSO	AOA	MVO	Proposed
SNR				
MIT-BIH ARR	69.254	73.154	78.154	83.65
MIT-BIH NSR	70.890	72.890	75.624	80.12

BIDMC-CHF	81.069	83.654	85.265	86.21
MSE				
MIT-BIH ARR	3.658e-10	3.789e-10	1.687e-10	2.369e-11
MIT-BIH NSR	5.065e-10	4.356e-10	3.651e-10	1.95e-10
BIDMC-CHF	6.087e-10	5.648e-10	3.987e-10	1.632e-10
ME				
MIT-BIH ARR	3.698e-4	1.687e-4	9.635e-5	6.954e-5
MIT-BIH	2.397e-3	1.589e-3	9.347e-4	7.158e-4

NSR				
BIDMC-CHF	3.087e-3	1.674e-3	8.146e-4	6.341e-4
MD				
MIT-BIH ARR	-3.658e-7	-3.458e-7	-2.39e-7	-1.10e-7
MIT-BIH NSR	-3.897e-7	-3.854e-7	-3.674e-7	-3.15e-7
BIDMC-CHF	-4.2287e-7	-4.125e-7	-3.978e-7	-3.87e-7
PRE				
MIT-BIH ARR	7.651e-8	6.974e-8	6.874e-8	5.624e-8

MIT-BIH NSR	7.047e-8	6.874e-8	6.814e-8	6.254e-8
BIDMC-CHF	7.369e-8	7.254e-8	7.156e-8	7.056e-8
NRME				
MIT-BIH ARR	1.957e-1	1.705e-1	1.548e-1	1.250e-1
MIT-BIH NSR	1.796e-1	1.684e-1	1.567e-1	1.354e-1
BIDMC-CHF	1.894e-1	1.782e-1	1.635e-1	1.405e-1
NRMSE				
MIT-BIH	1.960e-5	1.705e-5	1.678e-5	1.508e-5

ARR				
MIT-BIH NSR	1.987e-5	1.804e-5	1.735e-5	1.689e-5
BIDMC-CHF	2.222e-5	2.173e-5	2.014e-5	1.984e-5
CC				
MIT-BIH ARR	0.9998	0.9999	0.9999	1
MIT-BIH NSR	0.9998	0.9998	0.9999	0.9998
BIDMC-CHF	0.9989	09998	0.9999	0.9999

Figure 3.14 depicts the SNR of different optimization approaches like PSO, AOA and multi-verse optimization algorithm

(MVO) compared with the proposed approach. From this figure it is evident that the suggested approach gives higher SNR value than other optimization algorithms. The experimental findings illustrates that the proposed approach is superior to all other denoising techniques.

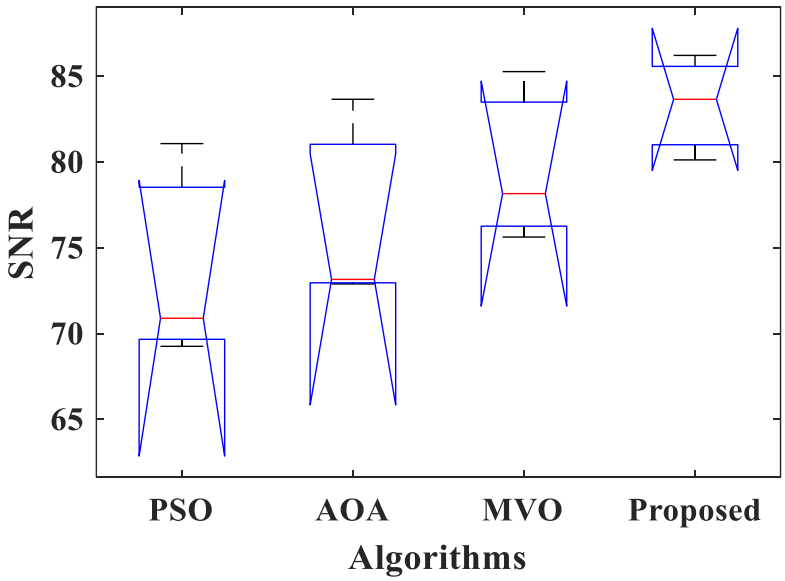

Figure 3.14: Various Optimization algorithms compared with proposed scheme in terms of SNR

Figure 3.15 compares the Mean Square Error (MSE) of several optimization techniques to the proposed methodology, including PSO, AOA, and multi-verse optimization algorithm (MVO). The recommended technique provides a less MSE value than previous optimization strategies, as seen in this graph. The experimental findings demonstrate that the proposed strategy outperforms every other optimization technique currently in use.

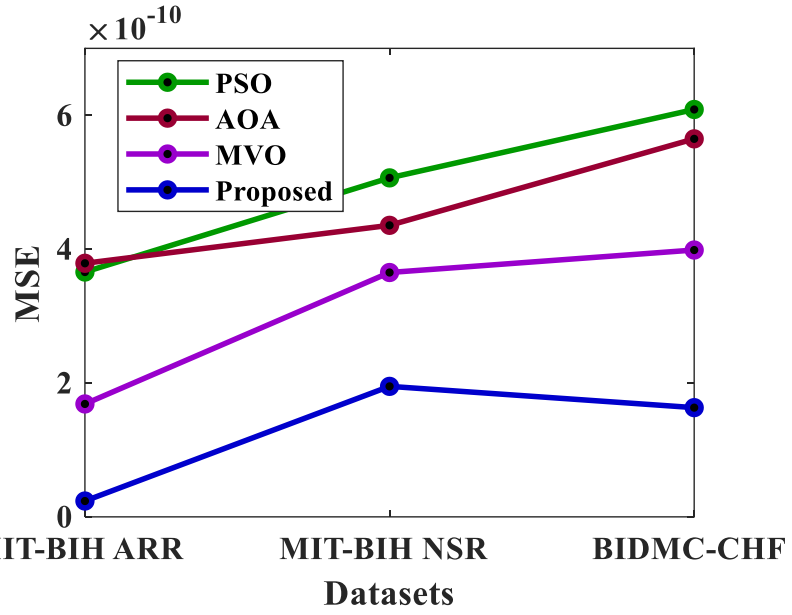

Figure 3.15: Various Optimization algorithms compared with proposed scheme in terms of MSE

Figure 3.16 depicts the maximum error (ME) of numerous optimization methodologies including PSO, AOA and multi-verse optimization algorithm (MVO) compared with the proposed approach. From this figure it is evident that the suggested approach gives lesser ME value than other optimization algorithms. The experimental findings illustrates that the proposed approach is superior to all other optimization techniques.

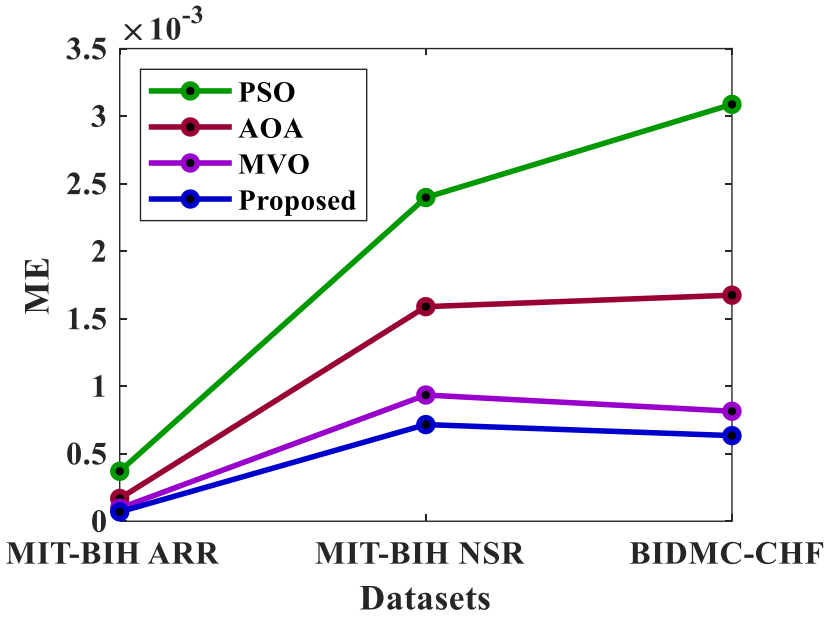

Figure 3.16: Various Optimization algorithms compared with proposed scheme in terms of ME

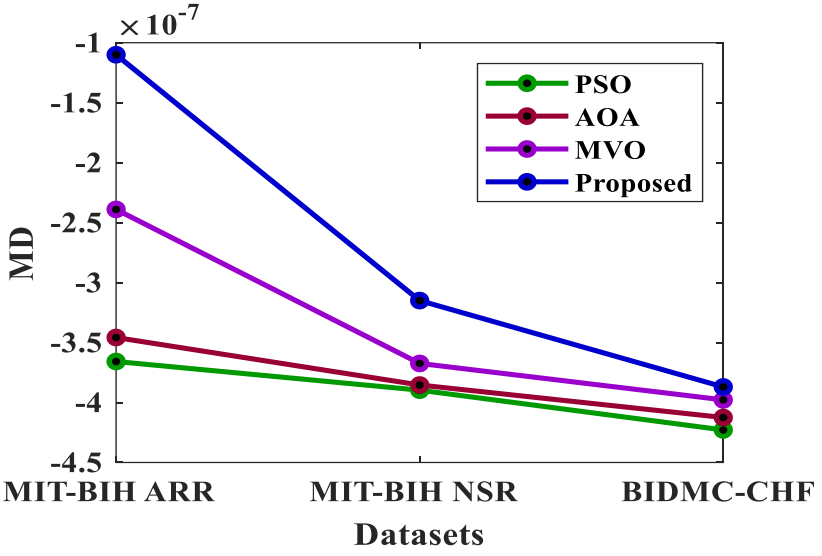

Figure 3.17: Various Optimization algorithms compared with proposed scheme in terms of MD

Figure 3.17 shows the mean difference (MD) between the suggested technique and other optimization methodologies including PSO, AOA, and MVO. This chart shows that the proposed technique generates a larger MD value than existing optimization approaches.

The peak reconstruction error (PRE) between the suggested approach and other optimization algorithms like PSO, AOA, and multi-verse optimization algorithm (MVO) is shown in Figure 3.18. The suggested approach produces a lower PRE value than existing optimization techniques, as seen in this graph. The results of the experiments reveal that the proposed strategy outperforms all other optimization strategies.

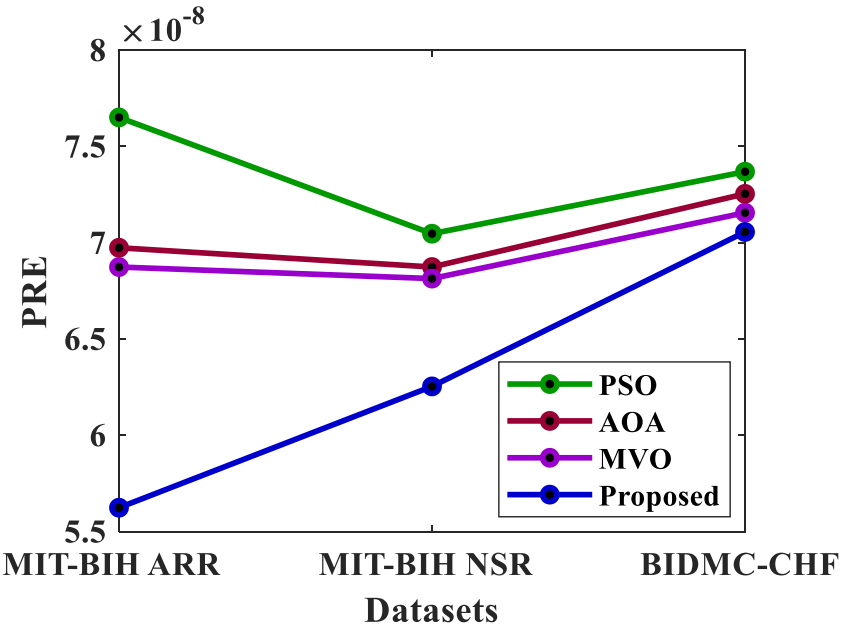

Figure 3.18: Various Optimization algorithms compared with proposed scheme in terms of PRE

Figure 3.19 depicts the correlation coefficient (CC) of numerous optimization methodologies including PSO, AOA and multi-verse optimization algorithm (MVO) compared with the proposed approach. From this figure it is evident that the suggested approach gives better CC than other optimization algorithms.

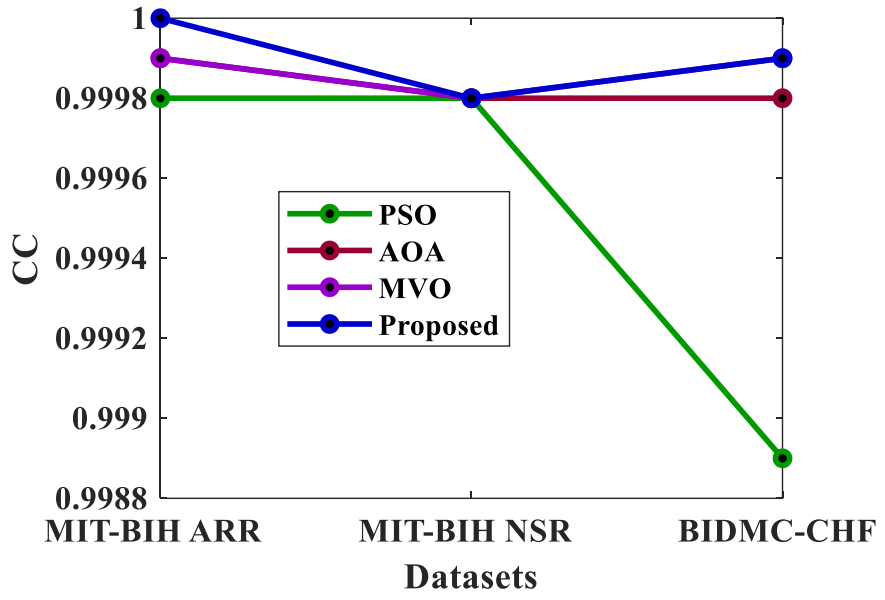

Figure 3.19: Various Optimization algorithms compared with proposed scheme in terms of CC

The normalized root maximum error (NRME) among the suggested approach and other optimization algorithms like PSO, AOA, and multi-verse optimization algorithm (MVO) is shown in Figure 3.20. The suggested approach produces a lower NRME value than existing optimization techniques, as seen in this graph. The results of the

experiments reveal that the proposed strategy outperforms all other optimization strategies.

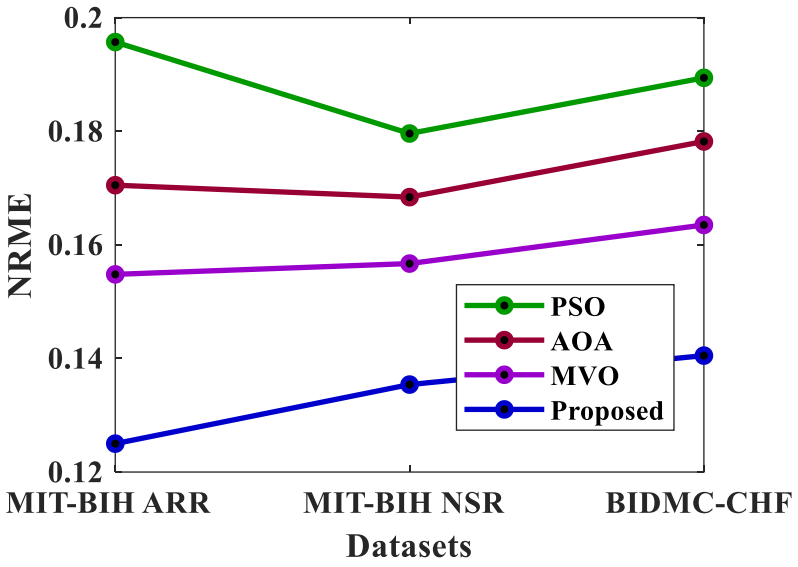

Figure 3.20: Various Optimization algorithms compared with proposed scheme in terms of NRME

The NRMSE between the suggested strategy and other optimization approaches like PSO, AOA, and multi-verse optimization algorithm is shown in Figure 3.21. In comparison to previous optimization techniques, the recommended methodology produces a significantly lower NRMSE. The results of the experiments reveal that the proposed strategy outperforms all other optimization strategies.

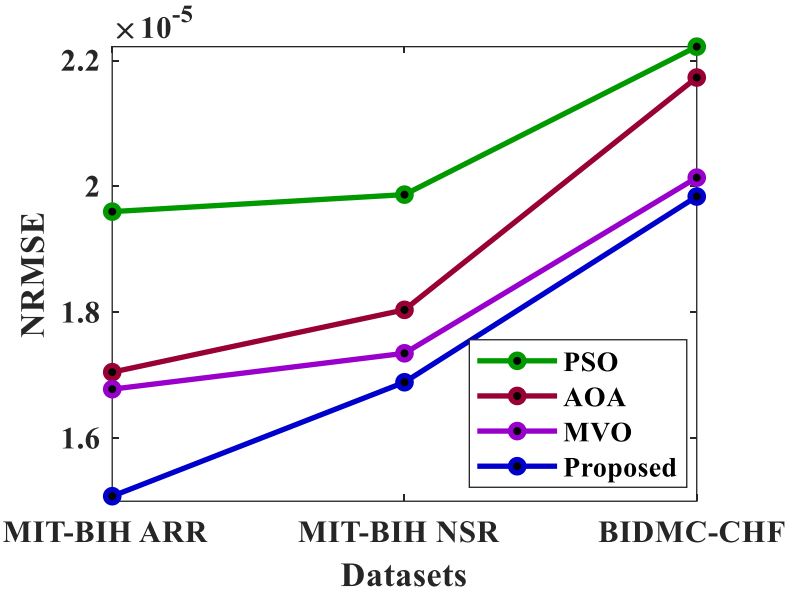

Figure 3.21: Various Optimization algorithms compared with proposed scheme in terms of NRMSE

Table 3.3 illustrates the Mann-Whitney U test for the proposed approach and the other existing approaches. On comparing this proposed approach produces best diagnosing value than the existing approaches.

Table 3.3: Mann-Whitney U test

Method	Mean	Sum of ranks	U value	P value
PSO	2.3333	7	8	0.2

Proposed	4.6667	14	1	
AOA	2.6667	8	7	0.4
Proposed	4.3333	13	2	
MVO	2.6667	8	7	0.4
Proposed	4.3333	13	2	

The use of analysis of variance (ANOVA) is advised for identifying significant factor or interaction effects. ANOVA is a valuable method for breaking down total variability into usable components like mean sum of squares (MS), F-value, sum of squares (SS), and degree of freedom (Df), among others. Table 3.4 illustrates the output parameters and the values obtained during the ANOVA test for various optimization algorithms with the proposed denoising approach.

Table 3.4: Variance Investigation (ANOVA)

Source	SS	Df	MS	F	Prob>F
Columns	152.979	3	50.9931	1.8	0.2242
Error	226.028	8	28.2535		
Total	379.008	11			

For the average of all datasets, Figure 3.22 illustrates the convergence curve of the suggested denoising technique and similar current algorithms. In comparison to previous methods, the suggested method demonstrated good convergence. The suggested technique is based on gain optimization using the HBO algorithm, with execution time being a critical aspect in the denoising strategy. When compared to current methods such as PSO, AOA, and MVO, the suggested technique requires less computing time.

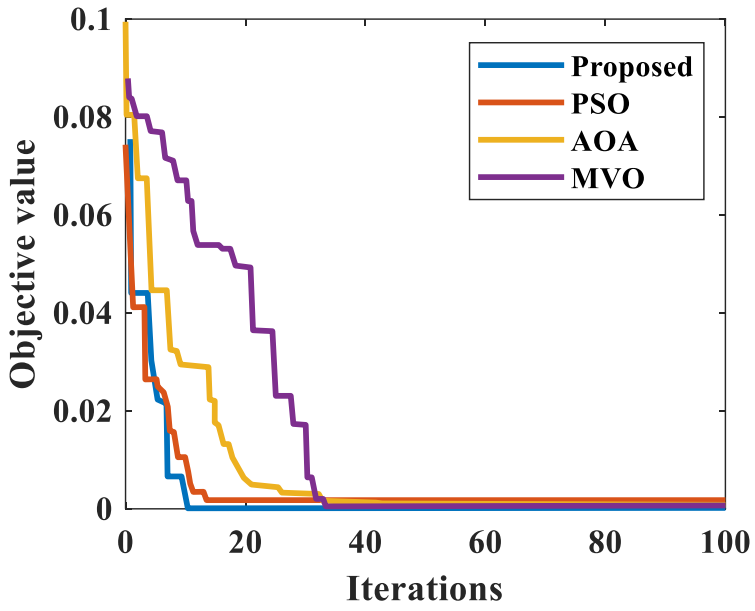

Figure 3.22: Convergence Curve for the proposed and existing denoising approaches

3.5 Summary

This study uses HBO, a novel bio-inspired metaheuristic algorithm, to implement an adaptive hybrid filter-based denoiser and demonstrate HBO's capacity to find high-quality solutions that outperform other metaheuristic algorithms such as PSO, AOA, and MVO. The HBO algorithm not only maintains a correct poise among exploration and exploitation, however, it also features a control parameter-free algorithm, which eliminates the need for a time-consuming control parameter tweaking process. EWT window function and filter parameters are adjusted by the proposed HBO algorithm. A comparison of the HBO approach with the RLS-based adaptive filter,

multichannel LMS, and DWT methods has been done to show the usefulness of the proposed adaptive hybrid filter. When compared to prior reported results, estimated results show that the proposed HBO based adaptive hybrid filter achieves a considerable improvement in NRMSE, SNR, MD, NRME, PRE, ME, and CC. As a result, the proposed strategy for denoising the cardiovascular signal is quite effective. As a consequence of the examined the findings and debates, it can be said that the suggested HBO algorithm supported by EWT and AHF can be employed efficiently for cardiovascular signal denoising.

CHAPTER 4

ECG SIGNAL DENOISING USING DISCRETE WAVELET TRANSFORM WITH AFRICAN VULTURE OPTIMIZATION ALGORITHM

4.1 Introduction

Electrocardiography (ECG), which is largely an electrical signal, depicts cardiac activity. It's displayed in the form of a graph. Electrodes (3 or 12 leads) are externally fastened to the thorax, legs, and hands to record the data. On the ECG, the potentials produced by cardiovascular muscle activity are depicted. It is commonly used by doctors to predict and treat a wide range of cardiovascular problems. The QRS complex, P, T, and U frequencies, can all be seen on an ECG, each of which is associated with a different phenomena that happens within a single cardiac cycle. The combination of these entities, as well as knowledge of the ECG scale, enables the computation of heart rate and the diagnosis of rhythm problems including atrial fibrillation, atrial flutter, cardiac arrhythmia, sinus tachycardia, and sinus bradycardia, among others. The QRS complex's axis deviation, for example, is a sign of ventricular hypertrophy, anterior and posterior fascicular block, and other illnesses that may be diagnosed via shape analysis.

An examination to ascertain the electrical potentials of the heart is called an electrocardiogram (ECG). The depolarization and repolarization of certain cells brought on by the movement of Na+ and k+ ions through the blood causes the electrical wave to be generated. Since the ECG signal is usually in the 2 mV region, a recording bandwidth of 0.1 to 120 Hz is required. Electrodes are applied to the patient's skin at the patient's current locations as part of a non-invasive technique for collecting the ECG. The ECG signal and heart rate serve as indicators of the cardiac illness of the human heart. A disturbance in heart rate or rhythm, or a change in the morphological pattern of the ECG signal, are both considered cardiac arrhythmias. The recorded ECG waveform is analysed to detect and diagnose it.

The ECG signal in a clinical setting is subjected to a variety of artefacts during capture. Random body and equipment noise, electrode contact noise, respirational movements, and electromyography artefacts are all major sources of noise. These disturbances decrease signal quality, frequency resolution, and have a significant impact on the morphology of critical ECG signals. For improved diagnosis, it is critical to eliminate ECG signal disruptions and increase ECG signal accuracy and reliability.

A noisy ECG signal has been investigated in a variety of methods. The signal is first filtered using high pass, low pass, and notch filters. On the other hand, these filters are static. The static filter's most significant drawback is that it eliminates a number of significant frequency components around the cutoff frequency. Static filters have set

filter coefficients. Because the noise's time variable behaviour is uncertain, fixed filter coefficients are difficult to use to reduce instrumentation artefacts. Adaptive filtering approaches have been created to get around the drawbacks of static filters. Other dynamic filters include the modified extended Kalman filter, wiener filter, adaptive Kalman filter, and other dynamic filters.

An essential stage in signal processing is the elimination of artefacts. A heart condition's diagnosis may be made using an ECG. ECG is a quick, painless, and non-invasive method of evaluating the cardiovascular system. The accurate extraction of information from a signal necessitates the precise characterisation of waveform morphologies and the absence of noise. While obtaining the ECG signals the signals are tainted by different type of artefacts including motion noise, electromyogram artefacts, and interference in power line and wandering baseline. It is difficult to eliminate these aberrations from the recorded ECG signal meanwhile an ECG is non-stationary. In this article, a novel denoising method that combines the discrete wavelet transform (DWT) and African vulture optimization (AVO) algorithm is proposed to denoise the white Gaussian noise found in ECG data.

Waveform morphologies must be well-characterized and noise-free to guarantee that the data obtained from a signal is correct. ECG, on the other hand, is a very little electric signal with amplitudes in the millivolt range. ECG noise comprises instrument interference, human activity, baseline drift, and other signal-related variables. The most

frequent noise in ECG data, baseline wander generates the most disturbances because of its magnitude. The ST segment as well as tiny waves like the P and T waves are frequently disrupted as a result of the signal deviating from its typical baseline level. As a result, researchers have proposed several strategies for decreasing signal noise.

A common signal processing technique called the wavelet transform (WT) creates a smooth signal in the time-frequency domain by using variables such the wavelet function name, thresholding techniques, selection rules, decomposition level, and threshold rescaling strategies. The literature has described a number of methods for addressing ECG components that have been impacted by various noises. Some of the solutions that have been proposed include WT, adaptive filters, neural networks, and non-linear filter bank designs.

The contribution of the work is as follows,

- The input of the design is thought to be the ECG signals from the MIT-BIH dataset. A clean signal is combined with white Gaussian noise to produce a noisy signal.

- The denoised ECG signal is split by the DWT and its parameters are optimized by the proposed Enhanced AVO algorithm. The AVO algorithm exploration phase is enhanced by the WOA optimization approach.

- After the decomposition, the noisy signal is transferred into the ASMF filter and its weight parameters are adjusted by the EAVO algorithm. Finally, the denoised ECG signals are attained from the suggested strategy.

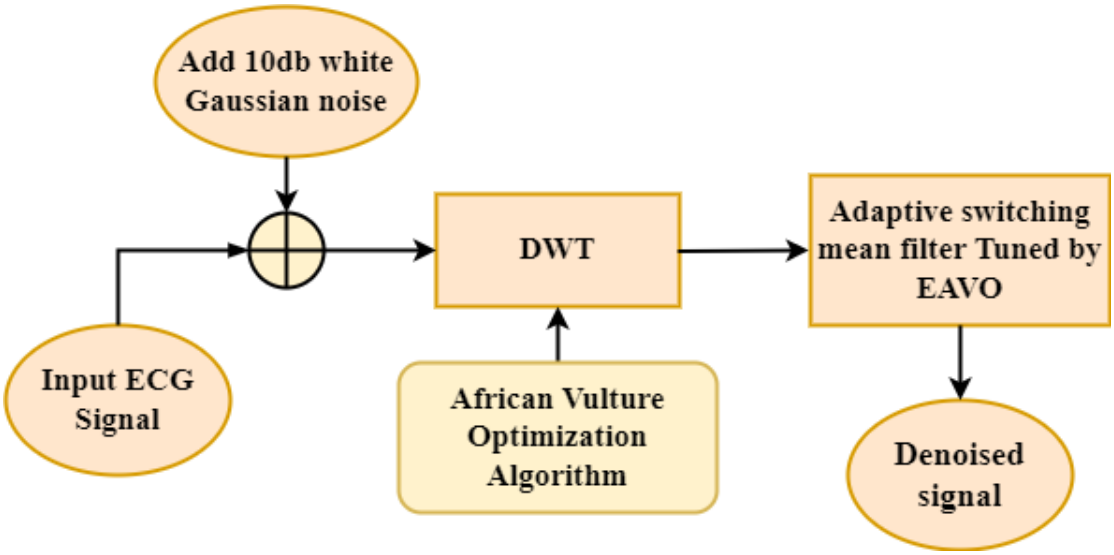

Figure 4.1: Proposed Approach Flow Diagram

4.2 Proposed Approach

The ECG signal is denoised in the suggested way utilising an adaptive switching mean filter and a discrete wavelet transform (DWT) optimised with the African vulture optimization (AVO) technique. The input ECG signals are recorded using the MIT-BIH ARR dataset and then exposed to white Gaussian noise. The distorted ECG data is denoised using the Discrete Wavelet Transform (DWT), and the threshold is optimised using the African Vulture Optimization (AVO)

method. In order to increase edge information and boost denoising performance, the denoised image is then reprocessed with an adaptive switching mean filter. Additionally, the proposed approach is contrasted with existing denoising techniques. Figure 4.1 displays the flow diagram of the proposed method.

4.2.1 DWT

The DWT is a wavelet transform that is utilized to extract wavelet coefficients from images at various sizes. In this situation, the larger coefficients in sub-bands will have more signal information than noise, whereas the lower coefficients in sub-bands will have more noise. These image noises can be decreased using a reconstruction approach that replaces the noisy coefficients with zeros and reverses the discrete wavelet transform. DWT stands for discrete wavelet series of discrete time signals, in which the wavelets, scaling function, and signal are all discrete in time. Filters are divided into two types: high and low pass. The high pass filter is responsible for image details, whereas the low pass filter is responsible for approximation. Using the horizontal and vertical dimensions, 2D DWT with one-dimensional decomposition is accomplished. High and low pass filters will be put into the photos in distinct rows and columns. The deconstruction occurs along the rows of photos initially in this manner. The data will be separated into columns after that. Low-low (LL), high-high (HH), low-high (LH), and high-low (HL) are the four deconstructed subband pictures produced by this

process (HH). These sub-bands' frequency components obscure the original image's whole frequency spectrum.

When a function $\Phi(t)$ meets the requirements stated in Eqn. (4.1) it has a Fourier transform for all $\Psi(\omega)$.

$$S_{\Phi} = \int_{0}^{+\infty} \frac{|\Psi(\omega)|}{\omega} d\omega < \infty \tag{4.1}$$

The basic wavelet is defined as the function $\Phi(t)$. By shifting and scaling the wavelet function as described in Eqn. (4.2), a wavelet sequence may be obtained.

$$\Phi_{a,b}(t) = \frac{1}{\sqrt{|a|}} \Phi\left(\frac{t-b}{a}\right) \tag{4.2}$$

An image's signal is a continuous two-dimensional signal. The continuous signal of the wavelet transform is given by equation (3).

$$f(x,y) = \frac{1}{S_{\Phi}} \int \frac{1}{a} \int_{-\infty}^{+\infty} \int_{-\infty}^{+\infty} W_f(a, b_1, b_2) \frac{1}{a} \Phi \times \left(\frac{x-b_1}{a}, \frac{y-b_2}{a}\right) dxdy \tag{4.3}$$

It's important to note that this filter is referred to as a quadrature mirror filter because the low pass and high pass filters is

interconnected. As stated by Nyquist's rule, half of the samples are deleted because half of the signal's frequency is discarded. The low pass filter g[n] output signal is then down-sampled by a factor of 2 and passed through an additional series of low pass and high pass filters to obtain the level-2 detailed and approximation coefficients. The cut-off frequency of the current set of filters is half that of the prior stage filter.

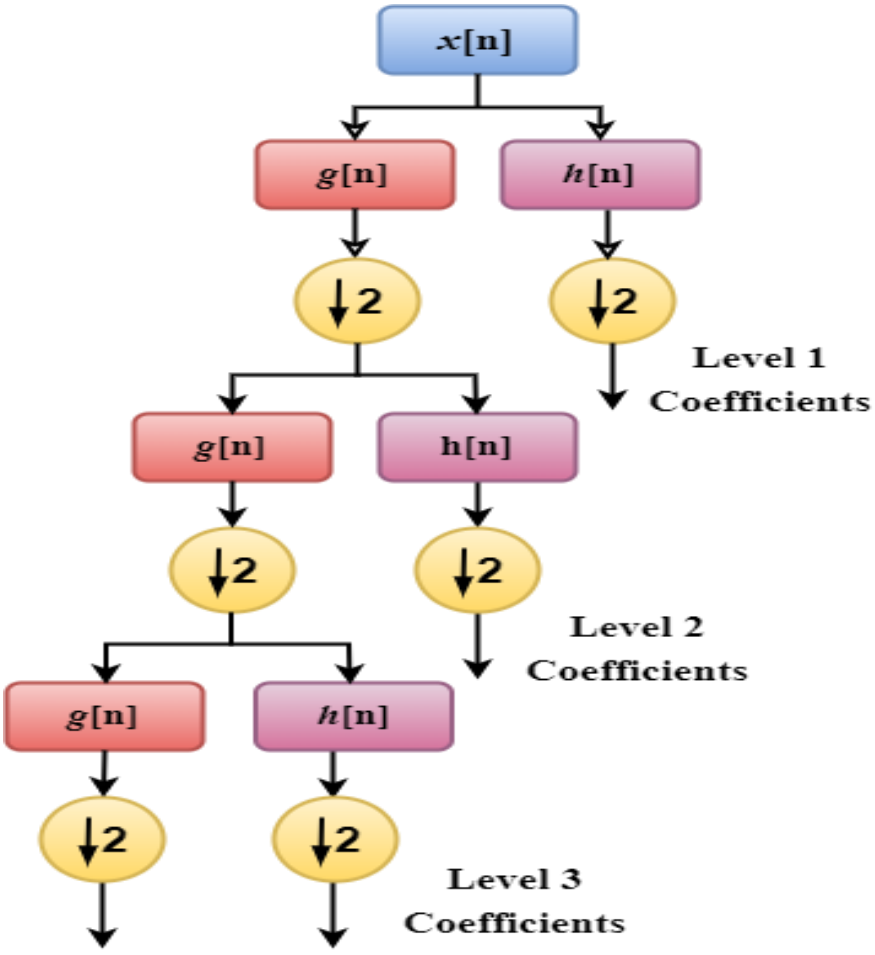

Figure 4.2: 3-level DWT block diagram

The main goal of employing DWT is to divide the input signal into various coefficient levels in order to adjust the input signals' high frequency. To put it another way, DWT divides the EEG signal into numerous frequency bands based on the assumption that the artefacts will have substantial amplitudes in each band. Fig. 4.2 illustrates the decomposition level L = 3 for denoising. In signal processing, signal noise removal is regarded as a difficult task. As a result, researchers have devised a number of solutions to this challenge, including the use of the filtering process. The solution is evaluated by the selected metaheuristic algorithm using the MSE objective function.

4.2.2 Adaptive switching mean filter

Some noises remain in the reconstructed signal after DWT-based denoising. The region amongst QRS complexes shows these disturbances very clearly. As a result, an ASMF filter is used to improve signal quality even more. ASMF is a powerful filtering technique that is utilized to eliminate impulse noise from signals. The core premise of ASMF is that signal samples in the same neighborhood should be identical. In this procedure, a specific window length is chosen, and the window center is put on an ECG sample at each iteration. If the variance among the ECG sample and windowed area's mean value is more than the threshold limit, the sample is considered corrupted, and its value is adjusted to match that of the mean. The ASMF operation's mathematical formulation is expressed in Eqn. (4.4).

$$\bar{X}_i = \begin{cases} q_i, & if\ |X_i^e - q_i \geq \alpha * \sigma_1| \\ X_i^e, & else \end{cases} \quad (4.4)$$

Where, ASMF operation input and processed ECG samples are represented into X_i^e and $\bar{X}_i$, respectively. The windowed region standard deviation denoted as q_i and i. Then the upper limit threshold value is chosen and the value varies from 0 to 1. The value of 0.1 is chosen empirically in this study, and a window of length of 9 samples is used.

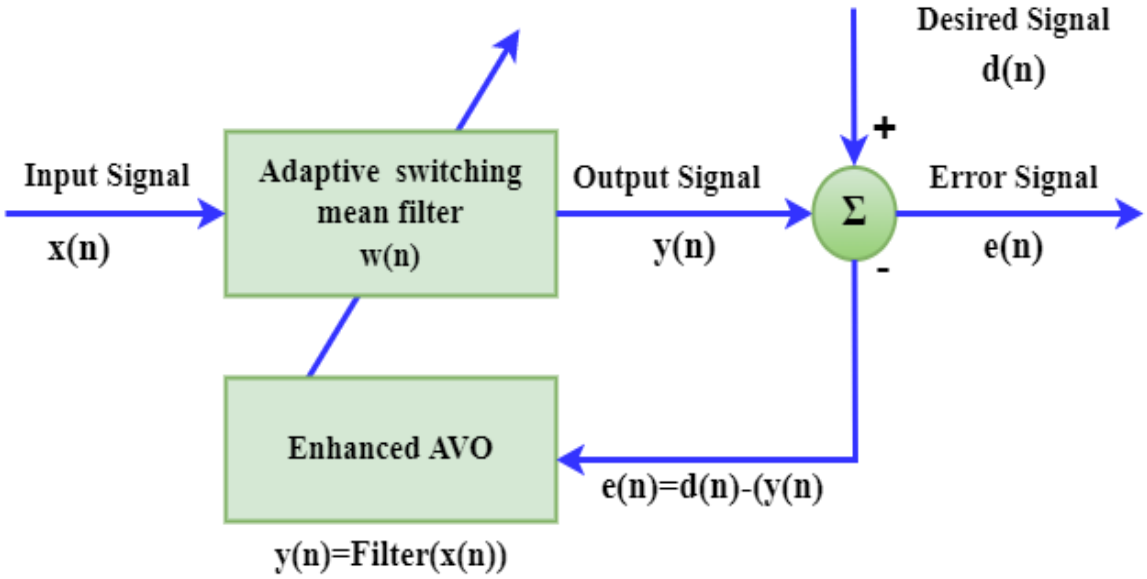

Figure 4.3: Adaptive switching mean filter

$$y(n) = \sum_{i=0}^{N-1} w_i(n) * x(n-i) \quad (4.5)$$

The total number of coefficients or weights is indicated by N. The $w_k(n)$ filter parameter signifies a specific time n and is valid for k

weight sequences. The open interval ranges from 0 to N this specific time changes. The fitness function is minimization of $^{e(n)}$, which is given in Eqn. (4.6),

$$obj2 = \min\{e(n)\} = d(n) - y(n) \tag{4.6}$$

4.2.3 African Vulture Optimization (AVO) Approach

The African Vulture Optimization imitates the foraging characteristics of African vulture. The following are the working principle of the AVO approach.

- In a given setting, there might be up to N vultures. In metaheuristic algorithms, it specifies the same number of population, and the number depends on the issue the researchers wish to apply to the AVOA.

- Many vultures may be physically segregated into two groups in a natural habitat, and the algorithm divides them into categories by first calculating the fitness function of all solutions (starting population). The finest response is designated as the best and first vulture, while the second response is designated as the second-best vulture. Others create a population that moves or replaces one of each performance's top two vultures.

- The rationale for group separation in this algorithm is that vultures' most important natural purpose may be stated as follows: group living to find food. Each vulture tribe has a unique incapacity to locate and consume food.

- Vultures' proclivity for eating and hours of searching for food allows them to flee the hungry trap. At the formulation stage, our anti-hunger compromises assume that the population's worst option is the weakest and most hungry, so the vultures strive to stay away from the worst and come up with the best solution. The strongest and best vultures in the AVOA are two of the best solutions, and the other vultures aim to approach the best.

This optimization algorithm consists of five phases that describes different characteristics of the vulture in its foraging phase.

- Clustering Population
- Starving Vultures
- Exploration Phase (Intial)
- Exploitation Phase (Medium)
- Exploitation Phase (Later)

- **Clustering Population:** In this phase the vultures cluster together and then move towards the source of food as described in Eqn. (4.4).

$$V_i^t = \begin{cases} TopVulture_1^t, & r_i^t = P_1 \\ TopVulture_2^t, & r_i^t = P_2 \end{cases} \tag{4.3}$$

Here, $TopVulture_1^t$ denotes the cluster of top vultures that are nearer to the food, P_1 and P_2 are arbitrary number that varies from 0 to 1.

- **Starving Vultures:** The degree of starvation of vulture is computed as in Eqn. (4.4).

$$D_i^t = (2 * rand_i^t + 1) * a^t * \left(1 - \frac{t}{T}\right) + h^t \tag{4.4}$$

Here, $rand_i^t$ refers an arbitrary number that varies from 0 to 1 and a^t is also an arbitrary number that varies from -1 to 1.

- **Exploration Phase:** The exploration phase is computed as follows,

$$A_i^{t+1} = \begin{cases} V_i^t - H_i^t * D_i^t, & r_1 \geq rand_{r1}^t \\ V_i^t - D_i^t + rand_{r2}^t * \left((min - max) * rand_{r3}^t + min\right), r_1 \geq rand_{r1}^t \end{cases} \tag{4.5}$$

$$H_i^t = |Ct * V_i^t - A_i^t| \tag{4.6}$$

Here, A_i^{t+1} denotes the i[th] vulture at *t+1* iteration and $rand_{r1}^t, rand_{r2}^t, rand_{r3}^t$ refers the arbitrary number that ranges from 0 to 1.

- **Exploitation Phase (Medium)**: For eradicating the imbalance in the food exploitation phase is divided into two: fighting for food and flying around. The location of a vulture is computed as,

$$A_i^{t+1} = H_i^t * (D_i^t + rand_{r4}^t) - h_i^t \tag{4.7}$$

$$h_i^t = V_i^t - A_i^t \tag{4.8}$$

On flying in the circular motion the vulture update the location based on the Eqn. (4.9).

$$A_i^{t+1} = V_i^t - (O_{i1}^t - O_{i2}^t) \tag{4.10}$$

$$O_{i1}^t = V_i^t * \left(\frac{rand_{r5}^t * A_i^t}{2\pi}\right) * \cos(A_i^t) \tag{4.11}$$

$$O_{i2}^{t} = V_i^t * \left(\frac{rand_{r6}^{t} * A_i^t}{2\pi}\right) * \sin(A_i^t) \quad (4.12)$$

- **Exploitation Phase (Later)**: This phase the vulture characteristics are divided into aggregation and attack. In aggregation the vulture location is updated based on the Eqn. (4.13).

$$A_i^{t+1} = \frac{W_{i1}^t - W_{i2}^t}{2} \quad (4.13)$$

In attacking phase the vulture location is updated based on the Eqn. (4.14).

$$A_i^{t+1} = V_i^t - |h_i^t| * H_i^t * Levy(dim) \quad (4.14)$$

Once the optimization process begins, EWOA makes a random, initial population and analyses the fitness function. Following the discovery of the optimum solution, the algorithm repeats the stages until the end condition is met. The main parameters are first updated. Finally, the method returns the optimal solution. The use of the best solution discovered so extreme to update the location of the remainder of

the resolutions ensures the convergence of this algorithm. As a result, the Enhanced AVO offers the most optimal solutions.

Pseudo code for Enhanced AVO
Inputs: population size N and maximum iterations T **Outputs**: Best fitness value

Initialize the random population
 	
while(stopping condition is not met) ***do***
 	
Compute fitness
 	
Set PBestVulture1 as the position of Vulture (First best solution)
 	
Set PBestVulture2 as the position of Vulture (Second best solution)
 	
for (each Vulture (P_i)) ***do***
 	
Select $X(i)$ using Eq. (10)
 	
Update the H using Eq. (12)
 	
if *(|H| ≥ 1)* ***then***
 	
if *($p_1 \geq rand p_1$)* ***then***

Update the location Vulture using Eq. (14)

else

Choose a arbitrary search agent ()

Current search agent position is modified by the Eq. (17)

end if

end if

end for

Check for any solutions that go beyond the limit and make necessary changes.

Compute fitness

Update X if better solution found $t = t + 1$

end while

return best solution

4.2.4 Adaptive Switching Mean Filter

Using an adaptive median filter, the filtering window size is changed based on the anticipated global noise density and the level of local corruption. For lesser noise ratios, an adaptive centre weighted

vector median filter is used; however, for greater noise ratios, noisy pixels are determined by comparing the difference between the vector pixel mean and projected variance. The window encompassing the detected noisy pixel is then re-evaluated, and the pixels are assigned exponential weights based on their spatial and radiometric similarity to other pixels. The weighted average of the pixels inside the window is used to replace the noisy pixels. When compared to other robust filters, the filter can maintain more signal information at greater noise ratios.

4.3 Experimental Results

The suggested denoising approach is simulated by MATLAB2018a software running on a Windows8.1 operating system. The White Gaussian noise is included in the ECG signals with the variances of 10dB to create a noisy signal. For experimentation purposes, the proposed approach is tested with three standard datasets BIDMC-CHF, MIT-BIH NSR and MIT-BIH ARR. Figure 4.4 illustrates the clean, noisy, and denoised ECG signals. The first collection of uniform test data for identifying readily accessible arrhythmias was the MIT-BIH dataset. Over 500 places worldwide have used this database since 1980 for basic heart dynamics research. 48 half-hour segments of 24-hour, 2-channel ECG recordings from 47 subjects were gathered by the BIH Arrhythmia Laboratory for this database. The patient's age, gender, and state of sickness are all included in each set of ECG data. The database allows associated institutions to exchange services and technical support while cutting R&D expenditures since it contains a wider range of ECG

abnormalities and more data types. The datasets, clean ECG signal, artefacts ECG signal, and denoised ECG signal are shown in Figure 4.4.

Table 4.1: Parameter description of proposed algorithm

Parameters	**Value**
Population size	40
Maximum iteration	200
r_1	0.8
r_2	0.2
k	2.5
p_1	0.6
Random search ability	0.1

Dataset	Clean ECG	Artefacts ECG	Denoised ECG
MIT-BIH ARR	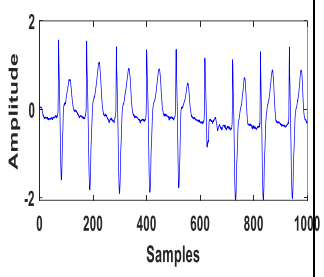	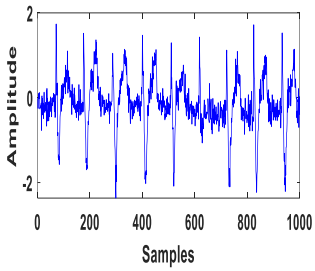	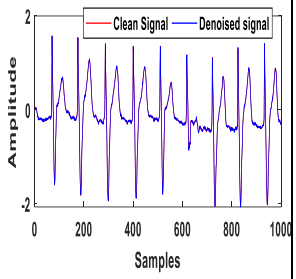
MIT-BIH NSR	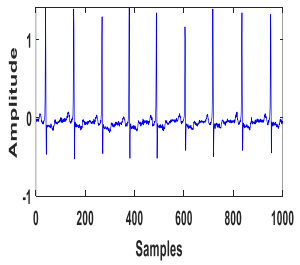	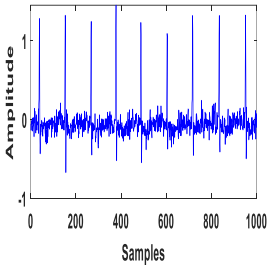	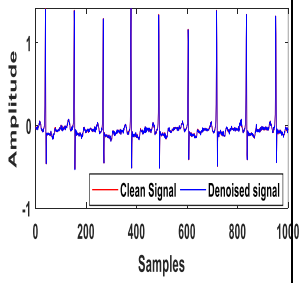
BIDM C-CHF	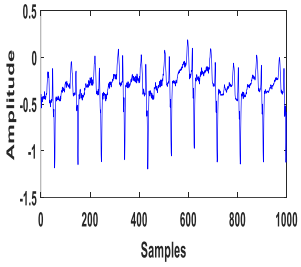	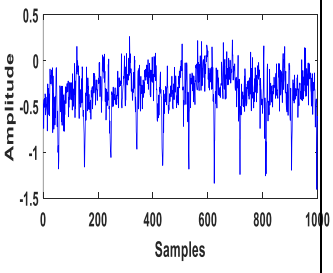	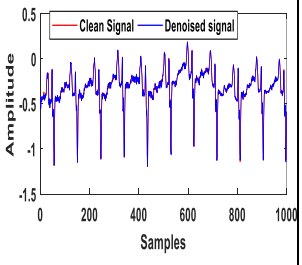

Figure 4.4: Original ECG Signal, Artefacts ECG and Denoised ECG Signal

For quantitative evaluation in denoising performance, the proposed strategy is utilized the following metrics such as peak reconstruction error (PRE), SNR, ME, MSE, correlation coefficient (CC), normalized root maximum error (NRME), normalized root-mean-square error (NRMSE), and MD are separately computed. These parameters are computed using $x0(p)$ is the pure signal; $y0(p)$ is the filtered outcome.

$$SNR = 10log_{10}\frac{\sum_{i=0}^{N-1}(x0(p_i))^2}{\sum_{i=0}^{N-1}(y0(p_i)-x(p_i))^2} \quad (4.15)$$

It's worth noting that the SNR measures noise suppression; consequently, the greater the SNR, the greater the denoising performance.

$$MD = \frac{1}{N}\sum_{i=0}^{N-1} x0(p) - y0(p) \quad (4.16)$$

$$NRMSE = \sqrt{\frac{\sum_{i=0}^{N-1}(y0(p_i)-x0(p_i))^2}{\sum_{i=0}^{N-1}(x(p_i))^2}} \quad (4.17)$$

$$PRE = \frac{x0(p)-y0(p)}{x0(p)} \quad (4.18)$$

$$ME = \max[abs(x0(p) - y0(p))] \quad (4.19)$$

$$NRME = 100 \times \sqrt{\frac{abs(x0(p)-y0(p))}{abs(x0(p))}} \quad (4.20)$$

$$CC = \frac{N[\sum_{i=0}^{N-1} x0(p_i) y0(p_i) - (\sum_{i=0}^{N-1} x0(p_i)) \sum_{i=0}^{N-1} y0(p_i))]}{\sqrt{[N \sum_{i=0}^{N-1} x0(p_i)^2) - (\sum_{i=0}^{N-1} y0(p_i))^2] \times [N \sum_{i=0}^{N-1} x0(p_i)^2) - (\sum_{i=0}^{N-1} y0(p_i))^2]}} \quad (4.21)$$

Table 4.2 describes the performance of the suggested approach including MSE, peak reconstruction error (PRE), SNR, normalized root-mean-square error (NRMSE), maximum error (ME), mean difference (MD), normalized root maximum error (NRME), and correlation coefficient (CC) is computed and are compared with other existing approaches such as RLS-based adaptive filter, Multichannel LMS, improved multiverse optimization with adaptive threshoding, Empirical Wavelet Transform with honey badger optimization and DWT-based baseline wander. The suggested technique delivers superior denoised signals than the other current approaches, based on the results.

Table 4.2: Performance of the Suggested Approach compared with other Approaches

Datasets	RLS-based adaptive filter	Multichannel LMS	DWT-based baseline wander	IMVO-AT	HBO-EWT	Proposed
	SNR					

MIT-BIH ARR	74.854	77.258	79.583	81.191	83.542	86.56
MIT-BIH NSR	71.526	73.819	75.925	77.953	79.549	84.45
BIDMC-CHF	73.765	75.471	80.163	82.616	85.643	87.28
	MSE					
MIT-BIH ARR	2.812e-10	1.943e-10	3.983e-10	2.904e-10	3.365e-10	2.356e-11
MIT-BIH NSR	3.419e-10	2.987e-10	2.654e-10	2.981e-10	2.450e-10	1.78e-10

BIDMC-CHF	3.731e-10	3.256e-10	3.465e-10	3.204e-10	2.915e-10	1.932e-10
	ME					
MIT-BIH ARR	8.348e-4	6.356 e-4	4.265e-4	8.338e-4	6.749e-4	6.945e-5
MIT-BIH NSR	2.945e-3	2.609 e-3	9.455e-4	3.549e-3	3.604e-3	7.578e-4
BIDMC-CHF	9.964e-4	7.843e-4	6.894e-4	9.624e-4	7.752e-4	6.431e-4
	MD					
MIT-BIH ARR	-7.86e-7	-4.590e-7	-3.933e-7	-7.752e-7	-4.150e-7	-1.10e-7

MIT-BIH NSR	-7.75e-7	-6.775e-7	-5.436e-7	-7.514e-7	-6.894e-7	-3.15e-7
BIDMC-CHF	-1.15e-6	-6.593e-7	-5.965e-7	-1.215e-6	-6.250e-7	-3.87e-7
	PRE					
MIT-BIH ARR	4.643e-7	3.864e-7	1.654e-7	4.804e-7	1.065e-7	6.464e-8
MIT-BIH NSR	9.568e-8	9.641e-8	8.644e-8	8.859e-8	8.264e-8	5.524e-8
BIDMC-CHF	1.505e-7	9.567e-8	8.664e-8	1.739e-7	8.364e-8	7.065e-8
	NRME					
MIT-	3.230e-	2.539e-1	3.214e-	2.562e-	2.567e-	1.250e-1

BIH ARR	1		1	1	1	
MIT-BIH NSR	2.704e-1	2.425e-1	2.439e-1	2.481e-1	2.450e-1	1.354e-1
BIDMC-CHF	2.264e-1	2.453e-1	2.958e-1	2.550e-1	2.519e-1	1.405e-1
	NRMSE					
MIT-BIH ARR	3.477e-5	3.691e-5	2.904e-5	3.365e-5	2.105e-5	1.581e-6
MIT-BIH NSR	3.145e-5	2.461e-5	2.981e-5	2.450e-5	2.119e-5	1.698e-6
BIDMC-CHF	3.294e-5	3.624e-5	3.204e-5	2.915e-5	2.353e-5	1.974e-6
	CC					

MIT-BIH ARR	0.9888	0.9899	0.9983	0.9993	0.9997	1
MIT-BIH NSR	0.9778	0.9856	0.9871	0.9944	0.9976	0.9997
BIDMC-CHF	0.9868	0.9871	0.9958	0.9985	0.9988	0.9998

Figure 4.5 depicts the correlation coefficient (CC) of various denoising methods such as RLS-based adaptive filter, Multichannel LMS, improved multiverse optimization with adaptive threshoding, Empirical Wavelet Transform with honey badger optimization and DWT-based baseline wander compared with the proposed approach. This chart clearly shows that the recommended method provides better CC than previous denoising techniques.

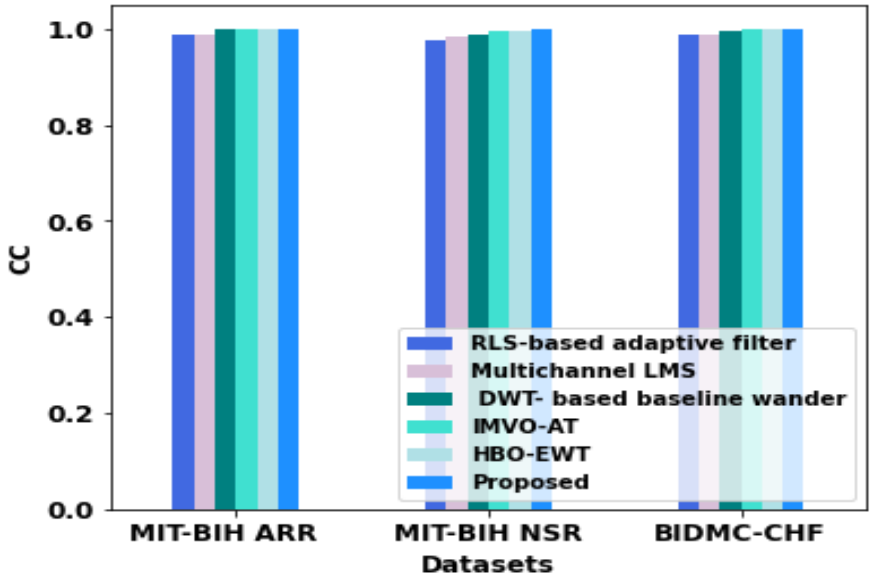

Figure 4.5: CC values of various denoising methods

Figure 4.6 defines the mean difference (MD) among the suggested technique and other denoising approaches methods such as RLS-based adaptive filter, Multichannel LMS, improved multiverse optimization with adaptive thresholding, Empirical Wavelet Transform with honey badger optimization and DWT-based baseline wander. This chart shows that the proposed technique generates a larger MD value than existing optimization algorithms. The suggested technique delivers superior denoised signals than the other current approaches, based on the results.

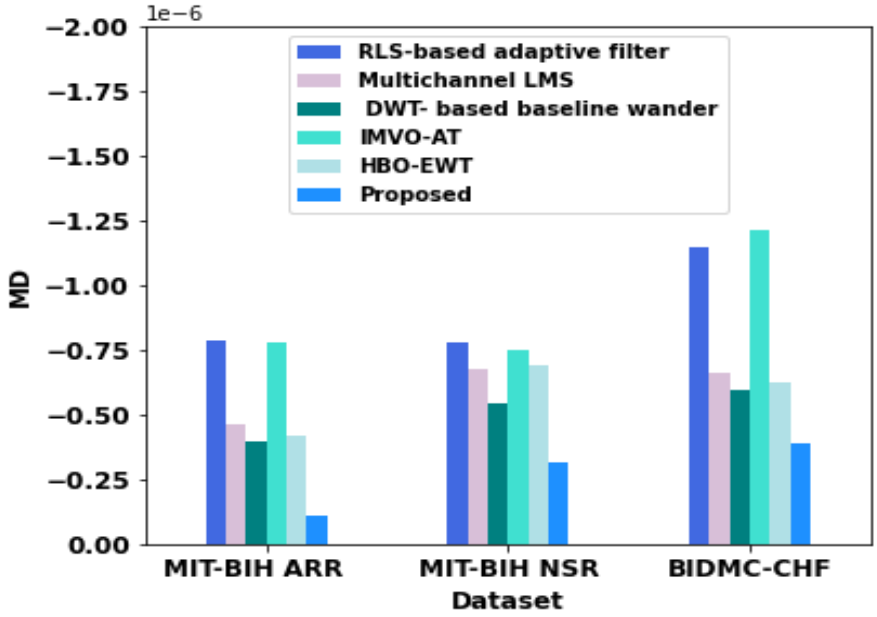

Figure 4.6: MD values of different denoising methods

Figure 4.7 depicts the maximum error (ME) of various optimization algorithms such as RLS-based adaptive filter, Multichannel LMS, improved multiverse optimization with adaptive thresholding, Empirical Wavelet Transform with honey badger optimization and DWT-based baseline wander compared with the proposed approach. From this figure it is evident that the suggested approach gives lesser ME value than other denoising techniques. The experimental findings illustrates that the proposed approach is superior to all other denoising techniques.

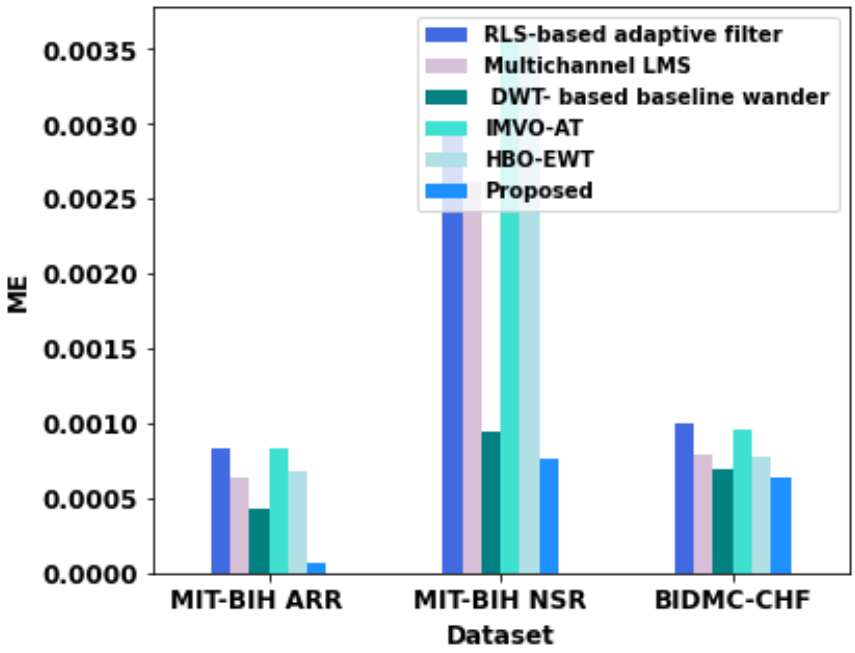

Figure 4.7: ME values of different denoising methods

Figure 4.8 compares the Mean Square Error (MSE) of several optimization techniques to the proposed methodology, including RLS-based adaptive filter, Multichannel LMS, improved multiverse optimization with adaptive thresholding, Empirical Wavelet Transform with honey badger optimization and DWT-based baseline wander. The recommended technique provides a less MSE value than previous denoising strategies, as seen in this graph. The experimental findings demonstrate that the suggested methodology outstrips all currently used denoising techniques.

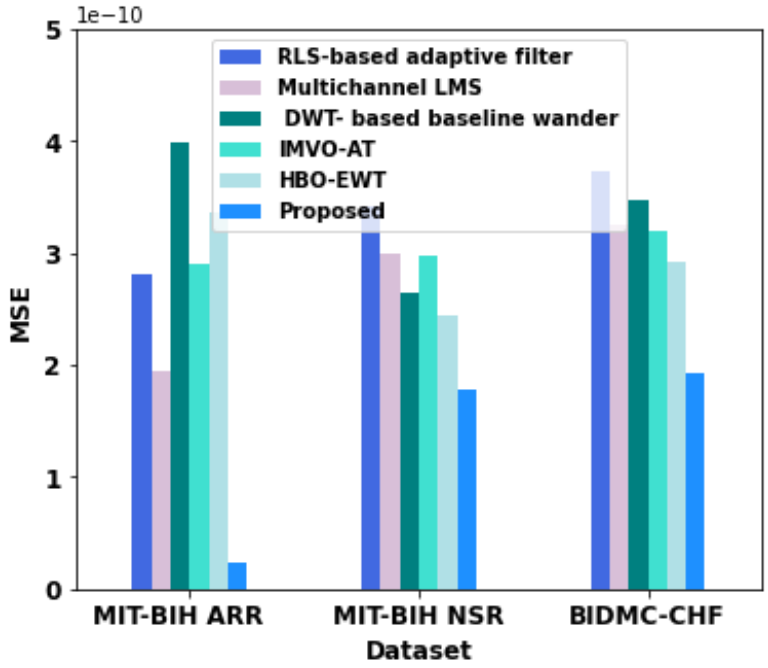

Figure 4.8: MSE values of different denoising methods

The normalized root maximum error (NRME) between the suggested approach and other optimization algorithms like RLS-based adaptive filter, Multichannel LMS, improved multiverse optimization with adaptive thresholding, Empirical Wavelet Transform with honey badger optimization and DWT-based baseline wander is shown in Figure 4.9. The suggested approach produces a lower NRME value than existing denoising techniques, as seen in this graph. The results of the experiments reveal that the proposed strategy outperforms all other denoising strategies.

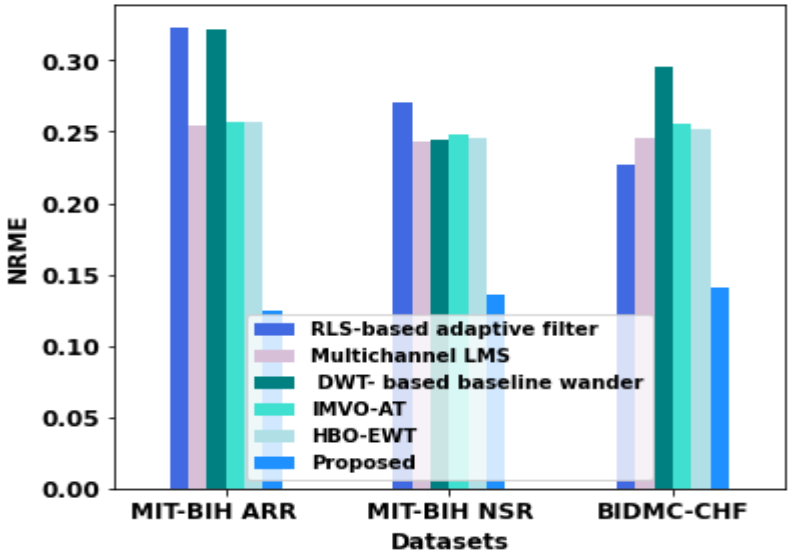

Figure 4.9: NRME values of different denoising methods

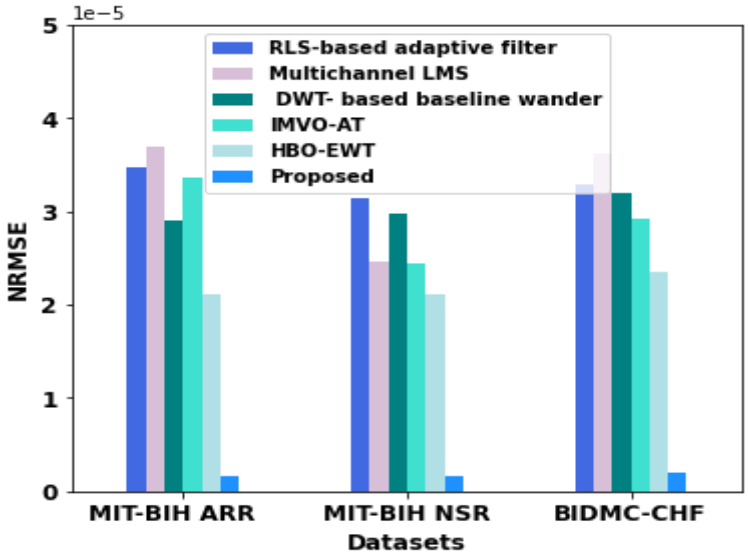

Figure 4.10: NRMSE values of different denoising methods

The peak reconstruction error (PRE) between the suggested approach and other optimization algorithms like RLS-based adaptive

filter, Multichannel LMS, improved multiverse optimization with adaptive thresholding, Empirical Wavelet Transform with honey badger optimization and DWT-based baseline wander is shown in Figure 4.11. The suggested approach produces a lower PRE value than existing denoising techniques, as seen in this graph. The results of the experiments reveal that the proposed strategy outperforms all other denoising strategies.

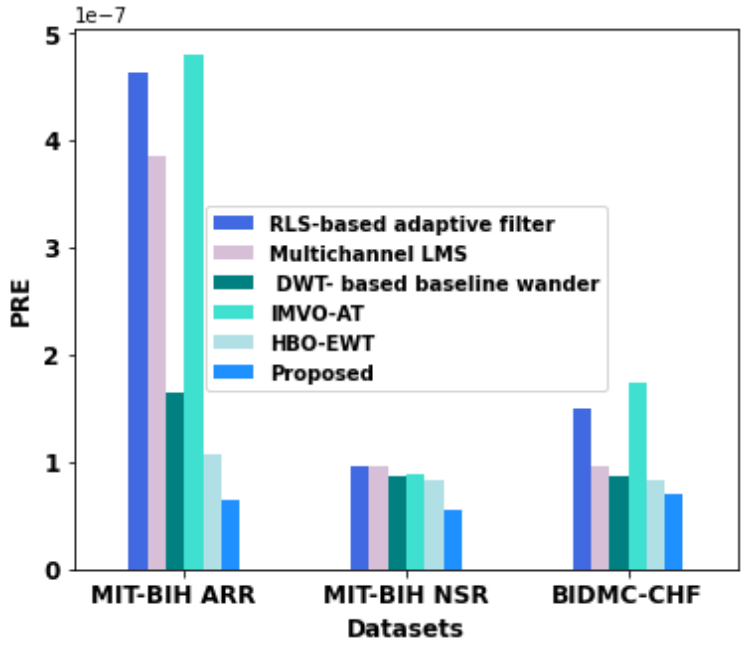

Figure 4.11: PRE values of different denoising methods

Figure 4.12 depicts the SNR of various approaches such as RLS-based adaptive filter, Multichannel LMS, improved multiverse optimization with adaptive thresholding, Empirical Wavelet Transform with honey badger optimization and DWT-based baseline wander

compared with the proposed approach. From this figure it is evident that the suggested approach gives higher SNR value than other existing approaches. The experimental findings illustrates that the proposed approach is superior to all other denoising techniques.

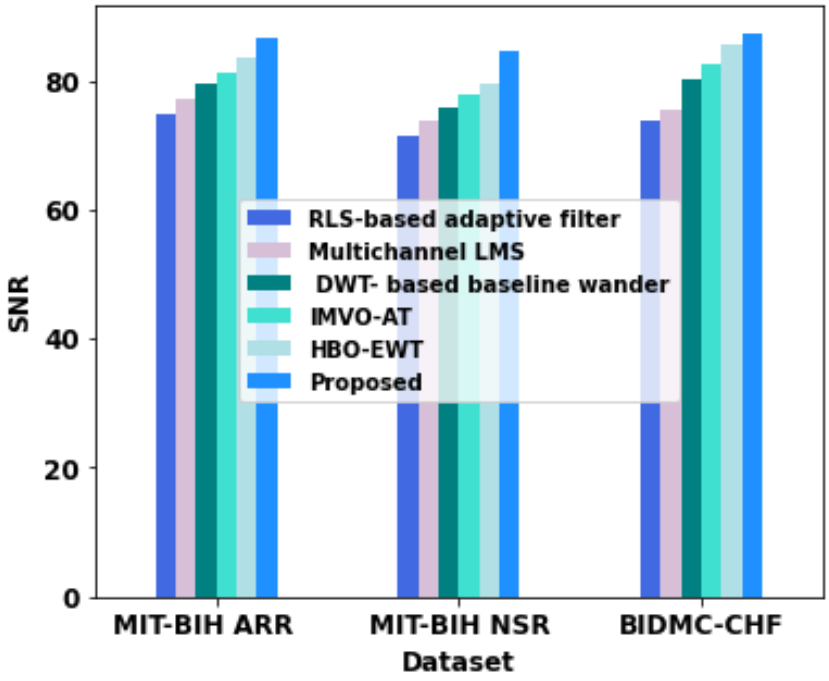

Figure 4.12: SNR values of different denoising methods

Table 4.3 describes the Wilcoxon signed rank test for the proposed approach versus the existing approaches.

Table 4.3: Wilcoxon signed rank test

Comparative hypothesis	Proposed VsPSO	Proposed VsAOA	Proposed VsMVO	Proposed VsIMVO	Proposed VsHBO
P-value	0.164	0.157	0.125	0. 125	0.05

For discovering interaction effects or significant factors, Friedman's analysis of variance (ANOVA) is recommended. ANOVA is a useful method for separating overall variability into useable components such as a degree of freedom (Df), sum of squares (SS), F-value, and mean sum of squares (MS). Table 4.4 displays the output parameters and values obtained from the ANOVA test for several optimization methods utilising the suggested denoising methodology.

Table 4.4: Friedman's test

Source	SS	Df	MS	F	Prob>F
Columns	30.3333	2	15.1667	4.04	0.1324

Interaction	2.3333	2	1.1667		
Error	87.3333	12	7.2778		
Total	120	17			

4.4 Summary

This study uses Enhanced AVO, a novel bio-inspired metaheuristic algorithm, to implement an adaptive switching mean filter-based denoiser and demonstrate WOA-AVO capacity to find high-quality solutions that outperform other metaheuristic algorithms such as PSO, AOA, MVO, IMVO, and HBO. The Enhanced AVO algorithm not only maintains a correct poise among exploration and exploitation but it is control parameter-free algorithm, which eliminates the need for a time-consuming control parameter tweaking process. The DWT wavelet parameter of window function and ASMF filter is optimized by the Enhanced AVO algorithm. To prove the effectiveness of the proposed denoising filter, EAVO method comparative analysis has been conducted with the RLS-based adaptive filter, multichannel LMS, IMVO-AT, HBO-EWT, and DWT- based baseline wander techniques. When compared to prior reported results, estimated results show that the proposed EAVO-based adaptive switching mean filter achieves a

considerable improvement in NRMSE, SNR, MD, NRME, PRE, ME, and CC. As a result, the proposed strategy for denoising the cardiovascular signal is quite effective. The results and discussions examined allow for the conclusion that the proposed hybrid algorithm, which is supported by DWT and filter, can be used effectively for cardiovascular signal denoising.

CHAPTER 5

CONCLUSION AND SCOPE FOR FUTURE WORK

5.1 Conclusion

The electrocardiogram (ECG) is a non-stationary biological signal used to diagnose cardiac issues. Noise reduction in electrocardiography signals is a key and important task since the artefacts that contaminate the data have similar frequency characteristics as the signal itself. Filtering techniques, for instance, have been demonstrated to be unsuccessful in eliminating these interferences. Electrocardiography signals, as a result, require an innovative and efficient denoising technique in order to achieve appropriate noise-removal performance.

The non-stationary electrocardiography data may be successfully denoised using empirical wavelet transform or discrete wavelet transform hybridized with machine learning approaches. The current thesis provides a unique connection for cleaning up ECG signals. A noisy signal is made up of a limited number of IMFs that represent the data's oscillatory mode. The first few IMFs (Instrinsic Mode Functions) capture the signal's noisy component, whereas higher order IMFs capture slower fluctuations like baseline wander.

Any complex signal's high and low frequency components may be separated using EWT-based techniques. The reconstruction method can omit those IMFs that capture noisy components. Denoising is performed by removing the unwanted bits of the signals. To verify the presented methodology, experimental testing of the novel proposed approach was done on various electrocardiogram data (MITBIH ECG Database).The findings suggest that the suggested approach is appropriate for ECG denoising and improves signal quality significantly. To reduce computational complexity, various ANCs that use sign-based versions of all three normalised algorithms have been successfully developed, and maximum data normalisation based processing has been applied to all algorithms to reduce the number of multiplications in the denominator part of the weight update recursion.

5.2 Future Work

Future research should focus on reducing all forms of noise from ECG signals using a single hybrid strategy that combines existing approaches. And also the work presented here might be expanded upon, as could the different options for future research. These are detailed briefly below. Other noise categories, such as foetal noise, donor heart noise, pacemaker noise, and so on, will require further ANC development. The use of fewer leads to extract data for current ECG recorders may result in processing problems that can be corrected using new algorithms that are still being developed. There is potential for the

creation of intelligent cardiac systems in which various algorithms may be utilised, with the appropriate adaptive algorithm activating for filtering based on the noise characteristics. New ANCs may be created utilising neural networks and fuzzy logic.